

Review: Quantum Metrology and Sensing with Many-Body Systems

Victor Montenegro,^{1,2} Chiranjib Mukhopadhyay,^{1,2} Rozhin Yousefjani,^{1,2,3}
Saubhik Sarkar,^{1,2} Utkarsh Mishra,⁴ Matteo G. A. Paris,⁵ and Abolfazl Bayat^{1,2,*}

¹*Institute of Fundamental and Frontier Sciences,*

University of Electronic Science and Technology of China, Chengdu 611731, China

²*Key Laboratory of Quantum Physics and Photonic Quantum Information, Ministry of Education,
University of Electronic Science and Technology of China, Chengdu 611731, China*

³*Qatar Center for Quantum Computing, College of Science and Engineering, Hamad Bin Khalifa University, Doha, Qatar*

⁴*Department Of Physics and Astrophysics, University of Delhi, Delhi 110007, India*

⁵*Universita di Milano, I-20133 Milano, Italy*

Quantum systems, fabricated across various spatial scales from nano to micrometers, are very delicate and naturally sensitive to the variations of their environment. These features make them excellent candidates for serving as sensors with wide range of applications. The size versatility as well as their sensitivity, allow quantum sensors to achieve unprecedented precision with ultra-high spatial resolution. The main power of quantum sensors is achieved when the probe is composed of several particles. In this situation, quantum features such as entanglement contribute in enhancing the precision of quantum sensors beyond the capacity of classical sensors, a phenomenon that is referred to as quantum enhanced sensitivity. Originally, quantum sensing was formulated for non-interacting particles which are prepared in a special form of maximally entangled states. These probes are extremely sensitive to decoherence and any interaction between particles is detrimental to their performance. An alternative framework for quantum sensing has been developed exploiting quantum many-body systems, where the interaction between particles plays a crucial role. In this review, we investigate different aspects of the latter approach for quantum metrology and sensing. Many-body probes have been used for sensing purposes in both equilibrium and non-equilibrium scenarios. Quantum criticality has been identified as a resource for achieving quantum enhanced sensitivity in both of these scenarios. In equilibrium, various types of criticalities, such as first order, second order, topological, and localization phase transitions have been exploited for sensing purposes. In non-equilibrium scenarios, quantum enhanced sensitivity has been discovered for Floquet, dissipative, and time crystal phase transitions. While each type of these criticalities, either in equilibrium or non-equilibrium scenarios, has its own characteristics, the presence of one feature is crucial for achieving quantum enhanced sensitivity and that is energy/quasi-energy gap closing. In non-equilibrium quantum sensing, time becomes another parameter which can affect the sensitivity of the probe. Typically, the sensitivity enhances as the probe evolves in time. Unlike criticality-based quantum sensors, the criteria which allows non-equilibrium probes to achieve quantum enhanced sensitivity is not fully explored. In this review, we provide an overview on recent progresses on different aspects of quantum metrology and sensing with many-body systems.

CONTENTS

I. Introduction	2	B. Bosonic many-body probes	12
II. Elements of Parameter Estimation	4	C. Spin chain probes with criticality-enhanced sensitivity	12
A. Global and local estimation theory	5	D. Quantum many-body probes with long-range interactions	13
B. Single-parameter classical estimation bound	5	V. Equilibrium Quantum Sensing: Localization Transition	14
C. Optimizing the classical bound: the QFI	6	A. Pseudo-random localization transition	14
D. Multi-parameter estimation	7	B. Stark localization	15
E. Geometry of parameter estimation	8	VI. Equilibrium quantum sensing: Topological Phase Transitions	16
F. Alternatives to QFI for Metrology	8	A. Symmetry protected topological sensors	16
III. Interferometric Quantum Sensing	9	B. Non-Hermitian Quantum Sensors	17
IV. Equilibrium Quantum Sensing: Second Order Quantum Phase Transition	9	VII. Resource analysis for critical quantum sensing	19
A. Free fermionic many-body probes	11	VIII. Non-Equilibrium Quantum Sensing: Dynamical Quantum Phase Transitions	20
		A. Dynamical quantum phase transitions quantified by Loschmidt echo	20

* abolfazl.bayat@uestc.edu.cn

B. Dynamical quantum phase transitions quantified by a time-averaged order parameter	20
IX. Non-Equilibrium Quantum Sensing: Discrete Time Crystal Phase Transitions	20
X. Non-Equilibrium Quantum Sensing: Floquet Phase Transition	21
XI. Non-Equilibrium Quantum Sensing: Dissipative Phase Transitions	23
A. Profiting from dissipation	24
B. Restoring quantum sensing advantage in noisy environments	24
C. Dissipative phase transition as a sensing resource	25
XII. Non-Equilibrium Quantum Sensing: Quantum Many-Body Scars and Sensing	27
XIII. Non-Equilibrium Quantum Sensing: Sequential Measurements Metrology	28
XIV. Global Sensing: Parameter Estimation with Minimal Prior Information	30
XV. Summary and Outlook	33
Acknowledgments	34
References	34

I. INTRODUCTION

The rapidly emerging quantum technologies are expected to revolutionize our lives in the coming decades [1]. In a broad sense, quantum technologies are developed in three directions, namely quantum simulation and computation [2, 3], quantum communication [4, 5], and quantum sensing [6]. Thanks to advancements in fabricating ultra-precise quantum devices, the progress in all these three aspects have significantly been accelerated. Quantum sensing [6] is one of the pillars of quantum technologies which allow for developing a new generation of sensors for detecting gravitational, magnetic and electric fields as well as estimating physical quantities with unprecedented precision, well beyond the capability of conventional classical sensors. The application prospect of quantum sensors is very wide and includes mining [7], environmental monitoring [8], biological imaging [9–11], space exploration [12], radar technology [13, 14], searching for fundamental particles [15–19] — the list goes on. There are several reasons that make quantum sensors superior over their classical counterparts. First, the even smaller sizes of quantum sensors, which can be fabricated at the atomic scales, allows for excellent spatial resolution [20, 21]. Second, the

natural delicacy of quantum superposition allows quantum sensors to detect very weak signals [22, 23]. Third, a combination of quantum particles can benefit from a unique property of quantum physics, namely entanglement, which allows for quantum enhanced precision in comparison with a classical sensor using the same amount of resources [24–26].

In order to quantify the precision of a sensor for estimating an unknown parameter θ , one needs to specify a proper figure of merit. In case of maximal-likelihood estimation theory, the imprecision of the estimation, as quantified by the variance of an *unbiased* maximal-likelihood estimator, is bounded through Cramér-Rao inequality [27, 28] by $1/MI(\theta)$, where M is the number of samples and $I(\theta)$ is a quantity called Fisher information, which will be defined and discussed later. Dependence on M is a direct consequence of central limit theorem, therefore the most important quantity which bounds the precision of a sensor is the Fisher information. In fact, in estimation theory, Fisher information is the conventional figure of merit for evaluating the performance of a sensor. Every sensing procedure exploits some resources such as time, particle number, system size, etc. The resource efficiency of a given sensor is determined by the scaling of Fisher information with respect to those resources. In other words, such scaling shows how the precision is enhanced by using more resources. In the absence of quantum features, the Fisher information at best scales linearly with the resource, which is known as standard (or shot-noise) limit. However, exploiting quantum features such as superposition and entanglement may result in super-linear scaling of the Fisher information with respect to the resource. This is known as quantum enhanced sensitivity and is one of the key properties that makes quantum sensors superior over their classical counterparts.

The notion of quantum enhanced sensitivity was first discovered in an interferometric setup introduced in the seminal paper of Giovannetti, Lloyd and Maccone [24]. In this paper, the authors show that a special form of entangled states, such as Greenberger–Horne–Zeilinger (GHZ) states, can enhance the precision of detecting a phase shift quadratically with respect to the probe size. Optical setups have since been used to experimentally confirm this effect quite extensively [29–31]. Even for matter-based platforms, the effect was tested experimentally in ion-trap systems [32] and then extended to various physical platforms like superconducting qubits [33] and nitrogen vacancy centers [34]. The original formulation [24] relies on the GHZ-type of entangled states which are difficult to create and extremely sensitive to decoherence and particle loss. In addition, in this strategy a very special form of unitary operation, namely phase shift, is assumed for encoding the information in the state of the probe. In fact, it has been shown that any disturbance to the considered unitary operation diminishes the precision [35]. All these challenges may prevent the original interferometric sensing procedure to scale up for large

system sizes or restrict it to special forms of interactions.

An alternative method to interferometric quantum sensing has emerged in many-body systems. There are several distinct features between the two methods for sensing external parameters: (i) while the interferometric sensing requires entangled GHZ-type state preparation, in many-body sensors entanglement is either inherently present in the spectrum of the system or generated freely during the dynamics; (ii) while interaction between particles is destructive in interferometric sensing, it plays a crucial role in many-body sensors; (iii) unlike GHZ-type states, many-body systems are more resistive against decoherence and particle loss; and (iv) in contrast to the interferometric sensors, the optimal measurement may depend on the unknown parameter which is supposed to be measured. While features (i)-(iii) show the benefits of many-body sensors over their interferometric counterparts, the feature (iv) shows that taking advantage of many-body systems for sensing is not free of challenge. These *pros* and *cons* motivate further investigations of many-body systems for developing a new generation of sensors. In general, there are two different approaches to exploit many-body systems for metrology purposes with quantum enhanced sensitivity. The first approach, which typically requires equilibrium states, such as the ground state, exploits quantum criticality for achieving quantum enhanced sensitivity. In the second approach, however, non-equilibrium dynamics of a many-body system is exploited to accumulate information about the parameters of interest. Further divisions can be considered for non-equilibrium probes as they might be used at non-equilibrium steady states or transient dynamics. All these methods for achieving quantum enhanced sensitivity are summarized in Fig. 1.

Quantum criticality has already been identified as a resource for sensing in both equilibrium and non-equilibrium many-body systems. Originally, quantum phase transition in the transverse Ising model has been explored for metrology purposes [36]. It has been then extended to various types of criticalities including, first-order [37–39], second-order [36, 40–53], topological [54–58], non-Hermitian systems [59–73], and Stark phase transitions [74–76]. Apart from these distinct types of criticalities at equilibrium, non-equilibrium quantum phase transitions can also demonstrate quantum enhanced sensitivity. This includes dissipative [77–86], Floquet [87, 88] and time crystal [89–93] phase transitions. Each type of quantum criticality comes with its own features and characteristics. For instance, second-order quantum phase transitions take place in the ground state of a many-body system and are accompanied by spontaneous symmetry breaking and long-range correlations which are described by Landau-Ginzburg formalism [94]. On the other hand, topological phase transitions neither show symmetry breaking nor follow the Landau-Ginzburg theorem [95] and Stark localization takes place across the entire spectrum and not just the ground state [96, 97]. While different types of quantum

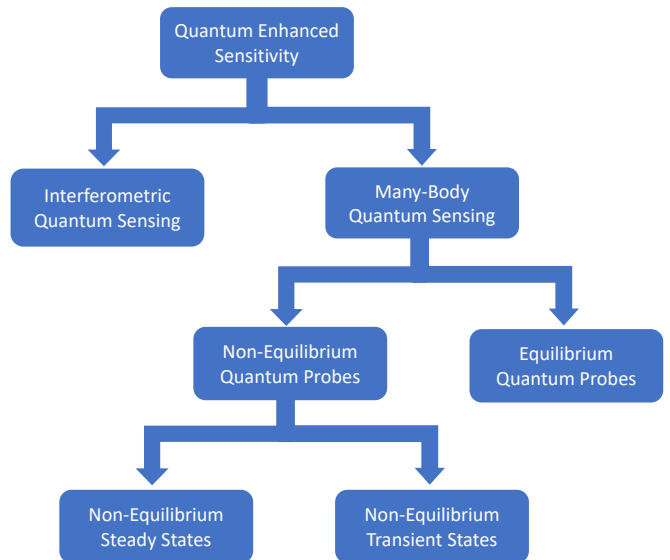


FIG. 1. **Schematic for achieving quantum enhanced sensitivity.** The main advantage of quantum sensors over their classical counterparts is manifested through quantum enhanced sensitivity. Various strategies have been discovered to achieve such enhancement. Originally, interferometric quantum sensors were proposed and realized for measuring a phase shift with quantum enhanced precision. Later, the capacity of quantum many-body systems for achieving quantum enhanced sensitivity was identified which is the subject of this review. Many-body systems have been used for quantum sensing in both equilibrium (e.g. criticality in the ground state) and non-equilibrium modes. In the non-equilibrium case, we can further divide the sensors into non-equilibrium steady states and transient dynamics.

criticalities have their own characteristics, one feature is common among all of them for showing quantum enhanced sensitivity which is energy/quasi-energy *gap closing*. This is an interesting observation which guides us in searching for finding new potential quantum sensors with the capability of achieving quantum enhanced precision. Interestingly, the realization of criticality-based quantum sensors are becoming viable in various physical platforms, including nuclear magnetic resonance systems [50] and Rydberg atoms [98].

Quantum criticality is in general a property of equilibrium states such as the Gibbs thermal state (which becomes the ground state at zero temperature limit) [99, 100]. Preparing such equilibrium states can be challenging in practice, demanding ultra-low temperatures or extremely long preparation times. In addition, criticality-enhanced quantum precision is only achievable around the phase transition point. This requires fine tuning and thus is mostly beneficial in the context of local sensing, where significant prior information about the parameter of interest is available. Therefore, as an alternative, one can use non-equilibrium dynamics of many-body systems for sensing unknown parameters. These setups are more experimental friendly as their initial state can be a

simple product state and entanglement is generated naturally during the dynamics. Non-equilibrium dynamics in many-body systems can be induced through different methods, including quantum quench [101–104], measurement quench [105–108] and external driving [109–111]. Apart from the probe size, in non-equilibrium quantum sensors, time is also a key resource which plays an important role and has to be included in the definition of standard limit and quantum enhanced sensitivity. In general, Fisher information scales as $I \sim t^\alpha L^\beta$, where t is time, L is the system size and α and β are two exponents [84]. In non-equilibrium sensors, the standard limit is defined as $\alpha=\beta=1$. Any situation with $\alpha > 1$ or $\beta > 1$ is called quantum enhanced sensitivity with the special case of Heisenberg limit, defined as $\alpha=\beta=2$. In certain systems in which the unitary dynamics preserves the number of excitations, the Fisher information may scale with the number of excitations too. In fact, in Ref. [112] it was shown that in excitation-preserving dynamics Fisher information scales as $I \sim t^\alpha L^\beta N^\gamma$, where N is the number of excitations and γ is its corresponding exponent. This is an interesting observation which shows how the sensitivity increases from single excitation subspace, i.e. $N=1$, to half filling, i.e. $N=L/2$. Unlike criticality-based quantum sensors, the criteria for achieving quantum enhanced precision is not yet well-characterized in non-equilibrium quantum many-body probes. For instance, we know that localized phases are not good for sensing [74–76, 113] but what features in extended phases are crucial for quantum enhanced sensitivity are not yet identified.

In practice, no quantum device is perfectly isolated from its environment and thus decoherence is an inevitable part of any quantum protocol. Consequently, any quantum dynamics is actually an open system evolution. Different formalisms have been developed for addressing open system dynamics, among them are: (i) master equation [114]; and (ii) non-Hermitian Hamiltonians [115]. In the former, the evolution of the system and its environment is described by a unitary operation. By tracing out the environment, the evolution of the system, typically within Born-Markov approximations, is thus characterized by the Lindblad (or Gorini-Kossakowski-Sudarshan-Lindblad) master equation [116]. In this formalism a quantum system initially prepared in a pure state may indeed evolve to a mixed state due to the action of jump operators — a signature of information leakage (irreversible process) to the environment. In non-Hermitian formalism, the environment is monitored for tracking a trajectory in which no jump operator action takes place [117, 118]. As a result, an initially pure quantum state remains pure throughout the dynamics, despite being evolved effectively as an open quantum system. Other mechanisms that address or profit from dissipation include decoherence-free subspaces [119, 120], dynamical decoupling [121, 122], and quantum reservoir engineering [123]. The latter technique involves adding an engineered Lindbladian term to the open system dynamics. This approach can be designed to steer the system into a

desired pure steady-state, effectively *cooling* the system to that state [124–127]. Both master equation and non-Hermitian formalisms have been investigated for quantum sensing. Indeed, a general joint (system plus environment) quantum Fisher information upper bound has been formulated [128]. Hence, one would expect that such open quantum system dynamics may also achieve quantum enhanced sensitivity provided that the system goes through a phase transition, which is again accompanied by an eigenvalue gap closing. In the master equation formalism, the phase transition is determined for the steady state of the system at the point that the eigenvalues of the Liouvillian operator shows gap closing [129]. An example of such systems with quantum enhanced sensitivity is boundary time crystals [89]. In the non-Hermitian systems, quantum enhanced sensitivity has been shown to emerge at the exceptional points [62, 70], where two or more eigenvalues and corresponding eigenstates coalesce, as well as in the cases of different types of gap closing in the complex energy plane [58].

In this review, we explore the capacity of many-body systems for serving as quantum sensors in both equilibrium and non-equilibrium regimes. Our paper is complementary to a few previous review papers on different aspects of quantum sensing. In Ref. [130], the theoretical aspects of quantum estimation theory are comprehensively discussed. On the other hand, Ref. [6] mostly focuses on experimental implementation of quantum sensors. More recent reviews have been dedicated for exploring Fisher information and its properties [131, 132]. In addition, recently an essay has also been dedicated to atomic, molecular, and optical platforms for realizing quantum sensors [133]. While quantum many-body sensors have received significant attention in recent years, these aforementioned recent progresses have not been covered in the previous review articles. This makes it timely to provide a review on the progress towards quantum many-body sensors.

II. ELEMENTS OF PARAMETER ESTIMATION

Precise measurements of relevant quantities are essential in science. In physics, high-precision measurements lead us to test the theory of special relativity [134–139], scrutinize the theory of general relativity via gravitational wave detection [134, 140], and validate the Standard Model of physics by confirming the existence of the elusive Higgs particle [141–144]. Thus, pursuing novel schemes and strategies for achieving high-precision measurements are highly desirable for advancing science. However, measuring a relevant quantity is only sometimes a straightforward procedure. Furthermore, quantities such as coupling strengths, temperature, and in general, those lacking corresponding quantum observables, such as entanglement or purity, can only be determined indirectly. Therefore, one requires to infer a relevant quantity of the system by indirect means. The art of

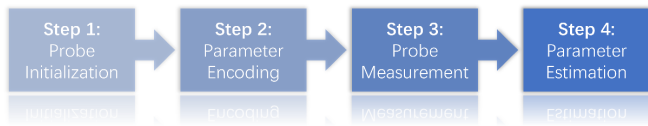


FIG. 2. **Sketch of parameter estimation steps:** Standard scheme for estimating an unknown parameter θ . An initial quantum state ρ dynamically encodes the parameter θ to be estimated as ρ_θ . To extract information about θ , a set of measurements via positive operator-valued measure (POVM) $\{\Pi_x\}$, are performed on the probe with random outcomes x . The resulting measurement outcomes are fed into a classical estimator $\tilde{\Theta}$ to infer the unknown parameter θ .

inferring such a relevant quantity by means of measuring another is known as parameter estimation [130, 145, 146].

The central aim of parameter estimation theory is to infer the unknown parameters of interest as precisely as possible. Any parameter estimation scheme is composed of four basic steps, see Fig. 2:

1. Choosing an adequate probe,
2. Encoding the unknown parameters dynamically into the probe,
3. Extracting information about the parameters of interest by performing measurements onto the probe,
4. Inferring the true (unknown) parameters via a classical estimator.

All the above steps need optimization to successfully estimate the parameters. It is important to note that the actual values of the parameters are always unknown by definition, and one must infer them indirectly. One common methodology to quantify the uncertainty in estimating a single unknown parameter θ is accessing the system of interest through measurements with observable O , which leads to estimating the error of θ using the error propagation formula [145]:

$$\delta\theta = \frac{\Delta O}{|\partial_\theta \langle O \rangle|}, \quad \frac{\partial}{\partial \theta} := \partial_\theta \quad (1)$$

where ΔO and $\langle O \rangle$ are the standard deviation and the expectation value of the outcomes associated with O , respectively. The denominator in Eq. (1) indicates that in order to decrease the error in the estimation of θ (i.e., $\delta\theta \ll 1$), one needs to increase the denominator, i.e., $|\partial_\theta \langle O \rangle| \gg 1$. To achieve this, it is necessary to find a set of outcomes with an expectation value $\langle O \rangle$ that varies significantly with respect to θ . Conversely, a set of outcomes that varies weakly with θ (i.e., flat slope $|\partial_\theta \langle O \rangle| \ll 1$) will result in a substantial error (i.e., $\delta\theta \gg 1$). While Eq. (1) offers a heuristic explanation of a necessary ingredient for estimating a parameter, a more rigorous and operational framework must be provided to determine a formal figure of merit for quantifying estimation performance. In fact, Eq. (1) does not take into account the entire probability distribution of the outcomes and cannot provide the framework to determine a proper figure of merit for quantifying the performance of an estimation strategy.

A. Global and local estimation theory

A suitable strategy to estimate a parameter usually depends on the amount of *a priori* information one has on the parameter itself. If no *a priori* information is available, the estimation strategy, i.e. the choice of the measure to be performed on the probe and the procedure employed to process data, should be *optimal in average* i.e. should be equally good for any value of the parameter. The set of techniques and methods used to choose and optimize the figure of merit in this case is known as *global estimation theory* [147, 148]. Once a global estimation has been performed an experimenter is left with some *a priori* information to be improved, i.e. one should look for figures of merits that select the best estimation strategy for a specific value or range of values of a parameter. This optimization problem is addressed by *local estimation theory* [147, 149, 150] which allows one to achieve the ultimate bound on precision. The quantum version of local quantum estimation theory [130, 151] is the fundamental tool of quantum probing, sensing and metrology and is the main subject of the present review, with the exception of Section XIV, where various aspects of global sensing are discussed.

B. Single-parameter classical estimation bound

Cramér and Rao [27, 28] first introduced such operational and formal framework for quantifying the performance in estimating a parameter, with the variance with respect to such parameter as the natural figure of merit. For the single-parameter case, where θ is the only unknown parameter to be determined, one gets the Cramér-Rao inequality (for *unbiased* estimators) as:

$$\text{Var}[\tilde{\Theta}] \geq \frac{1}{MI(\theta)}, \quad (2)$$

where M is the number of measurements (trials), $\tilde{\Theta} := \tilde{\Theta}(x)$ is known as the *estimator* of θ , with x being a set of measurement outcomes (discrete or continuous). Note that the estimator $\tilde{\Theta}$ is a function that only depends on the measurement outcomes x , and it maps the set of measurement outcomes to a parameter space with an estimated value of θ . The expression $I(\theta)$ is known as Fisher information (FI), denoted as:

$$I(\theta) = \int \frac{1}{p(x|\theta)} (\partial_\theta p(x|\theta))^2 dx, \quad (3)$$

for a continuous set of measurement outcomes, or $I(\theta) = \sum_i p(x_i|\theta)^{-1} (\partial_\theta p(x_i|\theta))^2$ for the discrete case. Here $p(x|\theta)$ is the conditional probability of obtaining outcome x given θ . Equation (2) sets the precision one can achieve with a particular measurement for a single trial. The equality is reached by using an optimal estimator.

The Fisher information $I(\theta)$ quantifies the sensitivity of the conditional probabilities with respect to the

parameter to be estimated. To enhance sensing precision, it is necessary to increase $I(\theta)$ by identifying conditional probability distributions that exhibit more significant changes as the unknown parameter varies. This results in $\partial_\theta p(x|\theta) \gg 1$, leading to $I(\theta) \gg 1$. The question of how to identify such advantageous scenarios is addressed in the following section.

C. Optimizing the classical bound: the QFI

The Fisher information defined in Eq. (3) is known as the classical Fisher information and is unique for a given measurement basis [131, 152]. Probability distributions that significantly vary with respect to the unknown parameter are preferred, as they yield larger values of classical Fisher information and, consequently, better parameter sensitivity. Thus, finding such probability distributions is of paramount importance. Classically, searching for them is an arduous task, as optimization needs to be performed over all possible measurement bases. Nonetheless, this optimization task can be achieved for quantum probes, leading to a tighter bound on the variance of the estimator [130, 151, 153–155]. Consider a quantum probe ρ encoding the unknown parameter θ as ρ_θ and a set of general quantum measurements $\{\Pi_x\}$. Π_x is a positive operator valued measure (POVM) with outcome x , such that $\int_x \Pi_x dx = \mathbb{I}$. The conditional probability of obtaining the outcome x for a given θ obeys the Born rule:

$$p(x|\theta) = \text{Tr}[\Pi_x \rho_\theta]. \quad (4)$$

Assuming regularity conditions, and since the trace and the derivative are linear operators, the derivative of the probability distribution $\partial_\theta p(x|\theta)$ translates into taking the derivative of the quantum state $\partial_\theta \rho_\theta$, specifically $\partial_\theta p(x|\theta) = \text{Tr}[\Pi_x \partial_\theta \rho_\theta]$. Here, the derivative of the quantum state satisfies the Lyapunov equation given by:

$$\partial_\theta \rho_\theta = \frac{1}{2} \{L_\theta, \rho_\theta\}, \quad (5)$$

with $\{*, \Delta\} = * \Delta + \Delta *$ being the anticommutator between operators $*$ and Δ , and L_θ is a self-adjoint operator called *Symmetric Logarithmic Derivative* (SLD). Following Ref. [130], the classical Fisher information $I(\theta)$ can be upper bounded as

$$I(\theta) \leq I_Q(\theta) := \text{Tr}[\rho_\theta L_\theta^2], \quad (6)$$

by incorporating the Schwartz inequality. Here, $I_Q(\theta)$ denotes the quantum Fisher information (QFI), leading to the quantum Cramér-Rao bound [130, 145, 151, 154–157]:

$$\text{Var}[\tilde{\Theta}] \geq \frac{1}{I(\theta)} \geq \frac{1}{I_Q(\theta)}. \quad (7)$$

Note that the derivative of the quantum state satisfies other expressions, e.g., the *Right Logarithmic Derivative*

(RLD) [156]. This gives rise to different quantum lower bounds. Hence, as opposed to the classical Fisher information, the QFI is not unique (see Ref. [131] for a thorough discussion and Ref. [156] for different achievable bounds).

The QFI of Eq. (6) accounts for the ultimate precision limit for the estimation of θ . Note that the QFI, as the maximization of the classical Fisher information over all possible measurements, depends on the quantum statistical model ρ_θ and the SLD L_θ only, and it does not depend explicitly on a particular measurement basis. The optimal POVM can be composed with the set of projectors over the eigenstates of L_θ with an associated optimal quantum estimator [130].

To saturate the quantum Cramér-Rao bound in Eq. (2), one needs both the optimal POVM (as determined by the support of L_θ) and an optimal classical estimator for post-processing data, such as the maximum-likelihood estimator in the limit of large data sets [27, 30, 151, 153, 158–160] (refer to Refs. [161, 162] for Bayesian analysis in the scenario of limited data). The optimal POVM ensures that the classical Fisher information equals the QFI, i.e., $I(\theta) = I_Q(\theta)$. This is crucial as it determines that the single-parameter quantum Cramér-Rao bound can always be achieved, provided that both the estimator and the measurement basis are optimal.

The SLD operator L_θ is an essential ingredient in the quantum parameter estimation framework, which can readily be obtained from the solution of the Lyapunov equation as [130]:

$$L_\theta = 2 \int_0^\infty e^{-t\rho_\theta} \partial_\theta \rho_\theta e^{-t\rho_\theta} dt, \quad (8)$$

being basis independent, and

$$L_\theta = 2 \sum_{n,m} \frac{\langle \phi_m | \partial_\theta \rho_\theta | \phi_n \rangle}{\epsilon_n + \epsilon_m} |\phi_m\rangle \langle \phi_n| \quad (9)$$

which is obtained from Eq. (8) using the spectral decomposition of ρ_θ , that is:

$$\rho_\theta = \sum_i \epsilon_i |\phi_i\rangle \langle \phi_i|, \quad (10)$$

where ϵ_i and $|\phi_i\rangle$ are the i -th eigenvalue and eigenvector of ρ_θ , respectively. From Eq. (9), it is straightforward to obtain the QFI in this basis as follows:

$$I_Q(\theta) = 2 \sum_{n,m} \frac{|\langle \phi_m | \partial_\theta \rho_\theta | \phi_n \rangle|^2}{\epsilon_n + \epsilon_m}, \quad \epsilon_n + \epsilon_m \neq 0. \quad (11)$$

It has been shown that it is also possible to separate the classical from the quantum contributions of the QFI by observing the dependence of the eigenvalues and eigenvectors with respect to the parameter θ . This leads to the following formula for the QFI [130]:

$$I_Q(\lambda) = I_\epsilon(\lambda) + 2 \sum_{n \neq m} \sigma_{nm} |\langle \phi_m | \partial_\lambda \phi_n \rangle|^2, \quad (12)$$

where $I_\epsilon(\lambda)$ is the (classical) Fisher information of the distribution of the eigenvalues of ρ_λ , and σ_{nm} may be written as [130]

$$\sigma_{nm} = \frac{(\epsilon_n - \epsilon_m)^2}{\epsilon_n + \epsilon_m} + \text{any antisymmetric term}. \quad (13)$$

The second term of Eq. (12) shows the detailed contribution arising from the dependence of the eigenstates of the quantum probe with respect to the parameter θ .

The QFI of Eqs. (6)-(11) applies to any quantum state. However, for pure quantum states $\rho_\theta = |\psi_\theta\rangle\langle\psi_\theta|$ such that $\text{Tr}[\rho_\theta^2] = 1$, the QFI adopts a simpler form given by [130, 145, 157]:

$$I_Q(\theta) = 4(\langle \partial_\theta \psi | \partial_\theta \psi \rangle - \langle \partial_\theta \psi | \psi \rangle \langle \psi | \partial_\theta \psi \rangle). \quad (14)$$

Particular instances of relevant quantum states, for example, two-qubit states in Bloch representation, a single-qubit dephasing along the z-axis in a magnetic field along the z-axis, and X-shape two-qubit states, can be found in [157].

Other formulas to evaluate the QFI for specific quantum statistical model have been found, which are useful in several situations of interest, e.g. unitary families [163], Bloch-sphere representation [164, 165], qubit X-states [166], and Gaussian states [167–173].

D. Multi-parameter estimation

Consider the situation where d unknown parameters $\theta = (\theta_1, \theta_2, \dots, \theta_d)$ need to be estimated. In this multi-parameter case, the Cramér-Rao inequality generalizes to (for the sake of simplicity $M = 1$) [130, 145, 157]

$$\text{Cov}[\tilde{\theta}] \geq I(\theta)^{-1}, \quad (15)$$

where $\text{Cov}[\tilde{\theta}]$ is the covariance matrix with elements

$$[\text{Cov}(\tilde{\theta})]_{ij} = \langle \tilde{\theta}_i \tilde{\theta}_j \rangle - \langle \tilde{\theta}_i \rangle \langle \tilde{\theta}_j \rangle, \quad (16)$$

and $I(\theta)$ is the classical Fisher information matrix with elements [157]

$$[I(\theta)]_{ij} = \int p(x|\theta) (\partial_{\theta_i} \ln[p(x|\theta)]) (\partial_{\theta_j} \ln[p(x|\theta)]) dx, \quad (17)$$

where the diagonal elements fulfill $\text{Var}[\tilde{\theta}_i] \geq [I(\theta)^{-1}]_{ii}$.

The matrix inequality in Eq. (15) means that $(\text{Cov}[\tilde{\theta}] - I(\theta)^{-1})$ is a positive semidefinite matrix. While the above is the general case, dealing with this matrix form is challenging. Hence, it is convenient to transform the matrix

inequality of Eq. (15) into a scalar bound by introducing a positive and real weight matrix \mathcal{W} such that [156]:

$$\text{Tr}[\mathcal{W}\text{Cov}[\tilde{\theta}]] \geq \text{Tr}[\mathcal{W}I(\theta)^{-1}]. \quad (18)$$

Similarly to the single-parameter scenario, it is possible to obtain a tighter bound of Eq. (15) leading to the multi-parameter quantum Cramér-Rao bound [130, 157]:

$$\text{Cov}[\tilde{\theta}] \geq I(\theta)^{-1} \geq I_Q(\theta)^{-1}, \quad (19)$$

where the matrix elements of QFI matrix $I_Q(\theta)$ are given by [130, 157]

$$[I_Q(\theta)]_{ij} = \frac{1}{2} \text{Tr}[\rho_\theta \{L_i, L_j\}]. \quad (20)$$

As before, one can convert the matrix inequality in Eq. (19) into a scalar bound using \mathcal{W} as follows:

$$\text{Tr}[\mathcal{W}\text{Cov}[\tilde{\theta}]] \geq \text{Tr}[\mathcal{W}I(\theta)^{-1}] \geq \text{Tr}[\mathcal{W}I_Q(\theta)^{-1}]. \quad (21)$$

As a particular case, one can consider \mathcal{W} to be the identity. This choice prioritizes the precision of θ as the sum of the variances of the unknown parameters

$$\sum_{i=1}^d \text{Var}[\tilde{\theta}_i] \geq \sum_{i=1}^d [I(\theta)^{-1}]_{ii} := \text{Tr}[I(\theta)^{-1}] \geq \text{Tr}[I_Q(\theta)^{-1}]. \quad (22)$$

While the above tighter estimation bound includes the SLDs L_i and L_j , other bounds can also be achieved by defining the *Right Logarithmic Derivative* [154] and the Holevo approach [174, 175]. However, the precision bound using the SLDs already contains the same information found in both the Holevo and the RLDs bounds [156]. For this reason, it is common to use Eq. (19) with their corresponding matrix elements defined in Eq. (20) as the ultimate precision limit for the multi-parameter estimation case.

One of the main differences between the single- and multi-parameter scenarios is that, while the classical Fisher information can be achieved in both scenarios, in principle, the QFI is attainable only in the single-parameter case and not for the jointly multi-parameter estimation [156]. This can be understood because, generally, there is no single symmetric logarithmic derivative L_i that defines an optimal measurement basis suitable for all the unknown parameters. To quantify this notion of incompatibility between parameters [176]—those that cannot be estimated optimally with a single set of measurements—the incompatibility matrix \mathbf{D} has been introduced [156, 177], also known as mean Uhlmann curvature [177], with elements:

$$D_{ij} = -\frac{i}{2} \text{Tr}[\rho_\theta [L_i, L_j]]. \quad (23)$$

The case $D_{ij} = 0$ for all i, j is known as the compatibility condition [176]. Recently, a genuine quantum incompatibility measure with a geometric character has also been

proposed [178], along with a comprehensive study of incompatibility under general p -local measurements [179].

The expressions given by Eqs. (6)-(11) to obtain QFI and SLD for single parameter estimation, and generalizations thereof to the multiparameter case all involve diagonalizing the quantum state ρ explicitly to find out its spectral decomposition. For quantum many-body density matrices whose dimensions increase exponentially with system-size, this generally presents a significant computational challenge. To overcome this, Ref. [180] noted that the Lyapunov equations can be expressed as a set of linear equations in the vectorization picture [181, 182], and thereby provided the following formula for the QFI matrix

$$[I_Q(\boldsymbol{\theta})]_{ij} = 2\text{vec}[\partial_{\theta_i}\rho]^\dagger (\bar{\rho} \otimes I + I \otimes \rho)^{-1} \text{vec}[\partial_{\theta_j}\rho], \quad (24)$$

where $\text{vec}(\cdot)$ denotes the vectorized form of a matrix and † denotes complex conjugation. The corresponding SLDs are given as

$$\text{vec}[L_i] = 2(\bar{\rho} \otimes I + I \otimes \rho)^{-1} \text{vec}[\partial_{\theta_i}\rho] \quad (25)$$

In case the quantum state ρ is not full-rank, the inverse is to be replaced by the Moore-Penrose pseudoinverse. Thus, the problem of fully diagonalizing a large matrix is replaced by matrix inversion. In optical systems, states are often expressed in the coherent state basis, which is a non-orthogonal basis. Accordingly, an extension of Eq. (24) for general non-orthogonal bases was achieved in Ref. [183].

E. Geometry of parameter estimation

Close links between Fisher information quantities and statistical distances have been found [151, 184]. In terms of the classical Fisher information, which quantifies the sensitivity of the probability distributions $p(x|\theta)$ concerning the unknown parameter θ , the notion of distinguishability between different probability distributions among M trials arises naturally (see Bengtsson and Życzkowski [185], and Kok and Lovett [186]). It turns out that distinguishing between two probabilities $p(x|\theta_1)$ and $p(x|\theta_2)$, taking ds (ds being the infinitesimal distance on the probability simplex space) along a line element $d\theta$, results in [185, 186]

$$\left(\frac{ds}{d\theta}\right)^2 = \sum_{\mu} \frac{1}{p^{\mu}} \frac{(dp^{\mu})^2}{d\theta^2} = \sum_{\mu} \frac{1}{p^{\mu}} \left(\frac{\partial p^{\mu}}{\partial \theta}\right)^2 := I(\theta), \quad (26)$$

which is the classical Fisher information of Eq. (3). Further analysis leads to:

$$(\delta\theta)^2 \geq \frac{1}{MI(\theta)}, \quad (27)$$

where $\delta\theta$ is the segment of the path in the probability simplex—rather than the variance of $\hat{\theta}$. Note that

the above has been derived solely from a distance measure (a metric) by distinguishing probability distributions on the simplex space. It has also been shown that for distinguishing two probability distributions, one can use the relative entropy (not a metric) for this purpose, and consequently, a close connection between the classical Fisher information matrix and the relative entropy emerges [145].

In quantum mechanics, on the other hand, the notion of distinguishing between normalized vectors in a complex Hilbert space can be addressed by the fidelity $F(\psi_1, \psi_2) = |\langle\psi_1|\psi_2\rangle|$ (not a metric). Indeed, this defines the Wootters distance [151, 184, 187]

$$ds_{\text{W}}^2 = (\arccos[F(\psi(\theta), \psi(\theta + \delta\theta))])^2, \quad (28)$$

with the Fubini-Study metric given by [188]

$$h_{\text{FS}} = \frac{\langle\partial_{\theta}\psi|\partial_{\theta}\psi\rangle}{\langle\psi|\psi\rangle} - \frac{\langle\partial_{\theta}\psi|\psi\rangle\langle\psi|\partial_{\theta}\psi\rangle}{\langle\psi|\psi\rangle^2}, \quad (29)$$

where $\psi := \psi(\theta)$. By setting $\langle\psi|\psi\rangle = 1$, it corresponds to the QFI for pure states (see Eq. (14)), that is

$$I_Q(\theta) = 4h_{\text{FS}}. \quad (30)$$

Extending the Fubini-Study metric to density matrices, one finds that the Bures metric is proportional to the QFI matrix [188] and is given by

$$I_Q(\boldsymbol{\theta}) = 4h_{\text{Bures}} = 8 \lim_{\delta\theta \rightarrow 0} \frac{1 - F(\rho_{\theta}, \rho_{\theta + \delta\theta})}{(\delta\theta)^2}, \quad (31)$$

where $\delta\theta$ is an infinitesimal increment of θ and the fidelity is the square root of the Uhlmann fidelity [189]

$$F(\rho_1, \rho_2) = \text{Tr}[\sqrt{\sqrt{\rho_1}\rho_2\sqrt{\rho_1}}]. \quad (32)$$

For pure states $\rho_1 = |\psi_1\rangle\langle\psi_1|$ and $\rho_2 = |\psi_2\rangle\langle\psi_2|$ the Uhlmann fidelity reduces to $F(\rho_1, \rho_2) = |\langle\psi_1|\psi_2\rangle|$.

F. Alternatives to QFI for Metrology

Gauging the precision of parameter estimation through the quantum Cramér-Rao bound is undoubtedly the most popular approach in the literature, thanks to its geometrical properties and its utility as a signature of multipartite entanglement. However, the Cramér-Rao bound suffers from two practical difficulties. Firstly, although this bound is asymptotically tight for single parameter estimation, it may perform quite poorly in the non-asymptotic regime and especially if the likelihood function is highly non-Gaussian. This is a known issue even in classical parameter estimation theory, and several alternate bounds have been proposed in statistical literature [190]. Perhaps the most well-known is the Ziv-Zakai bound [191], which is obtained by turning the continuous parameter estimation problem to a hypothesis

testing problem for each coarse-grained interval in the domain of the parameter. By noting that hypothesis-testing at each interval amounts to a quantum state discrimination problem, Tsang in Ref. [192] constructed a quantum version of the Ziv-Zakai bound. Although such bounds are not generally tight, they can be shown to perform significantly better for finite set of observations in highly non-Gaussian environments [193]. Extensions of the quantum Ziv-Zakai bound to multiparameter estimation [194] and noisy environments [195] have also been investigated. Lu and Tsang also considered the quantum generalization of the classical Weiss-Weinstein bounds [196]. In yet another direction, Liu and Yuan [197] obtained a tighter version of the Bayesian quantum Cramér-Rao bound valid for both biased and unbiased estimators. For a function $f(\theta)$ of the quantum parameter θ which is estimated via a (generally) biased estimator of bias $b(\theta)$ with a prior probability distribution $p(\theta)$ on a quantum state $\rho(\theta)$, Liu and Yuan's bound reads

$$\text{Var}[f(\theta)] \geq \int p(\theta) \left[\frac{[f'(\theta) + b'(\theta)]^2}{I(\theta)} + b^2(\theta) \right] d\theta, \quad (33)$$

where $I(\theta)$ is the QFI for $\rho(\theta)$ with respect to the parameter θ . One can note that this bound reduces to the biased version of the Bayesian Quantum Cramér-Rao bound bound for a uniform prior. Secondly, and of significant relevance to many-body sensing, the QFI is not fully expressible in terms of experimentally easily accessible one and two-point correlation functions [198]. This was addressed recently in Ref. [199], where an alternative functional dependent only on one and two-point correlators was proposed.

III. INTERFEROMETRIC QUANTUM SENSING

The first notion of quantum sensing has been formulated in a seminal paper by Giovannetti, Lloyd and Maccone [24]. In this case, the goal is to estimate the phase θ which is imprinted in quantum states through a unitary operation of the form $U(\theta) = e^{iH\theta}$, where H is a Hermitian operator with real eigenvalues E_k and their corresponding eigenvectors $|E_k\rangle$, such that $H|E_k\rangle = E_k|E_k\rangle$. This implies that the eigenvalues of the unitary operator $U(\theta)$ are given by $u_k = e^{iE_k\theta}$ while the eigenvectors do not depend on θ and remain the same as H , namely $U(\theta)|E_k\rangle = u_k|E_k\rangle$. The unknown parameter θ can be encoded in a quantum state through $|\Psi(\theta)\rangle = U(\theta)|\Psi_0\rangle$ for a given initial state $|\Psi_0\rangle$. In this case, one can easily show that the QFI of $|\Psi(\theta)\rangle$ is directly proportional to the variance of H

$$I_Q(\theta) = 4 (\langle \Psi(\theta) | H^2 | \Psi(\theta) \rangle - \langle \Psi(\theta) | H | \Psi(\theta) \rangle^2). \quad (34)$$

One can maximize the above QFI with respect to the initial state. In fact, the maximum of I_Q is achieved for the

initial state $|\Psi_0\rangle = (|E_{\min}\rangle + |E_{\max}\rangle)/\sqrt{2}$, where $|E_{\min}\rangle$ ($|E_{\max}\rangle$) is the eigenvector of H with the corresponding smallest (largest) eigenvalue E_{\min} (E_{\max}). Thus, the corresponding QFI becomes

$$I_Q = (E_{\max} - E_{\min})^2. \quad (35)$$

To analyse the scaling of I_Q , in Eq. (35), with respect to the system size one has to consider the details of the interaction in the Hamiltonian H . For a given interaction of $H = \sum_{\{j_1, \dots, j_k\}} h_{j_1 \dots j_k}^{(k)}$ where $h_{j_1 \dots j_k}^{(k)}$ represents a k -body interaction between particles at sites j_1 to j_k , the QFI, at best, scales as $I_Q \sim N^{2k}$ [200], which is known as the Heisenberg limit. This shows enhanced precision in comparison with classical scenarios in which Fisher information, at best, scales linearly with N . The source of this enhancement is the special form of the superposition between the two energy eigenstates with extreme eigenvalues. As a special case, it is worth considering a probe of N qubits which interact with a global magnetic field in the z direction. In other words, $H = \sum_{j=1}^N \sigma_j^z$, with σ_j^z being the z -Pauli operator which acts on qubit j . In this case, $|E_{\min}\rangle = |1, 1, \dots, 1\rangle$ and $|E_{\max}\rangle = |0, 0, \dots, 0\rangle$ and thus the optimal initial state will be the GHZ state $|\Psi_0\rangle = (|0, 0, \dots, 0\rangle + |1, 1, \dots, 1\rangle)/\sqrt{2}$ and, consequently, the QFI becomes $I_Q = N^2$.

The interferometric quantum phase sensing has been implemented experimentally [29–31, 201–203]. However, the scalability of this scenario might be challenging as: (i) initialization to a superposition between the two extreme eigenstates, namely $|E_{\min}\rangle + |E_{\max}\rangle$, is experimentally challenging; (ii) such superposition is highly susceptible to decoherence which transforms the superposition into a classical mixture with no quantum advantage for sensing; and (iii) it is only limited to a special class of unitary operations $U(\theta) = e^{iH\theta}$.

IV. EQUILIBRIUM QUANTUM SENSING: SECOND ORDER QUANTUM PHASE TRANSITION

It is interesting to consider a more general unitary operation $\tilde{U}(\theta) = e^{i(\theta H + \tilde{H})}$ for encoding the parameter θ , as $|\tilde{\Psi}(\theta)\rangle = \tilde{U}(\theta)|\Psi_0\rangle$. For such an unitary operation, the sensing performance is again quantified by QFI of the parameter θ denoted as $\tilde{I}_Q(\theta)$. Note that as far as $[H, \tilde{H}] \neq 0$, both the eigenvectors and eigenvalues of $\tilde{U}(\theta)$ depend on θ . In Ref. [35] it has been shown that for all choices of initial states $|\Psi_0\rangle$ and perturbing interactions \tilde{H} we always have $I_Q(\theta) \geq \tilde{I}_Q(\theta)$. This means that in the interferometric phase sensing scenario, the presence of perturbing interaction \tilde{H} is always destructive. For the case of sensing an external field, \tilde{H} can represent interaction among the particles of the probe. In such cases, the interaction between the constituents of the probe can reduce the performance of the system [35, 46, 200, 204].

An alternative method to interferometric sensing is to harness the interaction between the particles in strongly correlated many-body systems. The interplay between different parts of the Hamiltonian can induce phase transition in the system, also known as quantum criticality. Many-body systems exhibiting quantum criticality have been identified as resources for quantum enhanced sensitivity. In this section, we review various forms of quantum criticality for sensing and show that a common feature among all these systems is the emergence of a sort of “gap-closing” in their energy spectrum. This is an important observation as it clearly shows that any phase transition which is accompanied by gap-closing is a potential resource for quantum sensing.

As we have discussed in the previous section, despite the theoretical appeal, interferometry-based quantum sensing may face practical limitations. An alternative approach for achieving quantum-enhanced sensitivity is to exploit quantum criticality. The most conventional manifestation of quantum criticality is the second-order phase transition which describes a large set of phenomena. Second-order quantum phase transition occurs at zero temperature, where quantum fluctuations lead to spontaneous symmetry-breaking at the critical point. Interestingly, this opens up the possibility of quantum enhanced sensing near criticality [36]. Consider a many-body probe which is described by the Hamiltonian

$$H = \theta H_1 + H_2, \quad (36)$$

with H_1 representing the action of the target parameter θ on the probe, and H_2 representing the internal physics of the probe itself. The interplay between H_1 and H_2 often leads to rich phase diagrams with the strength of the parameter θ determining the relevant phase. When unhindered by thermal fluctuations, a second order quantum phase transition may occur at a specific value of $\theta = \theta_c$, where the ground state of the system undergoes a global transformation. There are several common features in second-order quantum phase transitions: (i) spontaneous symmetry breaking; (ii) the emergence of a scale invariance behavior for all observables in the system; (iii) the appearance of a diverging length scale ξ which behaves as $\xi \sim |\theta - \theta_c|^{-\nu}$, where ν is a critical exponent; and (iv) an anti-crossing between the ground and the first excited state whose energy gap vanishes at the transition point as the system sizes reaches thermodynamic limit. As we will discuss, a significant enhancement in sensitivity is often associated with the critical points in the phase diagram.

At this point, a distinction should be made between two different approaches to many-body critical quantum sensing. In the first approach, the ground state of a many-body system, potentially at criticality, is used as the *input* state for an interferometry-based quantum sensing. The critical ground state is a delicate superposition of several states which can reveal significant variance with respect to certain observables and thus maximizes the QFI in an interferometry-based sensing, as given in Eq.(34). For instance, in Ref. [205] many-body

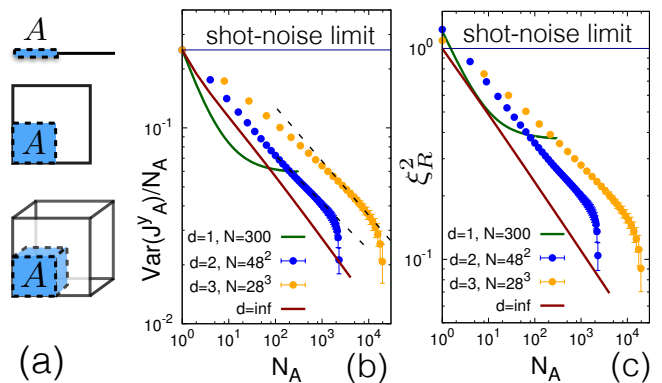


FIG. 3. **Sub-shot-noise scaling with critical quantum transverse field Ising chain probes for various dimensions.** In (b) and (c) x -axis is N_A , the number of spins inside any subsystem A as depicted in (a); y -axis is (b) variance of the estimator of y -component of collective spin operator $J = \sum_i S_i$ normalized by N_A , and (c) collective spin squeezing parameter ξ_R^2 . Figure taken from Ref. [207].

spin squeezed states are used as inputs to interferometric phase estimation protocols. Atom-interferometry based quantum metrology has grown substantially in recent years, and their detailed description lies outside the scope of the present review. We direct the interested reader to Ref. [206] for a comprehensive review. However, even for interferometric phase sensors with equilibrium probe states of genuinely many-body quantum systems, Frerot and Roscilde [207] showed the possibility of quantum criticality enhanced sensing. They considered the problem of estimating a phase angle ϕ for the collective spin operator $J = \sum_i S_i$, such that the unitary $U = \exp(i\phi J)$ represents the action of the interferometer. By considering the ground state of a transverse field Ising chain as the input of an interferometer, they showed that at the critical point, the scaling of precision of estimation of ϕ for a N -atom transverse field Ising chain in d -dimensions is given by

$$\delta\phi^2 \geq N^{-1-\frac{\eta-1}{d_m}}, \quad (37)$$

where η is the scaling exponent of the long-range correlation function of the order parameter, as defined by $\langle \sigma_i^x \sigma_{i+r}^x \rangle \propto r^{2-d-\eta}$, at critical point for a d -dimensional model, and $d_m = \min(d, d_c)$, with upper critical dimension $d_c = 3$ for the transverse field Ising chain. The results, plotted in Fig. 3, attest that sub-shot-noise scaling is indeed achievable with such probes.

The second approach, which is the main topic of this section, is that of Hamiltonian parameter estimation, where the many-body ground state is directly measured to gain access to the physical parameter in question. In the thermodynamic limit, where the system size $N \rightarrow \infty$, the QFI diverges [41, 208–212]

$$I_Q(\theta) \sim |\theta - \theta_c|^{-\alpha}, \quad (38)$$

where $\alpha > 0$ is the corresponding critical exponent. In

finite-size systems, at the transition point $\theta=\theta_c$ the QFI shows algebraic dependence on the system size

$$I_Q(\theta=\theta_c) \sim N^\beta. \quad (39)$$

The two expected asymptotic behaviors in Eqs. (38) and (39) can be merged in a single ansatz

$$I_Q(\theta) \sim \frac{1}{N^{-\beta} + A|\theta - \theta_c|^\alpha}, \quad (40)$$

with A being a constant. Note that in the thermodynamic limit (i.e. $N \rightarrow \infty$) one retrieves Eq. (38) and for finite system sizes at $\theta=\theta_c$ one recovers Eq. (39). The emergence of scale invariance behavior at the second-order quantum phase transition implies that the QFI follows a conventional finite size scaling ansatz [213]

$$I_Q(h) = N^{\alpha/\nu} g\left(N^{1/\nu}(\theta - \theta_c)\right), \quad (41)$$

where $g(\cdot)$ is an arbitrary function. This ansatz is routinely used for determining critical exponents α and ν using finite size systems. Plotting the rescaled QFI, namely $N^{-\alpha/\nu} I_Q(h)$, versus $N^{1/\nu}(h - h_c)$ collapses all the curves for different system sizes for the right choice of critical parameters, namely (θ_c, α, ν) . Since the two ansatzes in Eq. (40) and Eq. (41) describe the same quantity, they are not independent. In fact, by factorizing N^β form Eq. (40), one can show that the identity of both ansatzes imposes the following identity between the critical exponents

$$\beta = \frac{\alpha}{\nu}. \quad (42)$$

This shows that the three critical exponents are not independent from each other and knowing two of them is enough for determining the other. While the identity in Eq. (42) is valid for one-dimensional systems, its generalization to d dimensional probes is obtained as $\beta = \frac{\alpha}{d\nu}$ [47, 209, 210]. This is a remarkable discovery which shows that unlike the interferometry-based sensing scenarios, e.g. using GHZ states, the precision of criticality-based quantum sensing is not bounded by the Heisenberg scaling. In fact, super-Heisenberg scaling with $\beta > 2$ can be achieved if $\alpha > 2d\nu$. It is worth mentioning that for all realization of the second-order phase transition in the ground state, one can show that $\alpha=2$ [209, 210]. However, some non-ground state continuous phase transitions behave like the second-order phase transition with α different from 2 [74]. Therefore, for keeping generality of the paper, we keep α as a general parameter in our notations.

A. Free fermionic many-body probes

The above discussion on second-order quantum phase transitions is very general. It will be more insightful to go

through some examples and explicitly determine the scaling of QFI, namely $I_Q \sim N^\beta$, at the vicinity of the critical point. Free fermionic systems are an important class of many-body systems in condensed matter physics. In particular, they are analytically solvable which makes them an excellent toy model for understanding several complex phenomena, such as criticality. In addition, many spin chain systems can also be mapped to free fermion systems through Jordan-Wigner transformation and thus become solvable [99]. A general free fermion model with N particles can be described by Hamiltonian $\hat{H}(\theta)$ which in the Nambu formalism notation is written as [214]

$$\hat{H}(\theta) = \Psi^\dagger \tilde{H}(\theta) \Psi, \quad (43)$$

where $\Psi^\dagger = (\hat{c}_1^\dagger \hat{c}_1^\dagger \dots \hat{c}_N^\dagger \hat{c}_1 \hat{c}_2 \dots \hat{c}_N)$ is a $2N \times 1$ vector with $\hat{c}_i (\hat{c}_i^\dagger)$ being bare-particle annihilation (creation) operators and $\tilde{H}(\theta)$ being the $2N \times 2N$ Hermitian matrix containing information about θ . The collection of normalized eigenvectors $\{|E_k\rangle\}$ of \tilde{H} are expressible in terms of $N \times N$ -matrices U and V as

$$\{|E_k\rangle\} = \begin{pmatrix} U & \bar{V} \\ V & \bar{U} \end{pmatrix}, \quad (44)$$

with $\bar{\cdot}$ denoting complex conjugation and each column representing one eigenvector. The QFI for the ground state with respect to parameter θ can then be expressed as [215]

$$I_Q = \text{Tr} \left[(U^\dagger \frac{\partial U}{\partial \theta})^2 - \frac{\partial^2 U}{\partial \theta^2} \right] + \text{Tr} \left[(V^\dagger \frac{\partial V}{\partial \theta})^2 - \frac{\partial^2 V}{\partial \theta^2} \right] + 2\text{Tr} \left[U^\dagger \frac{\partial U}{\partial \theta} V^\dagger \frac{\partial V}{\partial \theta} \right] \quad (45)$$

This closed form of QFI can be used to study the scaling of QFI in free fermion systems. Another useful perspective for calculation of QFI for systems governed by generic quadratic fermionic Hamiltonians was provided by Carollo *et al* [216], where the SLD of fermionic Gaussian states associated with such quadratic Hamiltonians was considered. In this case, instead of the Dirac-representation of fermions $\{c_i, c_j^\dagger\} = \delta_{ij}$, $\{c_i, c_j\} = 0$, it is more convenient to work with the Hermitian Majorana representation given by fermion operators ω such that $\omega_{2j-1} = c_j + c_j^\dagger$, $\omega_{2j} = i(c_j - c_j^\dagger)$. Fermionic Gaussian states with n -fermionic modes and parametrized by the sensing parameter θ , can then be defined as states of the form $\rho(\theta) = \exp(-\frac{i}{4}\omega^T \Omega(\theta)\omega) / \text{Tr} [\exp(-\frac{i}{4}\omega^T \Omega(\theta)\omega)]$, where $\Omega(\theta)$ is a $2n \times 2n$ real anti-symmetric matrix and $\omega = (\omega_1, \omega_2, \dots, \omega_{2n})$ are the $2n$ Majorana fermions. Owing to the above Gaussian structure, such states can be completely described in terms of the second moment, i.e., the two-point correlation matrix $\Gamma_{jk}(\theta) = \frac{1}{2} \text{Tr}[\rho(\theta)(\omega_j \omega_k - \omega_k \omega_j)] = \tanh(i\Omega_{jk}(\theta)/2)$. Following the established mathematical approach for photonic Gaussian states [217], Carollo *et al* used the ansatz that the SLD in this case is also given by the quadratic form

$$L(\theta) = \frac{1}{2} \omega^T K(\theta) \omega + \xi^T(\theta) \omega + \eta(\theta), \quad (46)$$

with $\xi = 0$, and $\eta = \frac{1}{2}\text{Tr}[K(\theta)\Gamma(\theta)]$. The $2n \times 2n$ matrix K was ultimately shown to have been given in terms of the correlation matrix $\Gamma(\theta)$ and its eigenvalues $\{\gamma_k(\theta)\}$ with corresponding eigenvectors $|k(\theta)\rangle$ as

$$\langle j(\theta)|K(\theta)|k(\theta)\rangle = \frac{\left(\frac{\partial\Gamma}{\partial\theta}\right)_{jk}}{\gamma_j(\theta)\gamma_k(\theta) - 1}. \quad (47)$$

Recalling that QFI is just the expectation value of the square of the SLD operator and armed with the ease of calculating such moments for Gaussian systems, it is easy to calculate the QFI from this expression. Although strictly speaking this form of QFI technically only holds for full-rank states, one can nonetheless add an arbitrarily small white noise to the system to regularize the QFI.

B. Bosonic many-body probes

Apart from Fermionic systems, there are also Bosonic many-body quantum systems, e.g., interacting Bosonic atoms in a lattice, which are canonically described by the Bose-Hubbard Hamiltonian as

$$H = -t \sum_i \left(b_i^\dagger b_{i+1} + b_{i+1}^\dagger b_i \right) - \mu \sum_i n_i + U \sum_i n_i (n_i - 1) \quad (48)$$

where $b_i(b_i^\dagger)$ -s are the *Bosonic* annihilation (creation) operators and $n_i = b_i^\dagger b_i$ is the number operator at site- i . The Bose-Hubbard can be implemented by placing cold atoms in Harmonic oscillator traps [218–220]. At $T = 0$, the phase diagram consists of a Mott insulating phase ($t \ll U$) and a Superfluid phase ($t \gg U$). The quantum phase transition between these phases from the Mott insulator phase to the Superfluid phase involves the spontaneous breaking of the $U(1)$ symmetry of the Bose-Hubbard Hamiltonian. Quantum sensing in these atomic systems combines the theoretical formalism of photon-interferometry based metrology with reasonable ease of producing quantum states and robustness against particle loss. Considering a single-mode description of the resulting interacting BEC, where atom-atom interactions are described by a non-linear correction to the Harmonic trap potential, Gross *et al* obtained the first experimental demonstration of quantum-enhanced metrology in cold Bosonic atoms. Dunningham *et al* proposed the use of number-correlated squeezed BEC states [221], which are more robust to particle loss than NOON states. Another scheme by Dunningham and Burnett suggested that one can recreate the action of a (multiport) beam-splitter in an interferometer by simply tweaking the potential barrier between sites, thus enabling quantum-enhanced sensitivity [222, 223]. Heisenberg-limited quantum analogs of inertial guidance systems, also known as *atomic gyroscopes*, have been proposed in optical ring lattices [224]. While strictly not many-body systems, criticalities associated with superradiant phase transitions engineered in

optical cavities with Rabi or Jaynes-Cummings type interactions have also received renewed attention for the possibility of quantum-enhanced sensing [225]. Moreover, effect of engineering anisotropies between coupling strengths of rotating wave and counter-rotating atom-cavity interactions of such models have also been studied in detail [226, 227].

C. Spin chain probes with criticality-enhanced sensitivity

Spin chains are among the key models in many-body physics. They can be exploited as quantum probes in both static and dynamic scenarios. In this section, using explicit examples of critical spin chains, we study criticality in these models as a resource for quantum sensing. The most conventional type of criticality in spin chains is the second-order phase transition which has been described above in a general way. Some of these systems indeed support a second-order quantum phase transition, however this is not the only manifestation of criticality in spin systems. Consider a simple one-dimensional quantum Ising model in a transverse magnetic field h with the following Hamiltonian

$$H = h \underbrace{\sum_{i=1}^N \sigma_i^z}_{H_1} + J \underbrace{\sum_{i=1}^{N-1} \sigma_i^x \sigma_{i+1}^x}_{H_2}. \quad (49)$$

By factoring J and defining $\theta = h/J$, the Hamiltonian takes the general form of Eq. (36). One can analytically solve the transverse Ising model Eq. (49) through Jordan-Wigner transformation [228] which connects spin operators to fermionic ones as $c_i = \prod_{j=1}^{i-1} (-\sigma_j^z) \sigma_i^-$ (and equivalently $c_i^\dagger = \prod_{j=1}^{i-1} (-\sigma_j^z) \sigma_i^+$), where $\sigma^\pm = (\sigma^x \pm i\sigma^y)/2$. The corresponding QFI for the dimensionless parameter θ has been analytically calculated for the ground state [42, 43] and has been shown to scale quadratically with system size, namely $I_Q \sim N^2$ near the critical point $h/J \rightarrow \pm 1$. Recently, a modular approach effectively augmenting these systems with periodic coupling defects [215] has been proposed, which exploits the fact that multiple criticalities can be created in such a construction, all of which inherit the critical scaling behavior of the original chain. Alternatively, even for uniform chains, extending the ensemble measurement setup to real-time feedback control, i.e., adaptive strategies, allows one to overcome shot-noise scaling across the phase diagram [229].

Other quantum spin models have also been extensively studied in the literature for determination of quantum-enhanced scaling. In addition to their relevance for quantum sensing, such QFI-based analysis often reveals the nature of multipartite entanglement in many-body quantum systems. These include the 1D quantum XY models [46, 230, 231] with Dzyaloshinsky-Moriya interactions [232–234], XXZ models [163] which show Kosterlitz-

Thouless phase transition [235], and Heisenberg-type rotationally symmetric models [236, 237]. See Ref. [44] for more references and earlier reviews. In addition to spinless fermion models, metrological advantage was also investigated for short-range spinful Fermi gases and QFI was shown to be an order parameter in such systems [238]. Effect of lattice imperfections and disorder was considered in Ref. [48], whereby QFI analysis reveals that the two paradigmatic quantum disordered 1D lattices, namely Anderson [239] and Aubry-Andre models [240] belong to different universality classes. Experimental demonstration of quantum-enhanced critical sensing has also been recently performed [50] with a small NMR system. Extensions to multiparameter estimation by calculating the QFI matrix have also been considered [241, 242] along with experimental demonstration for NMR systems [243]. Departure from $T = 0$, i.e., ground state assumption has been considered in several directions. One is to consider metrology in finite-temperatures. Similar to other markers of quantumness, presence of a quantum critical region fanning out from the critical point at $T = 0$ has been detected with QFI [198]. Another popular direction of departure, namely, considering driven quantum many-body sensors instead of probes at equilibrium has been discussed in a later section of this review.

D. Quantum many-body probes with long-range interactions

Since local interactions are useful in quantum enhanced sensing, it is natural to ask whether criticality in models with longer-range interactions are also beneficial for metrology tasks. Unfortunately, exact results are rare for such systems and approximate methods, such as Density Matrix Renormalization Group (DMRG), are often unsatisfactory for generic Hamiltonians with long-range interactions because of an area law violation. However, QFI has indeed been studied in many systems showing interesting physics. Perhaps the most studied model is the Lipshin-Meshkov-Glick (LMG) Hamiltonian for N sites in 1D, which generalizes the anisotropic XY Hamiltonian by dropping the nearest-neighbour assumption. The Hamiltonian can be written as

$$H_P = \frac{J}{N} \sum_{i,j,i < j} (\sigma_i^x \sigma_j^x + \gamma \sigma_i^y \sigma_j^y) + h \sum_i \sigma_i^z, \quad (50)$$

where γ is the anisotropy parameter, J is exchange coupling, and h is the magnetic field. This model has been solved through Bethe ansatz [244, 245], or alternatively by a Holstein-Primakoff transformation [246, 247]. Considering J as the unit of interaction, this model has three estimable parameters, the magnetic field strength h , anisotropy γ , and the temperature T when system is in thermal equilibrium. At zero temperature, this system shows quantum criticality at $h=h_c=J$. In Ref. [248],

it has been shown that the QFI with respect to h diverges at criticality as $I_Q \sim (h - h_c)^{-2}$ (namely $\alpha=2$) in the symmetric phase ($h/J \geq 1$) and $I_Q \sim (h_c - h)^{-1/2}$ (namely $\alpha=1/2$) in the broken phase ($0 \leq h/J \leq 1$). Remarkably, these exponents for QFI do not depend on the anisotropy γ . While at the critical point h_c , one obtains $I_Q(h_c) \sim N^{4/3}$, indicating quantum-enhanced sensitivity, two-site reduced density matrices results in $I_Q(h_c) \sim N^{2/3}$ [249]. In [250], the authors considered the estimation of γ and T . In the thermodynamic limit near criticality, the leading contribution to QFI for both scales as $I_Q(h_c) \sim T^2$ at both phases, making this system attractive for thermometry. However, QFI for estimating anisotropy γ in the thermodynamic limit shows a divergence at $\gamma = 1$ and scales differently in the ordered phase ($h > 1$) compared to the symmetry-broken phase ($0 \leq h < 1$) following the formula

$$I_Q(\gamma) \sim \begin{cases} \frac{9}{4(h-1)^2} + \frac{25\beta^2}{12} + O(h) & h > 1 \\ \frac{9}{4(\gamma-1)^2} - \frac{25\beta^2(h-1)}{6(\gamma-1)} + O(h) & 0 \leq h < 1. \end{cases} \quad (51)$$

Garbe *et al* [251] have recently considered the influence of various driving protocols on QFI-based sensing in LMG and other fully connected systems. In LMG and other fully connected models, all interactions are equally strong, in contrast to models where all interactions except the nearest or next nearest are ignored. Thus, one may wonder what happens for models where long-range interactions are present, but the interaction strength is not distance agnostic, e.g., it decays following a power law [252]. Such models become extremely relevant for ion-trap based platforms, where the decay exponent can be fixed by tuning the lasers [253]. In Ref. [254], the authors considered a long-range Kitaev chain, which is an extension of the N -site tight-binding model, and whose Hamiltonian is given by

$$H_\theta = -\frac{J}{2} \sum_{j=1}^N (c_j^\dagger c_{j+1} + c_{j+1}^\dagger c_j) - \mu \sum_{j=1}^N (c_j^\dagger c_j - \frac{1}{2}) + \frac{\Delta}{2} \sum_{j=1}^{N-1} \sum_{l=1}^{N-j} \kappa_{\eta,l} (c_j c_{j+l} + c_{j+l}^\dagger c_j^\dagger), \quad (52)$$

where $\kappa_{\eta,l}$ is the coefficient for interaction between two sites l distance apart, J is the nearest neighbour coupling and μ is the chemical potential. The power-law decay is a specific case when $\kappa_{\eta,l} \propto 1/l^\eta$. The exponent η controls the range of interaction. For example, $\eta=0$ represents a fully connected graph in which all pairs interact equally while $\eta \rightarrow \infty$ represents nearest neighbor interaction. The following expression for QFI for estimating the parameter Δ was obtained in [254]

$$I_Q(\Delta) \sim \begin{cases} N^2 (\ln N)^{2(1-\eta)} & \eta \in [0, 1) \\ N^2 (\ln \ln N)^2 & \eta = 1 \\ N^2 & \eta > 1 \end{cases}. \quad (53)$$

Clearly, QFI scales in a super-Heisenberg manner if the long distance couplings decay slower than Coulombic, i.e. $\eta \leq 1$.

V. EQUILIBRIUM QUANTUM SENSING: LOCALIZATION TRANSITION

So far, second-order quantum phase transition in the ground state of many-body systems, manifested in different setups, has been investigated as a resource of enhanced precision sensing. In contrast, localization transitions, exemplified through Anderson and many-body localizations, affect the entire spectrum of the system and thus their impact is more drastic. Originally disorder is used for suppressing the effect of particle tunneling and thus inducing localization in which particles' wave functions extends only locally across a few sites. Localization takes place in both non-interacting (Anderson localization) and interacting (many-body localization) systems. The localization transition is energy dependent such that each eigenstate localizes at a different value of disorder [255–257]. Localization transition can also be induced by Floquet dynamics [258] pseudo-random potentials [259, 260] or Stark fields [97, 261]. In this section, we investigate the application of both single- and multi-particle systems under the effect of such localization effects for quantum sensing.

A. Pseudo-random localization transition

A paradigmatic model which exhibits localization-delocalization transitions has been studied for quantum sensing purpose [113]. It is represented by one-dimensional fermionic lattice in presence of a quasi-periodically modulated onsite potential, i.e., the potential varies from site-to-site. The Hamiltonian of the system is written as

$$\hat{H} = -t \sum_i (\hat{c}_i^\dagger \hat{c}_{i+1} + h.c.) + V \sum_i \cos(2\pi i \omega) \hat{c}_i^\dagger \hat{c}_i + U \sum_i \hat{n}_i \hat{n}_{i+1}, \quad (54)$$

where t is tunneling, ω is an irrational number, U is interaction strength, and V is the unknown parameter which we wish to estimate. In addition, the operator $\hat{c}_i^\dagger (\hat{c}_i)$ is fermionic creation (annihilation) operator at site i and $\hat{n}_i = \hat{c}_i^\dagger \hat{c}_i$ accounts for particle number. The non-interacting case, i.e. $U = 0$, is known as the Aubry-André-Harper (AAH) model [262]. In the AAH model

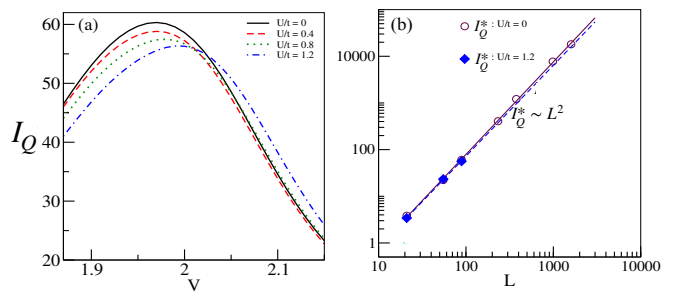


FIG. 4. **Quasi-random disordered probe.** (a) QFI as a function of V for different interaction strengths U (see Eq. 54) for particular case at half-filling ($L = 89$ and $n_f = 45$). The plot shows I_Q as a function of V for varied interaction strengths (up to the interaction strength comparable to the kinetic energy). (b) The maximum QFI, I_Q^* , as a function of L for $U=0$. The number of fermions n_f for $L = 21, 55, 89, 233, 377, 987$, and 1597 are $11, 28, 45, 116, 189, 494$, and 798 , respectively. The I_Q^* nearly saturates the Heisenberg limit, i.e., $I_Q^* \sim L^2$ for both, the bare system and a system with moderate interaction ($U=1.2$). Figure is adopted from [113].

with a single particle, there is an energy independent localization transition at a finite modulation strength, $V_c = 2$. For a given V , all the states are either localized (for $V > V_c$) or extended (for $V < V_c$) [263]. For finite size systems, proper scaling emerges at the transition for system sizes F_n with either odd or even sequences from the Fibonacci series and for ω to be approximated by $\omega_n = F_n / F_{n+1}$. Here F_n and F_{n+1} are two consecutive Fibonacci numbers with the property $\omega = \lim_{n \rightarrow \infty} (F_n / F_{n+1}) \rightarrow (\sqrt{5} - 1)/2$, which is the so-called golden ratio.

In addition to the single-particle case, one may consider the half-filled case in the presence of interaction U . The localization transition persists in the ground state in the presence of interaction [264, 265]. Moreover, further theoretical works have argued in favour of many-body localization (MBL) [266–268], albeit with different universality properties than the uncorrelated disordered systems.

Interestingly, the AAH model can be of potential use for quantum sensing of the strength of the quasi-modulated potential, V [113]. Figure 4 presents I_Q as a function of V for different interaction strength U and fixed L . Two observations are noted: First, the peak tends to shift towards a higher V^* (V^* is the value of V where I_Q is maximum in finite system of size L) with increasing U . This is expected as many-body localization transition is supposed to occur at $V_c > 2$ in the presence of interaction; and second, the value of I_Q tends to slightly decrease at V^* with increasing U . The scaling of the peak of the QFI which occurs at $V = V^*$, namely $I_Q^* = I_Q(V^*)$ is presented in Fig. 2(b) which reveals scaling of the form $I_Q^*(U=0) = L^{1.98(2)}$ in the non-interacting limit. Despite the lack of enough data points, it is evident that the effects of interaction on the scaling exponent re-

main pretty small in the range of weak to intermediate range.

B. Stark localization

Stark localization caused by an applied gradient field across a lattice has been exploited for ultra-precise sensing [74–76, 269]. The extended-localized transition in the limit of large one-dimensional systems takes place at an infinitesimal gradient field. This allows for sensing weak fields with great precision. This section is devoted to Stark probes and their capability to serve as a weak-gradient field sensor.

For one particle that tunnels to its neighbors in a one-dimensional lattice affected by a linear gradient field with strength h , the Hamiltonian is given by

$$H = J \sum_{i=1}^{L-1} (|i\rangle\langle i+1| + |i+1\rangle\langle i|) + h \sum_{i=1}^L i|i\rangle\langle i|, \quad (55)$$

where J is the tunneling rate. In this setup, the gradient-field strength h is the unknown parameter and aimed to be estimated. It is well known that in the thermodynamic limit (i.e. $L \rightarrow \infty$), all energy levels of the Hamiltonian Eq.(55) go through a phase transition from an extended to a localized phase at $h_c=0$ [96, 97, 270–272]. Focusing on the ground state, Fig. 5 (a) presents QFI as a function of h for different sizes of the probe. The initial plateaus represent the extended phase in which the QFI takes its maximum for $h \leq h_{\max}$. Clearly, h_{\max} skews to zero and tends to the critical point $h_c=0$, by increasing the length of the probe. The maximum values of the QFI, denoted by $I_Q(h_{\max})$ increase dramatically by enlarging the probe, evidencing divergence of the QFI in the thermodynamic limit. In the localized phase, namely $h > h_{\max}$, the QFI is size-independent and decays algebraically according to $I_Q \propto |h - h_{\max}|^{-\alpha}$ with $\alpha=2$ for the ground state. The scaling of the QFI with the system size at the critical point has been plotted in Fig. 5 (b). The QFI shows strong super-Heisenberg scaling, i.e. $I_Q(h_{\max}) \propto L^\beta$ with $\beta \simeq 6$. The inset of Fig. 5 (b) shows how β changes by getting distance from the critical point, i.e. h_{\max} . As the Stark localization transition happens in the entire energy spectrum of Eq. (55), one can inquire about higher energy eigenstates' scaling. Interestingly, one can obtain the super-Heisenberg scaling with $\beta \simeq 4$ for all excited eigenstates. Following section IV, establishing finite-size scaling analysis results in critical exponents $(\alpha, \nu) = (2.00, 0.33)$ and $(\alpha, \nu) = (4.00, 1.00)$ for the ground state and a typical eigenstate from the mid-spectrum, respectively. Indeed, three exponents β, α and ν obey $\beta = \alpha/\nu$ in Eq. (42), regardless of the energy level.

The offered quantum-enhanced sensitivity by Stark localization is not limited to the non-interacting probe. To

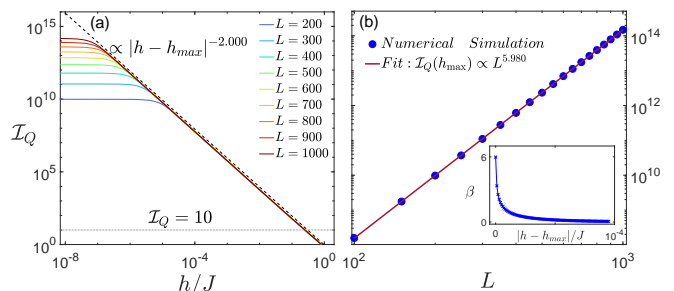


FIG. 5. **Single-particle Stark probe;** (a) QFI as a function of the Stark field h for single-particle Stark probe, prepared in the ground state of Eq. (55) with various sizes. The dashed line is the best fitting function to describe the algebraic behavior of the QFI in the localized regime when $L \rightarrow \infty$. (b) the maximum of the QFI at h_{\max} versus probe size L . The numerical results (markers) are well-fitted by function $I_Q \propto L^\beta$ (line) with $\beta=5.98$. The inset shows the scaling behavior far from the criticality. Figure is adopted from [74].

study the effect of the interaction, one can consider a one-dimensional probe of size L containing $N=L/2$ particles with tunneling to their next neighbor and interaction range that decay algebraically depends on the exponent $\eta > 0$. The Hamiltonian reads

$$H = J \sum_{i=1}^{L-1} (\sigma_i^x \sigma_{i+1}^x + \sigma_i^y \sigma_{i+1}^y) + \sum_{i < j} \frac{J}{|i-j|^\eta} \sigma_i^z \sigma_j^z + h \sum_{i=1}^L i \sigma_i^z, \quad (56)$$

with J and h as the coupling strength and the magnitude of the gradient field, respectively. By changing the exponent η , one can smoothly interpolate between a fully connected graph for $\eta=0$ and a standard nearest-neighbor one-dimensional chain for $\eta \rightarrow \infty$. In the following, after presenting the results for the probe with short-range interaction (i.e. $\eta \rightarrow \infty$), we investigate the impact of long-range interaction (i.e. $\eta < \infty$) to address this question that whether longer range of interaction can provide more benefits for sensing tasks.

Short-range interaction.— Fig. 6(a) represents the QFI as a function of h for various L obtained for the ground state [74]. By increasing the Stark field, the system goes through a phase transition from the extended phase to the localized one. Clearly, the QFI peaks at some h_{\max} which gradually moves to zero, indicating that the Stark localization transition in the many-body interacting probe takes place at an infinitesimal gradient field. While finite-size effects are evident in the extended phase ($h < h_{\max}$), in the localized phase ($h > h_{\max}$), the QFI is size-independent and decays algebraically as $I_Q \propto |h - h_{\max}|^{-\alpha}$ with $\alpha=4.00$. The scaling behavior of the Stark probe has been presented in Fig. 6(b) for both extended phase ($h=10^{-4}J$) and transition point ($h=h_{\max}$). The best fitting function to describe the numerical results (markers) obtained as $I_Q \propto L^\beta$ (lines) with $\beta=3.67$ and $\beta=4.26$, for extended

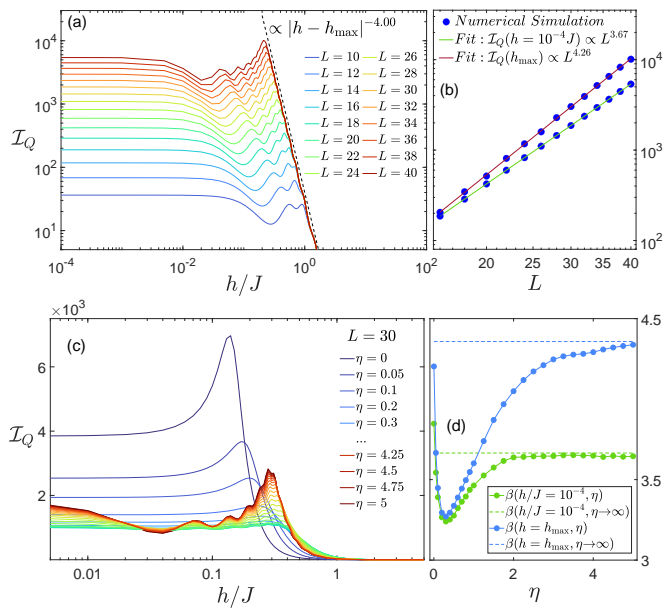


FIG. 6. **Many-body Stark probe;** (a) QFI versus h for many-body Stark probe with nearest-neighbor interaction prepared in the ground state of Eq. (56) with $\eta \rightarrow \infty$ and different sizes. The dashed line which is the best-fitting function shows the asymptotic behavior of the QFI in the localized phase. (b) the QFI versus L in extended phase, i.e. $h=10^{-4}J$, and critical point, i.e. $h=h_{\max}$. The numerical results (markers) are well-described by fitting function $I_Q \propto L^\beta$ (line) with $\beta=3.67$ and $\beta=4.26$ for the extended phase and critical point h_{\max} , respectively. (c) QFI versus h for many-body Stark probe prepared in the ground state of Eq. (56) with different η and $L=30$. (d) The obtained scales of the QFI, namely $\beta(h, \eta)$ versus range of the interaction η , in both extended phase ($h=10^{-4}$) and critical points ($h=h_{\max}$). Figure is adopted from [74, 75].

phase and transition point, respectively. Obviously, similar to the single particle probe, the many-body interacting probe also results in strong super-Heisenberg precision.

Long-range interaction.— To explore the advantages offered by long-range interactions in the Stark probe, Ref. [75] presents the QFI for a Stark probe of size $L=30$ prepared in the ground state of Hamiltonian Eq. (56) with different η 's. The results are shown in Fig. 6(c). Regardless of the range of the interaction, increasing h results in transition from extended phase to localize one, highlighted by a peak at $h_{\max}(\eta)$. Various η 's leaves different imprints on the QFI. By decreasing the range of the interaction the induced Zeeman energy splitting on each site changes from a uniform to nonuniform (resembling disorder) which cause diminution in QFI. The effect of nonuniform energy splitting gradually vanishes as the interaction tends to short-range. By considering a fitting function of the form $I_Q \sim L^\beta$, one can estimate the exponent β for various choices of (h, η) . The results are presented in Fig. 6(d) which clearly

shows the possibility of super-Heisenberg precision over a wide range of interactions.

Capturing the ultimate precision limit provided by the QFI, and equally saturating the Cramér-Rao bound in Eq. (7), demands an experimental-friendly measurement setup. In Ref. [74] it has been shown that a simple position measurement described by local projectors $\{\Pi_i = |i\rangle\langle i|\}_{i=1}^L$ results in CFI closely matches with the QFI in single particle probe. For many-body interacting case, the best observable to closely catch the QFI is obtained as $\mathcal{O} = \Pi_{i=1}^L \sigma_i^z$ [75, 76].

VI. EQUILIBRIUM QUANTUM SENSING: TOPOLOGICAL PHASE TRANSITIONS

Second order quantum phase transitions are known for various features including spontaneous breaking of a continuous symmetry, local order parameters, gap closing and scale invariance behavior. While such critical phenomena is usually good for quantum-enhanced sensitivity, it is not clear which of these features are responsible for achieving quantum enhanced sensitivity. Moreover, although these models are not as noise-sensitive as interferometric schemes, detailed analysis shows reduction in the QFI scaling with increasing noise [273]. Thus, building quantum many-body sensors based on beyond second-order phase transitions is crucial. There also exists phase transitions where the corresponding order parameter is global. These are called topological phase transitions and are characterized by discrete jump in topological indices of the ground state of the physical system such as the Chern number [274–276]. In addition, topological systems are expected to be naturally more robust against local noise and thus their performance as a sensor be less noise-affected. In this section, we consider two different topological sensors, namely Symmetry Protected Topological (SPT) systems and non-Hermitian topological probes.

A. Symmetry protected topological sensors

Topological phase transitions, exemplified through SPT transitions, are fundamentally different from conventional second-order quantum criticality. In fact, SPT transitions are characterized by: (i) the emergence of robust edge/surface states which are protected against symmetry-preserving local perturbations [277, 278]; (ii) an integer-valued nonlocal quantity called a topological invariant [279]; and (iii) the absence of long-range correlations and entanglement [280].

One of the simplest and earliest examples of many-body systems with SPT transition is the Su-Schrieffer-Heeger (SSH) model [281] which consists of one excitation in a 1D tight-binding lattice consisting of two different sublattices characterized by bonds of alternating

strengths. The Hamiltonian is given by

$$H_{\text{SSH}} = - \sum_{j \in L} \left(t_1 b_j^\dagger a_j + t_2 a_{j+1}^\dagger b_j \right). \quad (57)$$

where t_1 and t_2 are intra- and inter-site hopping rates. The parameter of interest is $\lambda = t_1/t_2$. For 2D and higher dimensional systems, the quintessential examples of topological systems are the so called Chern insulators and generalizations thereof (see Ref. [282] for a detailed review). For a simple system that has been realized in optical lattices with cold atoms [283], the spin-orbit coupled Hamiltonian is given by

$$\hat{H}^{\text{Ch}} = \sum_{\mathbf{k}} \begin{bmatrix} \hat{c}_{\mathbf{k},\uparrow}^\dagger & \hat{c}_{\mathbf{k},\downarrow}^\dagger \end{bmatrix} H_{\mathbf{k}}^{\text{Ch}} \begin{bmatrix} \hat{c}_{\mathbf{k},\uparrow} \\ \hat{c}_{\mathbf{k},\downarrow} \end{bmatrix}^T, \quad (58)$$

where $H_{\mathbf{k}}^{\text{Ch}} = \mathbf{B} \cdot \boldsymbol{\sigma}$ is the Bloch Hamiltonian with $\mathbf{B} = (2t_1 \cos k_x, 2t_1 \cos k_y, m_z + 2t_2(\sin k_x + \sin k_y))$ and $\boldsymbol{\sigma}$ the vector of Pauli matrices. Here \uparrow, \downarrow denote spin-1/2 up and down states, and m_z, t_1, t_2 are lattice parameters. The parameter to be estimated can be considered as $\lambda = m_z/t_2$. The eigenvectors form two bands that touch at phase transition at the Dirac points $(k_x, k_y) = \pm(\pi/2, \pi/2)$ for nonzero θ , and the phase boundaries are given by $\theta_c = \mp 4$ [282]. These SPT models are generically short-range entangled and their topological order are protected only under transformations with respect to some discrete symmetry.

For topological systems, Ginzburg-Landau theory fails since local order parameters do not exist and no continuous symmetry is broken. Hence the fidelity susceptibility or QFI based approach to detect topological phase transitions holds special relevance for such models, in addition to the practical task of building many-body quantum sensors. Extensive studies in this regard has been made on lower dimensional systems, including 1D Kitaev chain [284], and Kitaev's deformed toric code models [285] and honeycomb models [286, 287] in 2D. Gu and Lin [288] also pointed out that the critical exponent of fidelity for the honeycomb model is super-extensive and different for two sides of the critical point. Thus, fidelity susceptibility is indeed an useful tool for detecting topological phase transitions. In [55], the possibility of quantum enhancement of sensing in edge and ground states of topologically non-trivial single-excitation subspaces of generic free-Fermion Hamiltonians was investigated. For edge states, N^β scaling, with $\beta=2$ of QFI was obtained at the transition point and constant scaling away from criticality, as shown in the top panel of Fig. 7. Significantly, the optimal measurement for saturating the Cramér-Rao bound was revealed as a constant site-location measurement on the lattice for every value of the parameter θ . For many-body ground states, quadratic scaling of QFI was again obtained around the topological phase transition point, with classical linear scaling away from criticality, as shown in the bottom panel of Fig. 7. For multiparameter estimation, it has been suggested recently

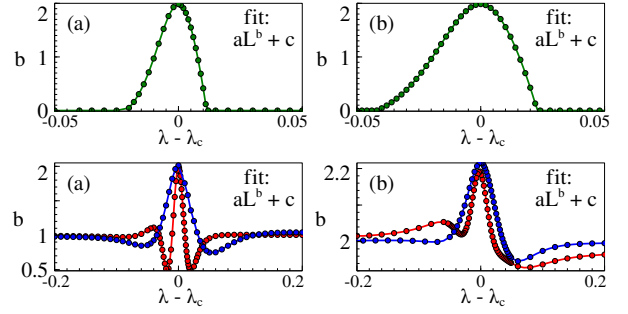


FIG. 7. **QFI scaling near transition.** Top panels : Scaling exponent of QFI of edge state (for $\lambda < \lambda_c$) and corresponding bulk state (for $\lambda > \lambda_c$) as a function of λ for (a) SSH model, and (b) Chern insulator model. Bottom panels : Scaling exponent of QFI of many-body ground state as a function of λ subject to PBC (blue) and OBC (red) for (a) SSH model, and (b) Chern insulator model. Figures taken from Ref. [55].

that the Berry curvature and related topological invariants (e.g., the Chern Number) act as physically relevant bounds for the QFI matrix used for multiparameter estimation [289]. Cai and his collaborators [57] have succeeded in experimentally demonstrating these bounds for a 2D Chern insulator system synthesized in an NV-center based setup.

B. Non-Hermitian Quantum Sensors

Non-Hermitian Hamiltonians provide an effective description of open system dynamics [290]. The topological systems bear many surprising features due to the unique properties of the eigenstates and complex eigenvalues [291]. In the absence of degeneracy, the eigenstates are linearly independent and form a complete basis, but they are not orthogonal. This stems from the fact that the right- and left-eigenstates are not the same. For a non-Hermitian Hamiltonian H_{NH} , they are defined as

$$H_{\text{NH}} |\psi_n^{\text{R}}\rangle = E_n |\psi_n^{\text{R}}\rangle, \\ \langle \psi_n^{\text{L}} | H_{\text{NH}} = E_n \langle \psi_n^{\text{L}} | \implies H_{\text{NH}}^\dagger |\psi_n^{\text{L}}\rangle = E_n^* |\psi_n^{\text{L}}\rangle, \quad (59)$$

where E_n is the corresponding eigenvalue. However, these states are biorthogonal [292], and upon normalization gives, $\langle \tilde{\psi}_m^{\text{L}} | \tilde{\psi}_n^{\text{R}} \rangle = \delta_{mn}$. Here, $|\tilde{\psi}_n^{\text{R}}\rangle = |\psi_n^{\text{R}}\rangle / \sqrt{\langle \psi_n^{\text{L}} | \psi_n^{\text{R}} \rangle}$, and $|\tilde{\psi}_n^{\text{L}}\rangle = |\psi_n^{\text{L}}\rangle / \sqrt{\langle \psi_n^{\text{L}} | \psi_n^{\text{R}} \rangle}$. This helps in writing down the completeness relation $\sum_n |\tilde{\psi}_n^{\text{R}}\rangle \langle \tilde{\psi}_n^{\text{L}}| = \mathbb{1}$ and the spectral decomposition $H_{\text{NH}} = \sum_n E_n |\tilde{\psi}_n^{\text{R}}\rangle \langle \tilde{\psi}_n^{\text{L}}|$. Non-Hermitian Hamiltonians can have degeneracies analogous to Hermitian systems, i.e. identical eigenvalues with distinct eigenstates. The points in the Hamiltonian's parameter space where this happens are known as diabolic points. There are also parameter values where more than one eigenvalues and the corresponding eigenstates can become identical. These are known as Exceptional Points (EP)

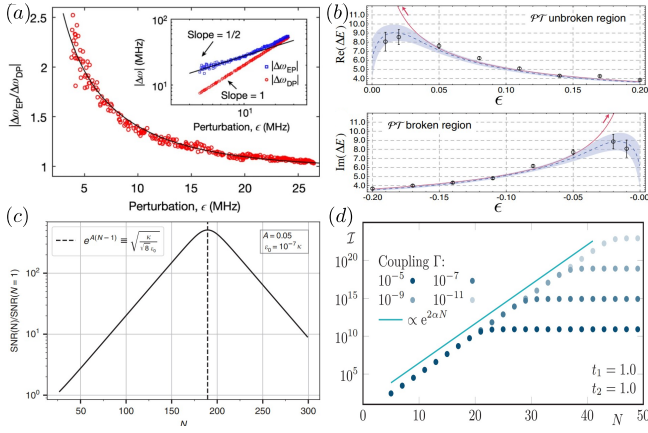


FIG. 8. **EP based and non-reciprocity based sensors.** (a) Energy splitting versus perturbation strength ϵ near EP shows enhancement over standard splitting near a diabolic point (DP). For EP of order 2 in Ref. [59], the black line shows the expected $\epsilon^{1/2}$ behavior. The inset shows scaling exponent of EP based sensor (blue squares) increasing from 1/2 (black line) as ϵ increases. The exponent for DP based sensor is 1 (red circles). Figure adapted from Ref. [59]. (b) For a PT-symmetric system in Ref. [60], EP of order 2 appears at the symmetry breaking point. The black circles are the experimental data for the energy splitting with perturbation ϵ . The red line shows the expected $\sqrt{|\epsilon|}$ behavior. In the PT-unbroken regime, the energies are real and the upper panel shows the splitting. In the PT-broken regime of the system considered, the real part of energy stays constant while the splitting is observed in the imaginary part (lower panel). As the EP is approached, deviation from the expected value occurs due to excessive noise. Figure adapted from Ref. [60]. (c) The signal-to-noise ratio (SNR) shows the exponentially enhanced sensitivity with system size N in the non-reciprocity based sensing protocol in Ref. [61]. It is based on the Hatano-Nelson model in Eq. (60) and $A = \log(J_R/J_L)/2$. The analysis is based on linear response theory which breaks down for very large N , due to amplification of noise. The expected value of N for this to happen with fixed values of other parameters is shown with dashed vertical line. Figure adapted from Ref. [61]. (d) QFI (\mathcal{I}) with respect to perturbation coupling the boundaries (Γ) as a function of system size N for the non-Hermitian SSH model based proposal in Ref. [56]. Here t_1 and t_2 are the intra- and inter-site hopping terms. The QFI increases exponentially with coefficient α (solid line) until it saturates to a value that increases with decreasing Γ . Figure adapted from Ref. [56].

and have no Hermitian counterpart. The right- and left-eigenstates corresponding to the EP are orthogonal to each other and the biorthogonal framework breaks down as the Hamiltonian is not diagonalizable anymore. If the Hamiltonian has parity-time (PT) symmetry, then in certain parameter regime, the eigenvalues are real and the Hamiltonian and the PT operator share the same eigenstates. This is known as the PT-unbroken phase. In the PT-broken phase, the eigenvalues can be complex. The PT-symmetry breaking point is an EP of the system.

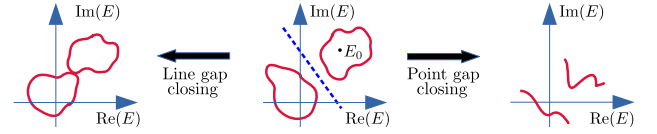


FIG. 9. **Non-Hermitian energy gaps.** Two types of gaps can occur in the complex energy plane (middle panel). Line gap (blue dashed line) separates two bands (red loops). Point gap resides inside a spectral loop (e.g. E_0). Line gap closes when the loops merge (left panel). Point gap closes when the loop shrinks to an arc (right panel).

EPs are branch point singularities in the complex energy manifold and generate non-trivial topology, quantified by winding of eigenvalues and eigenvectors [293]. Sensing based on EP was proposed first in Ref. [62] for coupled cavity systems – with photon loss and gain terms – that have resonant modes at EP. A non-Hermitian perturbation with strength ϵ would move the system away from the EP. For an EP of degree n (i.e. n eigenstates coalescing), the resulting energy splitting $\sim \epsilon^{1/n}$. In contrast, for Hermitian degeneracies or diabolic points, the leading order splitting is $\sim \epsilon$. The advantage of the EP based sensors can be quantified by the susceptibility $d_\epsilon \epsilon^{1/n} = \epsilon^{-(1-1/n)}$, which diverges as $\epsilon \rightarrow 0$. This was experimentally demonstrated with optical microring resonators [59, 63] and also with further imposition of PT symmetry [60, 64]. However, these schemes do not reveal the precision of the sensor which is the smallest change in ϵ that can be measured. The standard measurement is done by first implementing an excitation, followed by analyzing the resonant scattering output. The signal-to-noise ratio of the output is a measure of QFI, which sets the precision. As the eigenstates participating in the excitation-deexcitation process become more and more non-orthogonal while approaching EP, it was debated that the resulting quantum noise would overwhelm the advantage of EP based sensors [65, 66]. Experimental observation also confirmed this [67]. Signal enhancement was nevertheless predicted at specific frequencies [68] or with additional gain terms [69] and was also observed experimentally for systems slightly detuned from EP [70]. The effectiveness of EP based sensors is still a topic of active research [71].

In Ref. [69], another resource for enhanced signal was shown to be the non-reciprocity. For tight-binding non-Hermitian Hamiltonians, a concrete proposal based on the Hatano-Nelson model [294] was put forward in Ref. [61]. Here the non-reciprocity is provided by different hopping rates to left and right, namely J_L and J_R , in the 1D Hamiltonian

$$H_{\text{HN}} = \sum_j (J_L |j\rangle \langle j+1| + J_R |j+1\rangle \langle j|). \quad (60)$$

The imbalanced hopping terms generate a unique non-Hermitian topology even in the single-band structure, unlike Hermitian cases. Considering a N -site chain of coupled bosonic modes with a classical resonant drive at site

1, it was shown that the dynamics of the two quadrature modes are governed by a ‘doubled’ Hatano-Nelson Hamiltonian, with opposite reciprocities for the two modes. This imposes a \mathbb{Z}_2 symmetry which is broken by a perturbation on site N that mixes the two modes with strength ϵ . An input drive in terms of one mode would generate a large signal as the output in the other mode in the steady state. With judicious choice of the optimal homodyne measurement [295], the signal-to-noise ratio gives the QFI with respect to ϵ which scales exponentially with system size, namely $\text{QFI} \sim |\epsilon|e^{(N-1)\log(J_R/J_L)/2}$. This kind of exponential sensitivity was also reported in Ref. [56] with a similar coupled cavity system with input drive but here the perturbation term – with strength ϵ – connects the boundary modes (sites 1 and N). Here, the dynamics is governed by a non-Hermitian extension of the SSH model with balanced loss and gain terms on alternating sites. This breaks the sublattice symmetry, but makes the systems PT-symmetric. In the topologically non-trivial regime, the signal-to-noise ratio of the steady state output field scales exponentially with system size, i.e. $\text{QFI} \sim e^{\alpha N}$, where α is a positive coefficient. This behavior is closely connected to the acute spectral sensitivity of non-Hermitian topological systems [296–298]. In particular, exponential sensitiveness of the edge state energy E_0 to the coupling at the boundary ϵ (i.e. $\partial_\epsilon E_0 \sim e^{\alpha N}$), has also led to sensing proposal in Ref. [54]. These proposals function anywhere in the topologically non-trivial regime and does not require fine-tuning to an EP. An experimental confirmation of edge state sensitivity at the EP was also performed recently with an optical resonator setup [299]. Even in the absence of EP, superiority of sensing has been shown experimentally [72] and Heisenberg scaling in time has also been demonstrated with non-Unitary dynamics [73]. Such scaling behaviors are quite promising regarding sensing in open systems, although recent theoretical arguments cast doubts about actual advantages of non-Hermitian sensors over their Hermitian counterparts [300].

Beyond sensing boundary perturbations, non-Hermitian topology also can be used for estimating bulk Hamiltonian parameters. The notion of band gaps are extended in the non-Hermitian regime to two different gap structures: line gap and point gap (see Fig. 9) [301]. A spectral loop (for 1D systems) or finite spectral area (in higher dimensions) correspond to the presence of non-Hermitian skin effect in finite systems, where most of the eigenstates are localized at a boundary [302–305]. Changes in the bulk Hamiltonian parameters can make the spectral structure contract to a curve with zero spectral area. This signals a closure of the point gap, which makes the skin effect vanish. The corresponding localization transition in the eigenstates can be used for sensing, as was shown in Ref. [58], to achieve precision with Heisenberg scaling. This extends the role of gap closing for quantum-enhanced sensitivity to a truly non-Hermitian domain. For the aforementioned

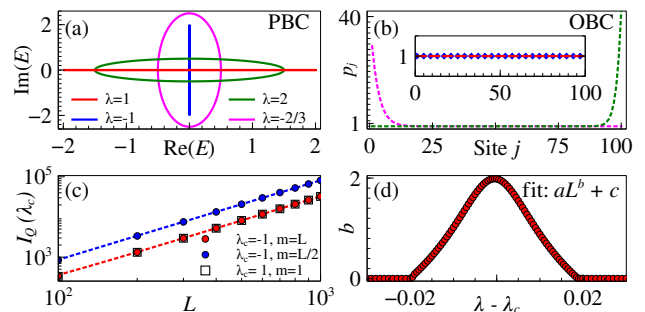


FIG. 10. **Bulk Hamiltonian parameter estimation with Hatano-Nelson model** with $\lambda = J_R/J_L$ in Eq. (60). (a) Bulk spectrum with periodic boundary conditions (PBC). (b) Cumulative site-population for open boundary conditions (OBC) eigenstates shows the non-Hermitian skin effect and its absence (inset). (c) Quadratic scaling of QFI with system size L at the transition $\lambda = \lambda_c = \pm 1$. (d) QFI Scaling exponent near transition. Figures taken from Ref. [58].

Hatano-Nelson model, this scaling can be obtained analytically (see Fig. 10). The robustness against local disorders is also shown by mapping it to a non-Hermitian Aubrey-André-Harper model [306]. Apart from extension to prototypical multi-band models [307] and 2D systems [308], experimental implementation is also possible in discrete-time non-Unitary quantum walk setups [309, 310].

VII. RESOURCE ANALYSIS FOR CRITICAL QUANTUM SENSING

As discussed above, various forms of criticality can achieve quantum enhanced sensitivity. The resource for achieving such enhanced precision is the system size N and the figure of merit is the QFI. However, in some cases the time T needed for accomplishing the sensing task has to also be considered as a resource. This might be due to practical issues, such as limited coherence time, or size dependence T which makes the sensing time extremely long for large system sizes. To account for such complexity, one can use normalized QFI as a figure of merit, namely I_Q/T [311–316]. For instance, in the case of many-body ground state sensing, one may consider an adiabatic approach for generating the complex ground state. This can be achieved by slowly evolving the system initialized in the ground state of a simpler Hamiltonian which is transformed into the desired Hamiltonian over the time interval T . If the transformation is slow enough, namely T is large, the quantum state remains in the ground state of the instant Hamiltonian throughout the evolution. This guarantees that at the end of evolution when the Hamiltonian takes the final form the system is in the desired ground state. When the system is adiabatically driven towards a second-order quantum phase transition, the required time T scales as $T \sim N^z$ [47], where z is the dynamical critical exponent showing how the en-

ergy gap ΔE vanishes at the critical point by increasing the system size $\Delta E_{\min} \sim 1/N^z$. Incorporating this into the scaling of the QFI across second-order quantum phase transitions in Eq. (39) leads to

$$I_Q(\theta=\theta_c)/T \sim N^{\beta-z}. \quad (61)$$

This clearly shows that the scaling diminishes as time is included in the resource analysis.

Similar results can be found for different quantum sensing strategies where the required time depends on the system size. For instance, in Ref. [89] quantum enhanced sensitivity, i.e. $\beta > 1$, is achieved for the steady state at the boundary time crystal transition when the figure of merit is the QFI I_Q . However, if one changes their figure of merit to normalized QFI, i.e. I_Q/T , with T being the time that the system reaches its steady state, the scaling with respect to system size is reduced to standard limit. However this situation changes for Stark probe presented in section V B. In Ref [74, 75], it has been shown that regardless of the number of particles and the range of the interaction, one always has $\beta - z > 1$ ensuring that the quantum enhanced sensitivity is always achievable for the Stark probes.

Note that a true resource analysis depends on the sensing scheme. If the time is not a restricting issue QFI can be used as the figure of merit. Equivalently, for those sensing schemes that time is a key limiting factor a better figure of merit is normalized QFI, namely I_Q/T .

VIII. NON-EQUILIBRIUM QUANTUM SENSING: DYNAMICAL QUANTUM PHASE TRANSITIONS

The footprints of the ground state quantum criticality in equilibrium can also be observed in non-equilibrium dynamics. For a closed system described by a time-independent Hamiltonian H , its time evolution which is described by Schrödinger equation as

$$|\Psi(t)\rangle = e^{-iHt}|\Psi(0)\rangle, \quad (62)$$

where $|\Psi(0)\rangle$ is the initial state. There are two different notions of dynamical quantum phase transitions which we will discuss separately in the following subsections.

A. Dynamical quantum phase transitions quantified by Loschmidt echo

By considering the projection of the time-evolved state with the initial state, one can define the Loschmidt echo, $\mathcal{L}(t) = |\langle \Psi(0) | \Psi(t) \rangle|^2$, interpreted as the return probability. One can define the rate of return probability \mathcal{G} , as

$$\mathcal{G} = - \lim_{N \rightarrow \infty} \frac{1}{N} \log L(t). \quad (63)$$

It is discovered that if $|\Psi(0)\rangle$ and $|\Psi(t)\rangle$ belongs to two different equilibrium phases, then the $\mathcal{G}(t)$ can be non-analytic at certain time $t=t_c$. On the other hands, if $|\Psi(0)\rangle$ and $|\Psi(t)\rangle$ belongs to the same equilibrium phase then $\mathcal{G}(t)$ is a regular function of time [317]. There are a few peculiarities to these cases [318] as well as extension in non-Hermitian systems [319, 320]. Such dynamical phase transitions has been proposed to provide quantum enhancement in parameter estimation [321]. The authors have proposed a negatively charged Nitrogen-Vacancy (NV^-) center in a nearby Carbon-13 nuclear spins as a platform for studying dynamical phase transitions. First, they have shown that the system undergoes a dynamical phase transition by a suitable choice of Gaussian time-varying magnetic field. Then it is shown that the Fisher information, for estimating coupling strength between the two Carbon-13 nuclear spins, improves at $t=t_c$ as compared to the regular times.

B. Dynamical quantum phase transitions quantified by a time-averaged order parameter

A second category of dynamical phase transitions in many-body systems is detected by time-averaged order parameter $\mathcal{O}(t)$. The time average of the order parameter in the evolved state $|\Psi(t)\rangle$ is given by

$$\overline{\langle \mathcal{O}(t) \rangle} = \lim_{T \rightarrow \infty} \frac{1}{T} \int_0^T dt \langle \mathcal{O}(t) \rangle. \quad (64)$$

The order parameter distinguishes an ordered phase when $\overline{\langle \mathcal{O}(t) \rangle} \neq 0$ from a disordered phase when $\overline{\langle \mathcal{O}(t) \rangle} = 0$. Such phase transitions have been identified for quantum-enhanced sensing [322]. In this paper, the authors have studied a fully connected spin model under sudden quenching. They focused on the LMG model which is given by

$$H_{LMG} = - \frac{\chi}{N} S_z^2 - \Omega S_x - \omega S_z \quad (65)$$

where $S_\alpha = \sum_{i=1}^N \sigma_{\alpha,i}/2$ are defined as collective spin operators and $\sigma_{\alpha,i}$ are the Pauli matrices for the i th spin-1/2 particle. The ground state criticality of the model occurs at $\Omega_c/\chi=0.5$ and $\omega_c/\chi=0$. The Fisher information in the long time state behaves as an order parameter and shows peak at the critical point. Moreover, the scaling of the long-time QFI at the critical point as a function of system size N reaches to a sub-Heisenberg limit for the transverse field, $I_{Q,B_x}^{t \rightarrow \infty} \sim N^{1.5}$ and $I_{Q,B_z}^{t \rightarrow \infty} \sim N^{1.75}$ for the longitudinal field.

IX. NON-EQUILIBRIUM QUANTUM SENSING: DISCRETE TIME CRYSTAL PHASE TRANSITIONS

Apart from dynamical phase transitions, discussed in Sec. VIII, there are other categories of phase transitions

which occur through non-equilibrium dynamics of many-body systems. An important class of such systems are discrete-time crystals (DTCs) which are defined in an isolated non-equilibrium quantum many-body system that undergoes periodic drives. Breaking the time translational symmetry results in the emergence of a new phase of matter known as the DTC phase with indefinite persistent oscillations [323–325]. Recently the long-range spatial- and time-ordered dynamics in the DTC phase have been harnessed in measuring an AC field [326, 327]. The optimal performance for long periods along with intrinsic robustness to the imperfections in the sensing protocol based on DTC phase allows one to hit the quantum standard limit in estimating the AC field. However, obtaining a true sensing enhancement based on a resource such as system size requires a wise mechanism for establishing DTC. In Ref. [93] the proposed mechanism results in a stable DTC with period-doubling oscillations that persist indefinitely even in finite-size systems. The time-dependent Hamiltonian that governs the dynamic in the considered spin-1/2 chain is

$$H(t) = JH_I + \sum_n \delta(t - nT)H_P, \quad (66)$$

$$H_I = \sum_{j=1}^{L-1} j\sigma_j^z \sigma_{j+1}^z, \quad H_P = \Phi \sum_{j=1}^L \sigma_j^x.$$

Here J is the spin exchange coupling, and $\sigma_j^{x,y,z}$ are the Pauli operators. For one period of evolution, the Floquet unitary operator reads

$$U_F(\Omega, \varepsilon) = e^{-iH_P} e^{-i\Omega H_I}, \quad (67)$$

here $\Omega = JT$, and Φ is tuned to be $\Phi = (1 - \varepsilon)\frac{\pi}{2}$, with ε as deviation from a $\pi/2$ x -rotation. While setting $\Omega = \pi/2$ results in a stable period doubling DTC that is robust against arbitrary imperfection ε in the rotating pulse, the system goes through a sharp second-order phase transition as the spin exchange coupling, namely Ω varies from $\frac{\pi}{2}$, denoting this variation as $\omega = |\Omega - \frac{\pi}{2}|$. Relying on this transition, a DTC quantum sensor has been devised to sense ω with benefits from multiple features. As it is clear from Fig. 11(a), in the DTC phase the QFI provides a plateau whose value depends on period cycles n , and in the non-DTC region it shows nontrivial and fast oscillations. By approaching the transition point, denoted by ω_{\max} (dashed line), the QFI shows a clear peak at all stroboscopic times. The extreme sensitivity to the exchange coupling across the whole DTC phase ($\omega < \omega_{\max}$) as well as at the transition point (ω_{\max}) providing quantum-enhanced sensitivity as $I_Q \propto L^\beta$ with $\beta > 3$ (see Fig. 11(b)). The obtained quantum enhancement is independent of the initial state and can be boosted by increasing imperfection in the pulse to a certain value.

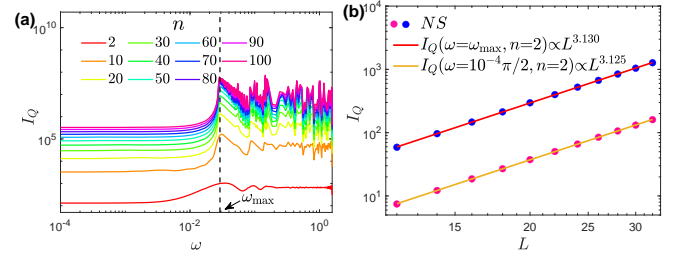


FIG. 11. **DTC quantum sensor**; (a) The QFI versus ω in stroboscopic times in a system of size $L=30$. The onset of the phase transition is determined by $\omega = \omega_{\max}$ (dashed line), the point where QFI peaks in different period cycles n 's. (b) The values of the QFI after $n = 2$ in DTC phase (for $\omega = 10^{-4}\pi/2$) and at transition points ($\omega = \omega_{\max}$) versus L . The numerical simulation (NS) is well-mapped by a function as $I_Q \propto L^\beta$ (solid lines) with $\beta > 3$. Results are obtained for $\varepsilon = 0.01$. Figure is adapted from [93].

X. NON-EQUILIBRIUM QUANTUM SENSING: FLOQUET PHASE TRANSITION

Quantum metrologically advantageous states can also be generated using the application of external time-periodic driving to the system. In this case, the frequency of the external driving can resonate with the lowest energies of the unperturbed systems. This resonance can be harnessed for quantum enhanced sensing [87, 88, 328–334]. This resonance phenomena has also been observed in gaped many-body quantum systems when the frequency of external driving matches with the lowest energy gap of the unperturbed Hamiltonian. [87, 88, 335]. Various important physical features of systems with time-periodic influence can be extracted by employing Floquet formalism. For a time-periodic Hamiltonian, $H(t + \tau) = H(t)$, with periodicity $\tau = 2\pi/\omega$, the solution of the Schrödinger equation follows from the Floquet theorem. The Floquet theorem gives an ansatz of the form $|\Psi(t)\rangle = \sum_\ell e^{-i\mu_\ell t} |\Phi_\ell(t)\rangle$. Here μ'_ℓ 's are eigenphase (the Floquet phase), $|\Phi_\ell(t)\rangle$ the Floquet modes, and $\ell \in \mathbb{Z}$. Substituting the ansatz to the Schrödinger equation, $H(t)|\Psi(t)\rangle = -i\hbar \frac{\partial |\Psi(t)\rangle}{\partial t}$, the Floquet modes satisfy

$$\left(H(t) - i \frac{\partial}{\partial t} \right) |\Phi_\ell(t)\rangle = \mu_\ell |\Phi_\ell(t)\rangle. \quad (68)$$

It can be noted that $|\Phi_\ell(t + \tau)\rangle$ is also a solution of the above equation with Floquet eigenphase μ_ℓ , therefore, one can write $|\Phi_\ell(t + \tau)\rangle = |\Phi_\ell(t)\rangle$. Furthermore, the time evolution propagator, describing the dynamics of the system, is given by

$$U(t, t_0) = \mathcal{T}_t \exp \left(-i \int_{t_0}^t H(t') dt' \right), \quad (69)$$

where \mathcal{T}_t represent time ordering operator. It is noted that $U(t + \tau)|\Psi(t)\rangle = |\Psi(t + \tau)\rangle$. Using the ansatz for $|\Psi(t)\rangle$ in the above equation, one gets $U(t +$

$\tau)e^{-i\mu_\ell t}|\Phi_\ell(t)\rangle = e^{-i\mu_\ell t}|\Phi_\ell(t + \tau)\rangle$. This shows that the Floquet modes are eigenvectors of the one time-period propagator $U(\tau, 0)$ with $\{e^{-i\mu_\ell \tau}\}$ the corresponding eigenvalues.

Properties of Floquet modes $\{|\Phi_\ell(t)\rangle\}$ and Floquet phases $\{\mu_\ell\}$ have been explored for sensing periodic magnetic fields due to clusters of few qubits [328]. Here, the effective magnetic field due to the cluster of spins is detected using a single qubit as a sensor. The initial state of the system is $|\psi(0)\rangle = \frac{1}{\sqrt{2}}(|\uparrow\rangle + |\downarrow\rangle) \otimes |\mathcal{B}(0)\rangle$, where $|\mathcal{B}(0)\rangle$ is the initial state of the detected spin cluster at time $t = 0$ and $|\uparrow\rangle, |\downarrow\rangle$ are the computational basis states of the electronic spin, respectively. At later times, due to the interaction with the sensor (the qubit state), the spin cluster state becomes entangled with the sensor. The magnetic field signal is detected from the data of temporal coherence of the time-evolved state of the detected spin cluster. The coherence can be expressed in terms of the eigenvalues and eigenstates of the one-period unitary evolution operator or Floquet operator. The coherence displays a dip which occurs at the avoided crossings of the Floquet eigenstates where $e^{i\mu_\ell} \approx e^{-i\mu_k}$ or when the Floquet gap, $\Delta_F = \mu_\ell - \mu_k$, vanishes. Thus, by measuring the location of the coherence dip, the energy-difference between Floquet states can be observed with precision higher than the one predicted by the average Hamiltonian theory. However, this method can only be applicable for a sensing around the resonance frequencies. Sensing of arbitrary frequency fields has been proposed using a single qubit as a sensor in Floquet systems [329]. In addition, periodically driven systems and the transition of Floquet eigenphases have been used for magnetic-field signal amplification [330]. In Ref. [331], an optimal control method is developed to estimate the amplitude, B , of a time-periodic magnetic field $B(t) = B(\cos(\omega t)\sigma_x + \sin(\omega t)\sigma_z)$. It is shown here that the QFI with respect to B can achieve super-Heisenberg scaling with interrogation time, t , by applying an optimal control pulse as compared to the one without control. A solid state sensor with an ensemble of high density Nitrogen Vacancy (NV) centers in diamonds has been investigated both theoretically and experimentally by Floquet formalism [332]. The system, here, is a dense ensemble of electronic spins. Each electronic spin act as an independent probe for the external signal. Thus, one would expect that, by increasing the number of particles in the system, the sensitivity can be improved. The improvement, however, is severely hindered by interaction between the spins, since a large spins are confined in a small volume, the spin-spin interaction is unavoidable. By applying a series of dynamical decoupling pulses, the interaction between the spins has been suppressed, which results in a larger coherence time. In this way the standard quantum limit is shown to be restored which is lost due to spin-spin interaction.

It is important to note that the above sensing protocols either do not employ interaction between the particles directly or use schemes to suppress the particle-particle interaction. Thus, the above schemes are equivalent to the

single-particle probe quantum metrology schemes with several rounds of repetition of the protocol. It is natural to extend the formalism to many-body systems with Floquet dynamics without applying any dynamical decoupling pulses and ask if still one can harness any property for improving the precision well beyond the standard limit. Sensing protocols have been developed in many-body systems using Floquet formalism for detecting both static [87] and periodic fields [88]. The Hamiltonian considered in those studies is

$$H(t) = -\frac{J}{2} \sum_{i=1}^N \left[\left(\frac{1+\gamma}{2} \right) \sigma_i^x \sigma_{i+1}^x + \left(\frac{1-\gamma}{2} \right) \sigma_i^y \sigma_{i+1}^y \right] - \frac{(h_0 + h(t))}{2} \sum_i \sigma_i^z, \quad (70)$$

where, σ^α ($\alpha = x, y, z$) are the Pauli matrices, J is the exchange coupling, $-1 \leq \gamma \leq 1$ is the anisotropic parameter, and the periodic-boundary conditions, i.e., $\sigma_{N+1}^\alpha \equiv \sigma_1^\alpha$, is imposed. Furthermore, the time-dependent field $h(t)$ is periodic with a period $\tau = \frac{2\pi}{\omega}$. Thus, the Hamiltonian is a time-periodic $H(t + n\tau) = H(t)$, where $n \in \mathbb{Z}$. In the absence of the periodic field, i.e. $h(t) = 0$, the Hamiltonian (70) shows quantum criticality at $h_0 = h_c = J$ for all values of γ [99]. Using Floquet formalism for solving the dynamics driven by the Hamiltonian in Eq. (70), one can estimate both the static field h_0 [87] and the amplitude of the periodic field $h(t)$ [88] even with partial accessibility to a block of spins. Note that partial accessibility implies that one only has access to a certain block of spins to perform measurement and gains information about the parameter of interest. It is to be emphasis here that the sensitivity to the parameter of interest naturally decreases as the accessibility reduces to smaller blocks. For example, it is shown that the QFI with respect to h_0 in the ground state of Eq. (70), when $h(t) = 0$, decreases as compared to the full system [87]. By driving the system periodically using an external drive field $h(t)$ the QFI can be made to exhibits peaks not only at the critical field, but at the points where the Floquet resonances occur. Thus, even with partial accessibility, the probe state becomes more sensitive with respect to the magnetic field h_0 when a suitable controlled driving magnetic field is applied such that the floquet gap closes.

By utilizing the time translation invariance of the Hamiltonian, the unitary dynamics in the integer multiple of time-period τ can be given by

$$U(\tau, 0) = e^{-iH_F \tau}, \quad (71)$$

where H_F is called the Floquet Hamiltonian and it describes the evolution of the system at the stroboscopic times $t = n\tau$. The knowledge of the state of the system at the later times $t = n\tau$ can be fully obtained by successive application of $U(\tau, 0)$. The $U(\tau, 0)$ admits spectral decomposition in terms of eigenvectors $\{|\mu\rangle\}$ and eigenvalues $\{\mu(\tau)\}$ of $U(\tau, 0)$ which depends on unknown parameter to be estimated. The eigenvalues are periodic

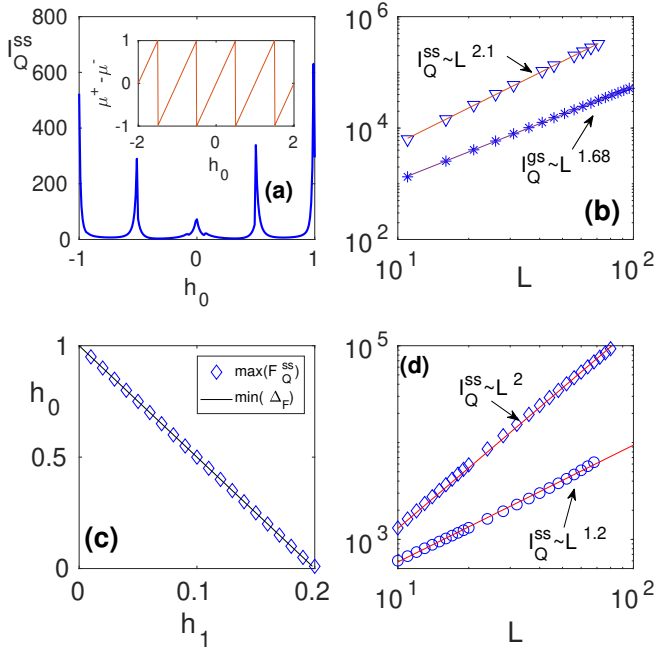


FIG. 12. **Driven enhanced sensing.** (a-b) DC field sensing for $h(t) = h_0 + h_1 \sin(\omega t)$. (a) Steady-state QFI I_Q^{ss} as a function of h_0 for $\gamma = 1$, $\omega = 1$, $h_1 = 1.5$, and the total system size $N = 6000$. (b) The scaling of QFI as a function of L in the steady-state (I_Q^{ss}) and the ground state (I_Q^{gs}). The total system size here is $N = 6000$ and the other parameters for the I_Q^{ss} and I_Q^{gs} are same as in panel (a). (c-d) AC field sensing of the form $h(t) = h_0 + h_1 \sum_{n=0}^{\infty} \delta(t - n\tau)$. (c) The line of maximum of I_Q^{ss} and minimum of Floquet gap. (d) Scaling of I_Q^{ss} as a function of L for points (h_0, h_1) such that $\Delta_F = 0$ in blue diamonds and for points $\Delta \neq 0$ in the blue circles. For (c-d), $\tau = 0.2$. Figure adapted from Refs. [87] and [88].

and are given by $\mu_\ell = \mu_\ell + n\omega$. Starting from a initial state, $|\Psi_0\rangle$, the time-evolved state can be written as $|\Psi(n\tau)\rangle = \sum_i e^{-i\mu_i n\tau} |\mu_i\rangle \langle \mu_i | \Psi_0\rangle^2$.

Since the system is continuously absorbing heat from the driving, it may heat up to an infinite temperature state which does not carry any information about the unknown parameter h_0 [336]. This time is exponentially large for most of the generic integrable finite-size and disorder-free many-body systems. Thus, a lot of information about the unknown parameter is gathered by performing measurements at the intermediate time, especially at the transient time. For a system with partial accessibility, one can only perform measurement on a block of size L . This practical limitation makes the sensing even more challenging as due to entanglement between the spins in the block and the rest of the system some information might get lost. To investigate the sensing with partial accessibility, the QFI has to be computed for the reduced density matrix $\rho_L = \text{Tr}_{N-L}(|\Psi(t)\rangle\langle\Psi(t)|)$. This reaches a non-trivial steady-state which serves as a potential probe state.

For static field sensing, i.e., for estimating h_0 , the time-dependent external driving field $h(t) = h_1 \sin(\omega t)$ is used as a control field to enhance field sensitivity. The QFI of the reduced density matrix ρ_L with respect to h_0 , denoted as I_Q^{ss} , tends to a steady-state [87]. It is shown that I_Q^{ss} exhibits Floquet resonances at $h_0 = h_c + l\omega$, $l \in \mathbb{Z}$. Thus, at these points of h_0 , the I_Q^{ss} displays peaks, as can be seen in Fig. 12(a). Moreover, the driving of the system with certain frequency ω recovers the Heisenberg scaling of $I_Q^{ss} \sim L^{\beta(\omega)}$ as a function of L which is absent in the ground state. In the ground state the QFI I_Q^{gs} scales with L as $I_Q^{gs} \sim L^{1.68}$ as shown in Fig. 12(b). While for the steady-state, the exponent $\beta(\omega = 2) = 2.06$, obtained in Fig. 12(b).

Now for periodic field sensing, the Hamiltonian in Eq. (70) is taken to be a a transverse -field Ising model ($\gamma = 1$) with a time-dependent magnetic field of unknown amplitude h_1 added to the Hamiltonian [88]. For simplicity, the form is taken as Dirac-delta pulse $h(t) = h_1 \sum_{n=0}^{\infty} \delta(t - n\tau)$. The aim is to estimate the unknown amplitude h_1 . The I_Q^{ss} is maximum and has a peak along a line in the $(h_0 - h_1)$ plane. Interestingly, this line corresponds to the line of vanishing Floquet gap. Moreover, in the steady-state, the Fisher information I_Q^{ss} with respect to h_1 exhibits the Heisenberg type scaling $I_Q^{ss} \sim L^\beta$. An important finding is that at the location of the vanishing Floquet gap, the exponent $\beta \approx 1.96$ while for points where the Floquet phases do not cross, the exponent decreases towards the standard limit.

XI. NON-EQUILIBRIUM QUANTUM SENSING: DISSIPATIVE PHASE TRANSITIONS

Physical systems unavoidably interact with their environment, often referred to as the bath or reservoir, which possesses a larger number of degrees of freedom than the system of interest. The study of open quantum systems, which involves understanding the interaction between our system and the environment, has led to remarkable theoretical findings and practical applications [116]. However, the presence of noisy environments causes the systems to lose their coherence (decohere) and, consequently, results in unavoidable detrimental effects on their dynamics. This issue is particularly relevant for upcoming quantum technologies, as fighting against decoherence is essential for achieving more efficient quantum probes [337], developing algorithms for specific quantum tasks [338], and quantum simulators with significantly longer coherence times [339]. Given that the interaction between the relevant system and its environment is inevitable, one might wonder whether it is possible to overcome or harness the detrimental effects of decoherence.

A. Profiting from dissipation

Since non-classical states are crucial for countless applications and theoretical advances, it would be highly desirable to have a mechanism where instead of avoiding dissipation, one could harness the very process of dissipation to one's advantage. The seminal work by Alfred Kastler in 1950 pointed in that direction [340]. The process, known as *optical pumping*, prepares any initial quantum state into a well-defined target state via selection rules of spontaneous emission. Building on Kastler's work, *coherent population trapping* was experimentally demonstrated in the 1970s by Arimondo and Orriols [341, 342]. In a nutshell, a three-level energy configuration with transitions levels $|a\rangle \longleftrightarrow |b\rangle$ and $|a\rangle \longleftrightarrow |c\rangle$ and Hamiltonian $H = \hbar\Omega(|a\rangle\langle b| - |a\rangle\langle c| + h.c)$ allows for a quantum state with a zero eigenvalue (a *dark state*). Remarkably, such a dark state, denoted as $|\psi_a\rangle \sim |b\rangle + |c\rangle$, decouples from the external pumping field Ω , thus allowing excitations that reach that energy level to remain there. In contrast, the *bright state*, denoted as $|\psi_b\rangle \sim |b\rangle - |c\rangle$, oscillates with the driving field Ω and the state $|a\rangle$. Indeed, this idea lies at the heart of laser cooling [343] as the ground state represents another specific quantum state. The paradigm shift of harnessing dissipation as a resource rather than a drawback has led to systematic studies of decoherence itself [124], the ability to prepare a quantum state from any arbitrary initial state [123], the use of atomic engineered reservoirs to create two-mode Einstein-Podolsky-Rosen-entangled states [125, 126], protection against noise through the engineering of pointer states [344], dissipative quantum computation [345], the creation of many-body states and non-equilibrium quantum phases [346], quantum memories using dissipative mechanisms [347], the generation of Bell states on an open-system quantum simulator [348], and the possibility to enhance sensing precision nearly to the Heisenberg limit [337].

Other proposals include decoherence-free subspaces [119, 120, 349–351], dynamical decoupling [121, 122, 349, 352], and reservoir engineering techniques [123–126, 344–346]. The latter technique has been utilized to prepare maximally entangled states of two qubits [353, 354], W-states [355, 356], and many-body entangled states [357, 358]. In the continuous variable scenario, this technique allows the study of multi-mode entanglement [359, 360] and the preparation of steady entanglement in bosonic dissipative networks [361]. Notably, it also enables the generation of quantum many-body entangled states which remains robust in the presence of dephasing, thermal effects, and exhibits scalability and robustness against disorder in the model parameters [362].

These approaches could provide efficient solutions for the fields of quantum computation, quantum communication, and quantum metrology where long-lived quantum states and quantum correlations are essential.

B. Restoring quantum sensing advantage in noisy environments

The previous section demonstrates the ability to deterministically prepare strongly correlated multi-mode and many-body quantum states by harnessing dissipation. Generating such quantum states is particularly advantageous for advancing quantum metrology. For instance, in lossless optical interferometry, the use of N00N states $|\Psi_{N00N}\rangle \sim |N, 0\rangle + |0, N\rangle$ in Mach-Zender interferometers enables achieving the Heisenberg limit of precision for phase estimation. Therefore, the deterministic production of N00N states is highly desirable. However, even if the N00N state is faithfully prepared, the loss of a single excitation destroys all the information about the unknown phase. This poses a significant challenge for quantum state preparation, as unavoidable noise can severely undermine sensing precision, even if states are efficiently prepared. In fact, in the asymptotic limit of the number of photons $N \gg 1$, it has been proven that phase estimation in the presence of losses can only improve the phase sensitivity up to a certain factor [363, 364]. Similarly, S. Knysh et al. [365] demonstrated that in dissipative systems and in the asymptotic limit $N \gg 1$, the scaling with respect to the number of photons N transitions from the Heisenberg limit towards the shot-noise limit. Interestingly, the crossover between the Heisenberg-to-standard scaling is solely a function of dissipation.

One solution to overcome photon losses was experimentally demonstrated by M. Kacprowicz et al. [366]. They employed a modified N00N state of the form $|\psi\rangle = x_1|2, 0\rangle + x_2|0, 2\rangle + x_3|1, 1\rangle$ with non-negative weights x_i , which enhances the robustness of phase estimation in the presence of single excitation loss. Remarkably, even if one excitation is lost, the modified N00N state remains maximally entangled. However, it is essential to note that the above approach still falls under the category of quantum probe preparation.

A more fundamental route to overcome noisy metrology was proposed by B. M. Escher et al. [128]. Their proposal involves treating the system in addition to the environment as a whole unitary process, aiming to restore quantum-enhanced sensitivity. This approach entails an upper bound given by

$$C_Q[\rho_{S+E}(\lambda)] \equiv I_Q[\rho_{S+E}(\lambda)] \geq I_Q[\rho_S(\lambda)], \quad (72)$$

where $I_Q[\rho_{S+E}(\lambda)]$ represents the QFI of the joint system plus environment ($S + E$), and $I_Q[\rho_S(\lambda)]$ denotes the QFI of the system (S) only, i.e. with the environment traced out. This framework enables the retrieval of information lost in the environment. Such a general approach has found applications in lossy optical interferometry and atomic spectroscopy in the presence of dephasing [128], force and displacement estimation using a noisy quantum-mechanical oscillator probe [367], and in variational approaches [368]. The proposed general protocol in the extended space entails a purified evolution and, remarkably, demonstrates that there is always a pu-

rification channel such that one can restore the quantum-enhanced limit of precision. However, observing the joint system plus environment might be practically very challenging. Hence, finding an alternative feasible route is highly desirable.

C. Dissipative phase transition as a sensing resource

As opposed to zero temperature (zero entropy) phase transitions lead by quantum fluctuations, dissipative phase transitions emerge due to the competition between the unitary (Hamiltonian) and the non-unitary (Lindbladian) system's parameters [369]. Leading to a phase transition in the steady-state as this competition varies. Indeed, in the thermodynamic limit, the competition between external drivings, the Hamiltonian evolution, and the dissipation mechanisms can trigger a non-analytical change in the steady-state of the system [129]. One of the first studies on general properties of the dissipative phase transitions was addressed by Kessler et al., [370] by investigating the steady-state properties of the central spin model

$$\dot{\rho} = -i[H_{\text{CSS}}, \rho] + J\gamma \left(S^- \rho S^+ - \frac{1}{2} \{S^+ S^-, \rho\} \right), \quad (73)$$

where the central spin system (CSS) Hamiltonian $H_{\text{CSS}} = H_S + H_I + H_{SI}$ decomposes in $H_S = J\Omega(S^+ + S^-)$, $H_I = \delta\omega I_z$, and $H_{SI} = a/2(S^+ I^- + S^- I^+) + aS^+ S^- I_z$. In the above, S^α and I^α are the collective electron and nuclear spin operators, respectively. $J\Omega$ is the Rabi frequency, $\delta\omega$ is the difference of hyperfine detuning ω , a is the individual hyperfine coupling strength, and γ the dissipation rate [370]. Interestingly, the character of the dissipative phase transitions, which may entail pure or mixed quantum states, was describe by having one or more steady states and occur and conjectured to happen when the Liouvillian spectral gap closes for both the real and imaginary parts [370], see Table. I.

A more rigorous (general) theory of Liouvillian spectra analysis was indeed addressed by Minganti et al., [129], confirming that the Liouvillian gap, i.e., $\text{Re}[\lambda_1]$ such that the Liouvillian superoperator \mathcal{L} satisfies $\mathcal{L}\rho_i = \lambda_i\rho_i$, is $\text{Re}[\lambda_1] = 0$ only at the critical point if the transition is of the first-order [see Fig. 13(a)], whereas for the second-order type, $\text{Re}[\lambda_1] = 0$ in the whole region of broken symmetry [129] [see Fig. 13(b)]. Consequently, the steady state of the system exhibits a divergent susceptibility with respect to parameters of the system [370]. Other analyses include the use of the Keldysh formalism [371, 372] and numerical approaches [373, 374].

Intense theoretical work has been pursued to understand the critical behavior at the dissipative phase transition [225, 373, 375–381], including photonic systems [382–393], lossy polariton condensates [380, 394], and spin systems [369, 370, 377, 395–398]. In addition,

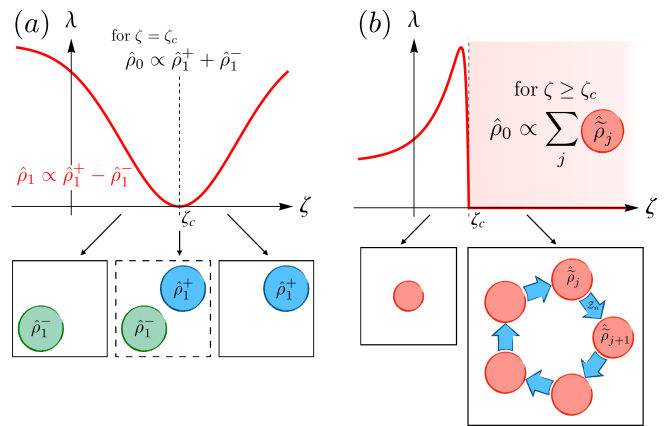


FIG. 13. Sketches illustrating the paradigms of first-order and second-order dissipative phase transitions: **(a) First-order case.** In the thermodynamic limit, both the real part $\text{Re}[\lambda_1]$ and the imaginary part $\text{Im}[\lambda_1]$ of the Liouvillian gap close when the parameter ζ (that triggers the transition) of the Liouvillian reaches its critical value ζ_c , i.e., $\zeta \simeq \zeta_c$. At the critical point $\zeta = \zeta_c$, the steady state $\hat{\rho}_{ss}$ is bimodal. Specifically, $\hat{\rho}_{ss}$ is a statistical mixture of $\hat{\rho}_1^+$ and $\hat{\rho}_1^-$, which represent two distinct phases of the system. **(b) Second-order case.** In the sketch, it is considered the breaking of a Z_n symmetry with $n = 5$. In the thermodynamic limit, the Liouvillian gap closes over the entire region $\zeta \geq \zeta_c$. Moreover, for $\zeta \geq \zeta_c$, all eigenvalues $\lambda_0, \lambda_1, \dots, \lambda_{n-1}$ of the Liouvillian are zero. When $\lambda \neq 0$ (here $\zeta < \zeta_c$), the steady-state density matrix $\hat{\rho}_{ss}$ is mono-modal. In the symmetry-broken phase ($\lambda = 0$ and $\zeta \geq \zeta_c$), $\hat{\rho}_{ss}$ is an n -modal statistical mixture of density matrices $\hat{\rho}_j$, which are mapped one onto the other under the action of the symmetry superoperator Z_n . Figure taken from [129].

exact steady-state expressions [386, 399, 400] and approximate methods for their evaluation based on variational approaches have been pursued [37, 401]. The presence of phase symmetry breaking in a single qubit-laser system [77], semiclassical first-order dissipative phase transition in Kerr parametric oscillators with parity symmetry breaking [38], and second-order transitions in the two-photon Kerr resonator [53]. The universality class of driven-dissipative systems has also been extensively addressed [372, 394, 398, 402, 403] with in-depth analysis of the phase diagram and critical exponents of a dissipative transverse Ising spin chain [404]. From a geometric perspective, the Uhlmann curvature has been proposed to shed light upon the nature of criticality [405], and a recent method based on the coherent anomaly approach has been proposed for determining critical exponents [406].

In addition to the above extensive theoretical findings, several experiments have already been realized in various systems, including trapped ions [407], ultra-cold atoms [78, 408–411], cavity-polariton [412, 413], superconducting circuits [82, 414], Rydberg atom ensembles [376, 415], to name a few.

Dissipative phase transitions have been extensively

	TPT	QPT	DPT
System operator	Hamiltonian $H = H^\dagger$	Hamiltonian $H = H^\dagger$	Liouvillian \mathcal{L} - Lindblad
Relevant quantity	Free energy $F(\rho) = \langle H \rangle_\rho - T \langle S \rangle_\rho$	Energy eigenvalues $E_\psi : H \psi\rangle = E_\psi \psi\rangle$	“Complex energy” eigenvalues $\lambda_\rho : \mathcal{L}\rho = \lambda_\rho \rho$
State	Gibbs state $\rho_T = \underset{\rho \geq 0, \text{Tr}(\rho)=1}{\text{argmin}} [F_\rho]$ $\rho_T \propto \exp[-H/k_B T]$	Ground state $ \psi_0\rangle = \underset{\ \psi\ =1}{\text{argmin}} [\langle \psi H \psi \rangle]$ $[H - E_{\psi_0}] \psi_0\rangle = 0$	Steady state $\rho_0 = \underset{\ \rho\ _{\text{tr}}=1}{\text{argmin}} [\ \mathcal{L}\rho\ _{\text{tr}}]$ $\mathcal{L}\rho_0 = 0$
Phase transition	Non-analyticity in $F(\rho_T)$	$\Delta = E_{\psi_1} - E_{\psi_0}$ vanishes	ADR = $\max[\text{Re}(\lambda_\rho)]$ vanishes

TABLE I. **Non-exhaustive comparison of thermal phase transitions (TPT), quantum phase transitions (QPT) and dissipative phase transitions (DPT):** The concepts for DPT parallel in many respects the considerations for QPT and TPT. $\|\cdot\|_{\text{tr}}$ denotes the trace norm and S the entropy. Note that if the steady state is not unique, additional steady states may come with a non-zero imaginary part of the eigenvalue and then appear in pairs: $\mathcal{L}\rho = \pm iy\rho$, ($y \in \mathbb{R}$). Table and caption taken from [370].

studied in quantum optics, particularly in the context of cooperative resonance fluorescence [416–421]. Notably, the quantum optical model used to explain cooperative resonance fluorescence has also been employed to investigate *Boundary Time Crystals* (BTCs), which are open quantum many-body systems situated at the boundary of a large bulk undergoing everlasting oscillations of a certain observable in the thermodynamic limit [422–424]. Time crystals are intriguing phenomena resulting from the breaking of time-translational symmetry [425–427]. They have been studied for both discrete and continuous temporal symmetry breakings.

Discrete time crystals and their potential for serving as quantum sensors in closed quantum systems were discussed in Sec. IX. Here, the focus is on the case of continuous symmetry breaking, which is responsible for the emergence of BTC, the Liouvillian spectral gap closes only for the real part, while the imaginary part forms band gaps [129, 422, 428], see Fig. 14. This is the most distinctive feature of BTC as the presence of bands give rise to everlasting oscillations in their stationary dynamics [422, 429]. BTCs have been studied using mean-field analysis [423] and through continuous monitoring [430]. Recently, a correspondence between second-order dissipative phase transitions and dissipative time crystals in the thermodynamic limit [428] and a thorough analysis of genuine multipartite correlations in a BTC have been put forward [431].

BTCs serve as valuable probes for addressing key issues in quantum sensors, namely: (i) they avoid the need for specific quantum many-body probe preparation through open dynamics and inherently benefit from dissipation, and (ii) an undemanding measurement basis can extract a fair fraction of the ultimate sensing. In concrete terms, the BTC probe is governed by the following non-unitary

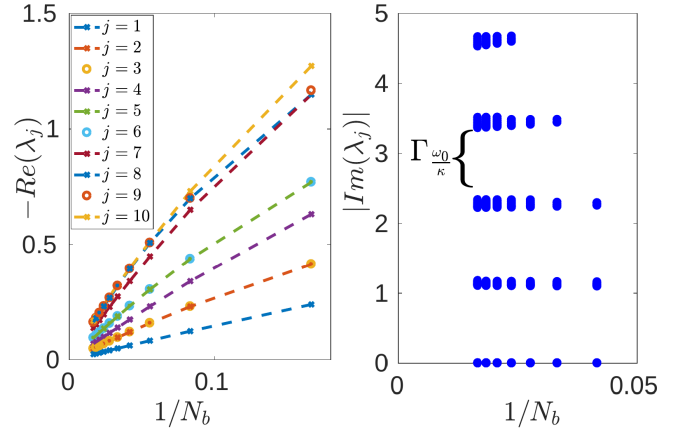


FIG. 14. **BTC Liouvillian spectra analysis: (Left)** Finite size scaling for the real part of the Liouvillian eigenvalues in the BTC phase. The index j labels the eigenvalues. The Liouvillian eigenvalues λ_j are ordered as a function of their real part ($|\text{Re}(\lambda_j)| \leq |\text{Re}(\lambda_{j+1})|$, and $j = 0$ has zero real part). In the $\omega_0/\kappa > 1$ phase, they scale to zero as a power-law of the inverse system size. **(Right)** The imaginary parts of the eigenvalues show a band structure, with a fundamental frequency separation $\Gamma_{\omega_0/\kappa}$. For fixed excitation thresholds (λ_j is selected such that $\nu = \frac{j^2}{N_b} \leq \epsilon$) [N_b being the system size of the boundary], the width of the bands remains finite in the thermodynamic limit (here $\nu < 0.025$). The widths of the bands tend to decrease as lower excitation thresholds are considered. The eigenvalues are plotted in units of κ . Figure taken from [422].

dynamics [416, 422, 423]

$$\frac{d}{dt}\rho = -i\omega[\hat{S}_x, \rho] + \frac{\kappa}{S} \left(\hat{S}_- \rho \hat{S}_+ - \frac{1}{2} \{ \hat{S}_+ \hat{S}_-, \rho \} \right) = \mathcal{L}[\rho], \quad (74)$$

where N non-interacting spin-1/2 particles are described by a (pseudo-)spin of length $S=N/2$. The collective an-

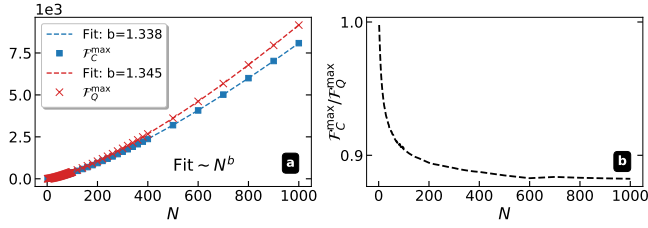


FIG. 15. **BTC quantum-enhanced sensing:** (a) Maximal quantum (classical) Fisher information \mathcal{F}_Q^{\max} (\mathcal{F}_C^{\max}) as a function of the system size N . Fitting functions with super-linear coefficient $b > 1$, evidencing quantum-enhanced sensing using a suboptimal observable. (b) Efficiency ratio $\mathcal{F}_C^{\max}/\mathcal{F}_Q^{\max}$ as a function of the system size N . Figure from [89].

gular momentum operators are given by $\hat{S}_\alpha = 1/2 \sum_j \sigma_\alpha^{(j)}$, where $\sigma_\alpha^{(j)}$ ($\alpha=x,y,z$) is the Pauli matrix at site j . In Eq. (74) ω is the single particle coherent splitting, $\mathcal{L}[\rho]$ is the Liouvillian operator, and κ is the effective collective emission rate. Deviations of Eq. (74), including local pumping and anisotropies in the coherent splitting, shows the robustness of such BTC probes even in this noisy case [432]. Such modified master equation faithfully represents state-of-the-art experiments [433, 434]. The steady-state $\rho_{SS} = \rho(t \rightarrow \infty)$ of the boundary undergoes a phase transition from an unbroken symmetry phase (determined by $\omega < \kappa$) to a boundary time crystal phase with everlasting total spin oscillations (determined by $\omega > \kappa$).

Quantum-enhanced sensitivity using the BTC probe of Eq. (74) can be evidenced in Fig. 15(a) via QFI analysis [89]. As seen from the figure, the maximum of the QFI \mathcal{F}_Q^{\max} grows polynomially with the system size N . A fitting function of the form $\mathcal{F}_Q^{\max} = aN^b + c$ ($c \rightarrow 0$) reveals a coefficient $b = 1.345$. Interestingly, in Fig. 15(a), a simple measurement basis of the total magnetization also scales super-linearly with the system size N . A fitting function of the same form as above exhibits quantum-enhanced sensitivity with a coefficient $b = 1.338$. To show the performance between the QFI and the classical Fisher information, in Fig. 15(b), the ratio between their maximum values is plotted, showing an asymptotic performance of 90% — a fair fraction achieved with a sub-optimal measurement basis.

XII. NON-EQUILIBRIUM QUANTUM SENSING: QUANTUM MANY-BODY SCARS AND SENSING

Quantum many-body scars (QMBSs) [435–437], observed in isolated interacting many-body systems, are known for violation of the eigenstate thermalization hypothesis [438–440] and, hence, exhibiting non-equilibrium dynamics. Recently, the potential applica-

tion of QMBSs in quantum sensing, using either their long-lived coherence time [441] or their strong multipartite entanglement [442, 443], has been identified. In Ref. [441], the authors consider N spin-1 particles in a 1D lattice with Dzyaloshinskii-Moriya interaction (DMI). The aim is to estimate the strength of an unknown magnetic field h which acts uniformly on particles. The Hamiltonian reads

$$H(\phi) = \sum_{i < j} \frac{J}{(i-j)^2} [\cos \phi (S_i^x S_j^x + S_i^y S_j^y) + \sin \phi (S_i^x S_j^y - S_i^y S_j^x)] + \frac{h}{2} \sum_{i=1}^N S_i^z, \quad (75)$$

where $S_i^{x,y,z}$ are the spin-1 operators, and J as the coupling strength. The interaction part of the Hamiltonian rotates between a pure XX interaction for $\phi=0, \pm\pi$ and DMI for $\phi = \pm\pi/2$. Spins that are prepared in the initial product state $|\psi_{t=0}\rangle = \otimes_{i=1}^N (|+1\rangle + |-1\rangle)/\sqrt{2}$ are allowed to evolve under the action of Hamiltonian H for a sensing time t . Then the local observable $\mathcal{O}_\theta = e^{-i\theta} \otimes_{i=1}^N (|+1\rangle\langle -1| + h.c.)$, with properly tuned θ , will be measured. In the absence of interaction between spins, i.e. $J=0$, the time evolved state can be obtained as $|\psi_t\rangle = \otimes_{i=1}^N (e^{-ith/2}|+1\rangle + e^{ith/2}|-1\rangle)/\sqrt{2}$ which results in the estimation error $\delta h = 1/\sqrt{NtT}$ without restriction on t . Generally, the interactions between the spins through generating entanglement and thermalization scramble quantum information irreversibly and, hence, deteriorate the sensing performance. In this case, one needs to complete the sensing task in an optimal time t^* which is much smaller than the thermalization time, resulting in the minimal value of the estimation error $\delta h^* = \min_t \delta h$. In Fig. 16(a), the minimal error δh^* , for optimal time t^* and $N=10$, as a function of ϕ and the coupling strength J is presented. Clearly, regardless of the interaction strength, the minimal error can be obtained for $\phi = \pm\pi/2$. For clarifying the relationship between all the parameters, in Figs. 16(b) and (c) for selected values of J and ϕ , the minimal error $\sqrt{T}\delta h^*$ is plotted. The numerical simulation (markers) are well fitted by the function $\delta h^* = 1.09/\sqrt{Nt^*T}$ (solid line). The same approach can be followed to formulate the optimal time of sensing t^* , see Figs. 16(d) and (e). The numerical simulation is well fitted by $t^* = 0.53/|J \cos \phi|$ (solid line). Clearly, for $\phi = \pm\pi/2$, i.e. when the interaction between spins is purely DMI, one has a diverging optimal sensing time $t^* \rightarrow \infty$ and its associated vanishing error, even for strong interactions. The origin of this quite surprising result is QMBSs, as it has been shown in Ref. [441]. For proving this connection, the authors start by introducing the spin-1/2 operators for two local basis states $|\pm 1\rangle$ of each spin-1 particle. The corresponding operators are $\tilde{S}_i^\pm = |\pm 1\rangle\langle \mp 1|$, and $\tilde{S}_i^z = [\tilde{S}_i^+, \tilde{S}_i^-]$ with the associated collective operators as $\mathcal{J}^\pm = \sum_i \tilde{S}_i^\pm$, and $\mathcal{J}^z = (1/2) \sum_i \tilde{S}_i^z$. It has been shown that the symmetric

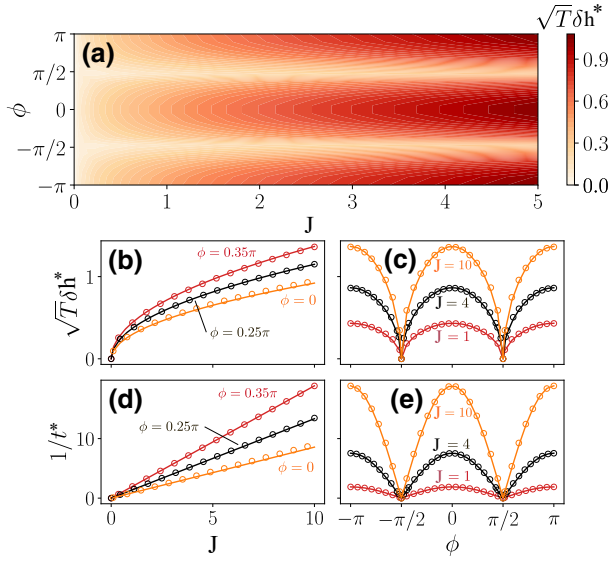


FIG. 16. **Quantum Scar based sensor;** (a) the minimal error δh^* obtained numerically for optimal sensing time t^* , in a system of size $N=10$, versus J and ϕ . (b) and (c), some cross-sections of panel (a). The numerical simulation (markers) is well fitted by the function $\delta h^* = 1.09/\sqrt{Nt^*T}$ (solid line). (d) and (e) the optimal sensing time t^* and its behavior for different values of the coupling strength J and ϕ . The numerical simulation (markers) can be closely described by the fitting function $t^* = 0.53/|J \cos \phi|$ (solid line). This figure is adapted from Ref. [441].

Dicke states $\{|\psi(s)\rangle\}_{s=0}^N$ defined as

$$|\psi(s)\rangle = \sqrt{\frac{(N-s)!}{s!N!}} (\mathcal{J}^+)^s (\otimes_{i=1}^N |-1\rangle) \quad (76)$$

are the scar states of Hamiltonian Eq. (75) with $\phi = \pm \pi/2$ [444]. In other words, the eigenstates $|\psi(s)\rangle$, defined by $H(\phi = \pm \pi/2)|\psi(s)\rangle = h(s - N/2)|\psi(s)\rangle$, violate the eigenstate thermalization hypothesis as they show a subvolume-law entanglement growth. Rewriting the initial product state $|\psi_{t=0}\rangle = \otimes_{i=1}^N (|+1\rangle + |-1\rangle)/\sqrt{2}$ in terms of the elements of the Dicke-scar subspace results in $|\psi_{t=0}\rangle = \sum_{s=0}^N \sqrt{\frac{N!}{2^N s!(N-s)!}} |\psi(s)\rangle$. The time-evolved state in this subspace is obtained as $|\psi_t^*\rangle = \otimes_{i=1}^N (e^{-it^*h/2}|+1\rangle + e^{it^*h/2}|-1\rangle)/\sqrt{2}$ results in $\delta\lambda = 1/\sqrt{Nt^*T}$, despite the presence of strong interaction. Therefore, the initial state which is prepared in the Dicke-scar subspace of Hamiltonian $H(\phi = \pm \pi/2)$ can result in a vanishing estimation error via its long-lived coherence property $t^* \rightarrow \infty$. More discussion on the advanced role of quantum many-body scar in quantum-enhanced sensing can be found in Refs. [441–443].

XIII. NON-EQUILIBRIUM QUANTUM SENSING: SEQUENTIAL MEASUREMENTS METROLOGY

Previous sections have demonstrated that placing the probe at the critical point of a general phase transition or a special highly entangled state, such as GHZ-type and N00N-type states, leads to quantum-enhanced sensitivity—see Secs. IV–VII for more details. These sensing advantages primarily exploit quantum superposition to achieve enhanced sensitivity. However, not all quantum probes experience a phase transition, and experimental limitations prevent us from generating arbitrary superpositions of many-body states. Therefore, it becomes essential to explore other features of quantum mechanics to attain quantum sensing advantages.

Measurement represents another distinct feature that sets apart the classical from the quantum world. Indeed, the concept of wave-function collapse due to projective measurements on the quantum system has sparked several discussions within quantum theory itself [445–448]. In quantum many-body probes with partial accessibility, measurements can only be conducted locally on a subsystem. However, in these scenarios, even though the measurement is local, the wave function collapse is global and affects the entire system’s wave function. This intriguing phenomenon has been the subject of intensive studies [449–458], such as a unique feature for quenching many-body systems [105, 106, 459, 460], leading to potential new types of phase transitions [107, 461–465].

In conventional sensing strategies, data is collected through independent and identical (IID) probability distributions. This means that after measuring the probe, one needs to reset it to its original quantum state for another round of experiments or, equivalently, use identical copies. Note that the formulation of the Cramér-Rao inequality (see Eq. (2)) assumes the resetting of the probe after each measurement or equivalently using M identical probes at once. A simple yet versatile sensing strategy has been devised using sequential measurements on the probe at regular time intervals [466–471]. This innovative sequential sensing scheme is of significant importance in quantum metrology for several reasons: (i) it avoids extremely time-consuming resetting times, (ii) it avoids the need for highly correlated or complex initial states, and (iii) available experimental measurements suffice for evidencing quantum-enhanced sensitivity. The sequential measurement sensing scheme, see Fig. 17, is an iterative sensing protocol:

- (i) A quantum probe $\rho^{(i)}(0)$ freely evolves to $\rho^{(i)}(\tau_i)$,
- (ii) At time τ_i a positive operator-valued measure (POVM) $\Upsilon_{\gamma_i} = \Pi_{\gamma_i}^\dagger \Pi_{\gamma_i}$, where $\Upsilon_{\gamma_i} \geq 0$ and $\{\Upsilon_{\gamma_i}\}$ are the elements of the POVM with random outcome γ_i , is performed on the probe, updating the quantum state into

$$\rho^{(i+1)}(0) = \frac{\Pi_{\gamma_i} \rho^{(i)}(\tau_i) \Pi_{\gamma_i}^\dagger}{p(\gamma_i)}, \quad (77)$$

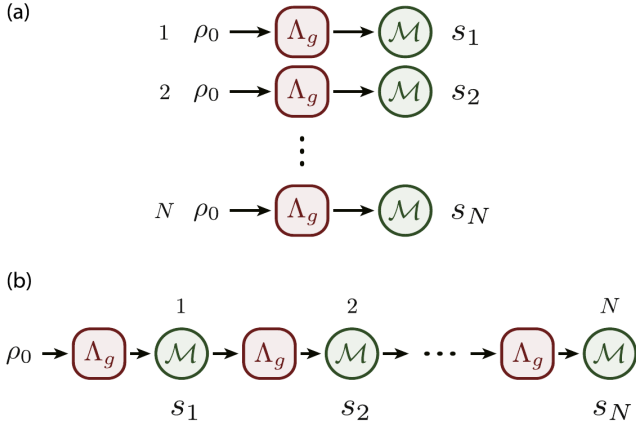


FIG. 17. **Comparison between standard and sequential measurements sensing strategies:** (a) Standard strategy for estimating a parameter g of a quantum system, where measurement data $\{s_1, \dots, s_N\}$ are collected by *independent and identical* experiments. Every time the experiment is performed, the system is reset to some specific known initial state ρ_0 . (b) Sequential scheme for estimating a parameter g of a quantum system, where the measurements are performed sequentially to collect data $\{s_1, \dots, s_N\}$ *without resetting the state of the system every after the measurement* and the initial state ρ_0 can be arbitrary. Figure taken from [466].

where

$$p(\gamma_i) = \text{Tr}[\Pi_{\gamma_i} \rho^{(i)}(\tau_i) \Pi_{\gamma_i}^\dagger], \quad (78)$$

is the probability associated to γ_i at step i ,

- (iii) The outcome γ_i is recorded and the new initial state $\rho^{(i+1)}(0)$ is replaced in (i),
- (iv) The above steps are repeated until n_{seq} measurements outcomes are consecutively obtained,
- (v) After gathering a data sequence $\boldsymbol{\gamma} = (\gamma_1, \dots, \gamma_{n_{\text{seq}}})$, the probe is reset to ρ_0 and the process is repeated to generate a new trajectory.

In general, the data collected from sequential measurements are non-IID, meaning that the measurement data are not independent of each other—i.e., one deals with effectively different probes at each measurement step. It is essential to emphasize that, unlike standard sensing schemes, there is no need for specific maximally entangled probe, the need for supporting quantum phases, feedback mechanisms, or quantum control. Naturally, standard sensing scheme reduces to the particular case of $n_{\text{seq}}=1$.

By harnessing the sequential measurements followed by free evolution at regular time intervals, the sequential sensing scheme has led to significant advancements, including Hamiltonian identification [472], sequential measurements sensing schemes [466, 468, 473–488].

Quantum-enhanced magnetometry powered by sequential measurements sensing in quantum many-body probes has been investigated for short number of sequential measurement sequences. An unknown local magnetic

field $\mathbf{B}=(B_x, 0, B_z)$ is aimed to be estimated using N interacting spin-1/2 particles with Heisenberg Hamiltonian [469]

$$H = -J \sum_{j=1}^{N-1} \boldsymbol{\sigma}_j \cdot \boldsymbol{\sigma}_{j+1} + B_x \sigma_1^x + B_z \sigma_1^z, \quad (79)$$

where $\boldsymbol{\sigma}_j=(\sigma_j^x, \sigma_j^y, \sigma_j^z)$ represents a vector composed of Pauli matrices acting on qubit site j , J denotes the exchange interaction, and $\mathbf{B}=(B_x, 0, B_z)$ stands for the local magnetic field to be estimated located at first site. For the sake of simplicity, a ferromagnetic state $|\psi(0)\rangle = |\downarrow\downarrow\downarrow\dots\rangle$ is probed at site N in the σ_z basis at regular time intervals $J\tau = N$. The latter allows enough time for the quantum correlations to spread throughout the spin chain. It has been shown [469] that a *synchronization-like* magnetization dynamics occurs between the first and last sites. This opens up the possibility of extracting information about the local magnetic field (located at the first site) by observing the dynamics of the readout qubit (located at the last N site). Remote sensing holds special significance in biology, where non-invasive sampling of organic tissues is desirable to protect the biological material (see quantum illumination techniques [156]).

From a practical perspective, both measuring and initializing the probe at each sequential step consume time, which is a crucial resource in actual experiments. Sequential measurements metrology accounts for these technical constraints straightforwardly by considering the total interrogation time as follows:

$$T = M(t_{\text{init}} + t_{\text{evo}} + t_{\text{meas}} n_{\text{seq}}), \quad (80)$$

where t_{init} , t_{evo} , and t_{meas} are the initialization, evolution, and measurement times, respectively. Typically, $t_{\text{init}} \gg t_{\text{meas}} \gg t_{\text{evo}}$. Eq. (80) shows that for a fixed total time T , increasing the number of sequences n_{seq} reduces the number of sequential trials M . However, the total number of measurements $M \times n_{\text{seq}}$ increases with an increase in n_{seq} for a fixed time T . By introducing the dimensionless average squared relative error given by: $\delta B_x^2 = \int f(\widehat{B}_x | \boldsymbol{\Gamma}) (|\widehat{B}_x - B_x| / |B_x|)^2 d\widehat{B}_x$, where $f(\widehat{B}_x | \boldsymbol{\Gamma})$ is the posterior distribution of obtaining B_x given the observed data $\boldsymbol{\Gamma} = \boldsymbol{\gamma}_1, \boldsymbol{\gamma}_2, \dots, \boldsymbol{\gamma}_M$, where each sequential run $\boldsymbol{\gamma}_k$ contains n_{seq} spin outcomes, and $|\widehat{B}_x - B_x| / |B_x|$ corresponds to the relative error of the estimation. δB_x^2 accounts for both the uncertainty and the bias in the estimation simultaneously. For short number of sequential measurements, it has been shown that a suitable fitting function of the form $\delta B_x^2 \sim T^{-\nu} n_{\text{seq}}^{-\beta}$ with $\nu = 1$ and $\beta > 1$, evidences quantum-enhanced sensitivity for estimating B_x with respect to the number of sequential measurements n_{seq} and a given total protocol time T . Hence, one can consistently achieve higher sensitivity by employing sequential projective measurements on a probe subsystem for a finite and experimental-friendly sequence of measurements.

Despite the above, the investigation of sequential measurement sensing schemes is usually limited to short

lengths of measurement sequences due to the exponential growth of measurement outcomes with the number of sequences— $(2^N)^q$ for N measurements on q spins. Thus, evaluating all probabilities distributions becomes intractable. For estimating sensing precision with a large number of sequential measurements, indirect approaches have been proposed, such as functional analysis of the measurement outcomes, showing a Fisher information increasing linearly with the number of sequential measurements n_{seq} [466], namely $I_C(\lambda) \simeq \frac{n_{\text{seq}}}{\sigma^2} (\partial_\lambda \langle S \rangle_*)^2$, or via correlated stochastic processes [489]. Moreover, single-trajectory based sensing [470, 490] utilizing maximum-likelihood estimators [491] (with convergence proof [492]) has recently been proposed. This approach demonstrates that a single sequential run (a trajectory) with $n_{\text{seq}} \gg 1$ is enough to achieve estimation with arbitrary precision. Recently, using a Monte Carlo methodology, a comprehensive analysis of sequential measurements metrology for $n_{\text{seq}} \gg 1$ has been presented. This analysis evaluates the increment in Fisher information as [493]:

$$\mathcal{F}_\lambda^{(n)} = \mathcal{F}_\lambda^{(n-1)} + \Delta \mathcal{F}_\lambda^{(n)}; \quad \Delta \mathcal{F}_\lambda^{(n)} := \sum_\gamma P_\gamma f_\lambda^{\gamma, (n)}, \quad (81)$$

where $\mathcal{F}_\lambda^{(j)}$ represents the classical Fisher information at step j , $\Delta \mathcal{F}_\lambda^{(n)}$ is the increment of the classical Fisher information after performing one more measurement following the recording of $(n-1)$ measurements, and $f_\lambda^{\gamma, (n)}$ is the classical Fisher information obtained from the n -th measurement $p(\gamma_n)$ in trajectory γ . Utilizing this approach, one can examine the behavior of the classical Fisher information for arbitrarily large numbers of sequential measurements. Conducting local projections on a quantum many-body probe leads to probe's finite memory, attributed to repeated local projections and free evolution, resulting in a rank-1 matrix [493]. This probe's finite memory is linked to the transition from super-linear to linear scaling of classical Fisher information. After losing memory of an early state, classical Fisher information scales linearly with n_{seq} , limiting the extractable information capacity of the quantum probe in sequential measurements.

For the quantum many-body probe described in Eq. (79), Figs. 18(a)-(b) demonstrate a correspondence between the transition from super-linear to linear scaling of classical Fisher information and the probe's finite memory. Specifically, the classical Fisher information increment $\Delta F_B^{(n_{\text{seq}})}$ becomes nearly constant at around the same n_{seq} where the averaged fidelity $\langle F \rangle_{\text{traj}}$ also becomes nearly constant. This averaged fidelity measures the similarity between two distinct initial states following the same trajectory [493] (a single trajectory is composed of n_{seq} measurement steps). In Fig. 18(c), the classical Fisher information $\mathcal{F}_B^{(n_{\text{seq}})}$ is plotted as a function of n_{seq} . This plot clearly shows a transition from non-linear to linear behavior, in agreement with the quantum-enhanced sensing shown for short sequential measurements [469] and the linear scaling with indirect methods for large

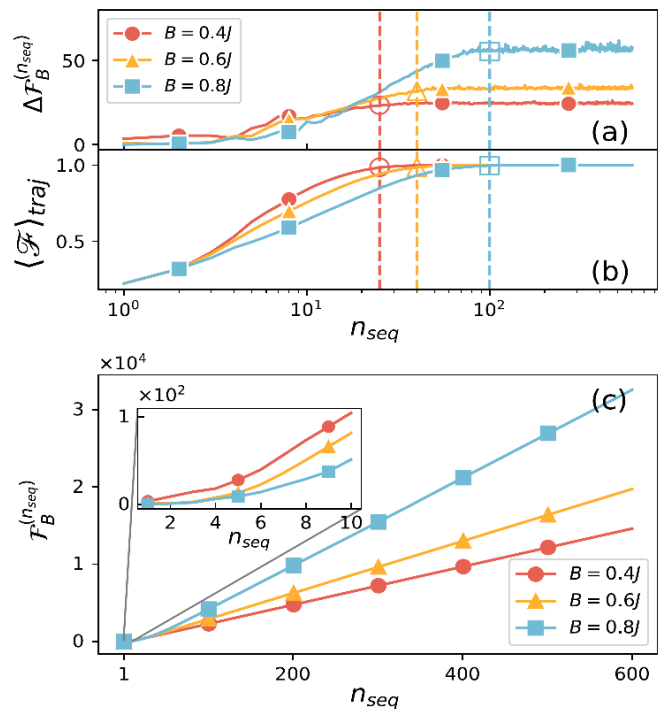


FIG. 18. **Sequential measurements metrology for the quantum-many body probe of Eq. (79) and large number of consecutive measurements n_{seq} :** (a) Classical Fisher information increment $\Delta F_B^{(n_{\text{seq}})}$ as a function of n_{seq} , (b) Fidelity averaged over 10^4 different trajectories (each trajectory evaluates the fidelity between two distinct initial states following the same trajectory) as a function of n_{seq} , (c) classical Fisher information $\mathcal{F}_B^{(n_{\text{seq}})}$ as a function of n_{seq} . Figure taken from [493].

n_{seq} [457]. The Monte Carlo-based methodology discussed above for arbitrarily large n_{seq} it has been addressed for both quantum many-body probes and light-matter probes [493].

XIV. GLOBAL SENSING: PARAMETER ESTIMATION WITH MINIMAL PRIOR INFORMATION

An implicit assumption underlies all preceding discussions: the assumption that sufficient information about both the unknown parameter of interest and the control parameters is available beforehand. This scenario is known as *local estimation theory* [147, 149, 150, 160, 494–496], where the unknown parameter varies within a very narrow interval. It is important to note that the limitations of local estimation theory have been identified in a wide range of contexts. This is because the Cramér-Rao inequality of Eq. (2) presents some subtleties, including: (i) although the bound performs excellently for unbiased estimators, a typical unbiased estimator, such as the maximum likelihood, is sometimes infeasible due

to the large data set needed to saturate the bound asymptotically [497] (see also Rubio et al. [161, 162] for metrology with limited data). Furthermore, in practice, most estimators are biased [498]; (ii) regularity conditions of the Cramér-Rao bound are hard to verify [499]; and (iii) a limiting variance may not coincide with the variance of a limiting distribution [498].

In contrast to local estimation theory, *global estimation theory* applies when no prior information is available. Therefore, the unknown parameter varies within a broader sensing interval. Consequently, the choice of measurement to be performed on the probe and the analysis of the estimation data should be optimal on average, that is it should be equally effective for any possible value of the parameter [147, 148].

One of the earliest studies on global sensing, aimed at overcoming the limitations of local estimation theory, was proposed by van Trees [498, 500] (a stronger type of inequality is also provided by Klaassen [501]). The van Trees inequality addresses the comprehensive concept of global sensing, where the unknown parameter λ varies according to some prior distribution $z(\lambda)$, determining that the average variance is given by the Bayesian Cramér-Rao bound or posterior Cramér-Rao bound [130, 500]:

$$\overline{\text{Var}[\hat{\lambda}]} = \int z(\lambda) \left[\hat{\Lambda}(x) - \lambda \right]^2 dx d\lambda \geq \frac{1}{Z_F}, \quad (82)$$

where $\hat{\Lambda}(x)$ is the estimator of λ (mapped from the measurement outcomes x), and Z_F can be demonstrated to be

$$Z_F = \int z(\lambda) I(\lambda) d\lambda + M \int z(\lambda) [\partial_\lambda \log z(\lambda)]^2 d\lambda, \quad (83)$$

where the first term accounts for the average of the classical Fisher information over the prior distribution $z(\lambda)$ and the second term is the classical Fisher information of the prior distribution itself [500]. A quantum bound can also be derived [130] by substituting $I(\lambda)$ with $I_Q(\lambda)$. A very narrow prior distribution reduces Z_F to the local classical Fisher information bound, i.e., $\int z(\lambda) I(\lambda) d\lambda \rightarrow I(\lambda)$. Examples of van Trees global estimation are: collisional thermometry (where a series of ancillas is sent sequentially to probe the system's temperature) utilizing Bayesian inference, and the significance of prior information using the modified Cramér-Rao bound associated with van Trees and Schützenberger [502]; Bayesian thermometry approach based on the concept of thermodynamic length, applicable in the regime of non-negligible prior temperature uncertainty and limited measurement data, exemplified using a probe of non-interacting thermal spin-1/2 particles [503]; ultimate bounds in Bayesian thermometry approach for arbitrary interactions and measurement schemes (including adaptive protocols) are explored. Notably, a derivation of a no-go theorem for non-adaptive protocols that does not allow for better than linear (shot-noise-like) scaling, even having access to arbitrary many-body interactions, is presented [504].

Note that, in general, van Trees bound is not tight and cannot be saturated. To achieve a tighter bound a systematic and general metric evaluating the performance of global sensing and its significance for quantum many-body probes with criticality has been examined in Ref. [51]. The global sensing procedure involves considering a modified quantum Cramér-Rao bound, which introduces the average uncertainty of the estimation as follows:

$$\overline{\delta\lambda^2} := \int_{\Delta\lambda} \delta\lambda^2 z(\lambda) d\lambda \geq g(\mathbf{B}) := \int_{\Delta\lambda} \frac{z(\lambda)}{M\mathcal{I}_Q(\lambda|\mathbf{B})} d\lambda, \quad (84)$$

where $z(\lambda)$ is the prior distribution of the unknown parameter λ to be sensed, M is the number of measurements, $\mathcal{I}_Q(\lambda|\mathbf{B})$ is the QFI, $\mathbf{B}=(B_1, B_2, \dots)$ are external tunable parameters interacting with the probe, and the unknown parameter varies over a sensing interval

$$\Delta\lambda \in [\lambda^{\min}, \lambda^{\max}], \quad \text{with} \quad \lambda^{\text{cen}} := \frac{\lambda^{\min} + \lambda^{\max}}{2}. \quad (85)$$

The minimization of the right-hand side of Eq. (84) with respect to the control parameters \mathbf{B} defines the figure of merit for determining the optimal probe, namely:

$$g(\mathbf{B}^*) := \min_{\mathbf{B}} [g(\mathbf{B})]. \quad (86)$$

Note that, in general, the optimal measurement basis varies across $\Delta\lambda$, and no measurement setup can saturate the modified global Cramér-Rao bound of Eq. (84) over the entire interval. Note that it has been proven that the van Trees inequality is always smaller than the mean classical Cramér-Rao lower bound, that is [505]: $\overline{\text{Var}[\hat{\lambda}]} \geq \int z(\lambda) \frac{1}{I(\lambda)} d\lambda \geq \frac{1}{Z_F}$. This indeed shows that the average uncertainty g is a tighter bound than the one given by the Van Trees.

Eq. (86) has been evaluated for the transverse Ising quantum many-body probe:

$$H = J \sum_{i=1}^L \sigma_x^i \sigma_x^{i+1} - \sum_{i=1}^L (B_z + \lambda_z) \sigma_z^i, \quad (87)$$

where L is the system size, σ_α^i ($\alpha=x, z$) represents the Pauli operator at site i , $J > 0$ denotes the exchange interaction, B_z corresponds to the controllable magnetic field that can be adjusted, λ_z stands for the field to be estimated, and periodic boundary conditions are imposed. Assuming that the unknown parameter varies over a wide region $\Delta\lambda_z$, the protocol introduced in Ref. [51] systematically optimizes the quantum many-body probe to deliver the best sensitivity performance on average. In the case of single-parameter estimation, the control field B_z acts as an offset of the critical point, see Fig. 19(a). However, when the phase diagram becomes more complex or in the presence of multi-parameter estimation, such an offset becomes non-trivial, see Fig. 19(b).

By defining the size of the probe L as the relevant sensing resource, it has been demonstrated that the QFI

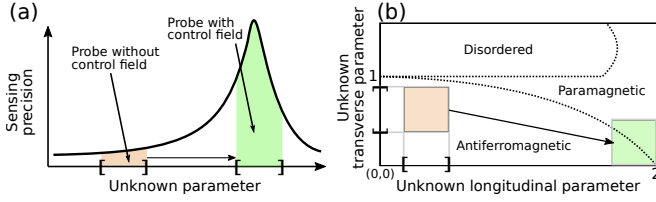


FIG. 19. **Sketch of phase diagram and the role of global sensing:** (a) The global sensing scheme tunes the quantum probe to operate optimally on average. This procedure ensures that the control fields will optimize the probe to exploit the critical point. (b) As the phase diagram becomes more complex, the probe’s offset becomes non-trivial. In general, the minimization of $g(\mathbf{B})$ (see Eq. (84)) systematically optimizes the probe to exploit criticality across the entire phase diagram. Figure taken from [51].

scales super-linearly with L over a moderate wide interval of $\Delta\lambda_z$ [51]. Fig. 20(a) shows the fitting coefficients a and b obtained from the fitting function $g(B_z^*, \Delta\lambda_z) \sim aL^{-b} + c$, as a function of the interval $\Delta\lambda_z/J$. Here, $\Delta\lambda_z/J \rightarrow 0$ represents local sensing. As the figure illustrates, the b coefficient decreases from the (expected) Heisenberg limit ($b = 2$) to the standard limit ($b = 1$) as the interval $\Delta\lambda_z$ increases. The global sensing protocol still demonstrates quantum-enhanced sensitivity for sensing intervals $0 \leq \Delta\lambda_z \lesssim 0.07J$. In Fig. 20(b), even under the seemingly standard limit (i.e., $b = 1$), the global sensing strategy still delivers superior sensing precision compared to a non-optimized probe. This superiority arises from the global sensing strategy, which ensures probe optimization by minimizing $g(\mathbf{B})$ over the prior distribution.

Thermometry, the process of estimating the temperature of a sample, plays a crucial role in quantum thermodynamics [506, 507] and has various applications, such as determining macroscopic objects in their ground state [508, 509]. In certain scenarios, local estimation for thermometry may not be sufficient, making an alternative estimation strategy highly important. Note that the bound in Eq. (84) may not be saturated as, in general, the optimal measurement setup vary for different values of the unknown parameter λ . In some cases that the optimal measurement is not a function of λ the bound can indeed be saturated. An example of such scenario is thermometry for which energy measurement is optimal, independent of the temperature of the system. This allows to design an optimal probe for measuring temperature over an arbitrary interval. In Ref. [510], it is shown that optimization of the probe reduces to optimizing the energy eigenvalues. Interestingly, for the case of local thermometry, where temperature varies over a narrow interval, the optimal probe contains only two distinct eigenenergies, with a unique ground state and full degeneracy for the rest of the spectrum. The energy gap between the ground state and the rest of the spectrum depends on the temperature [511] and can be obtained by solving a nonlinear equation [510]. Using the global

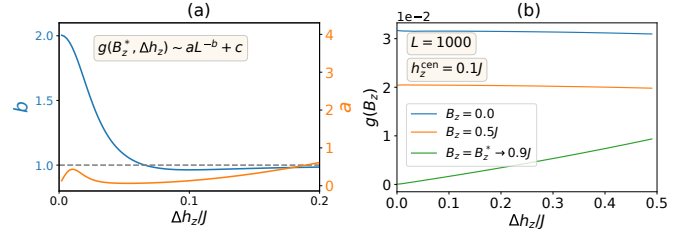


FIG. 20. **Global sensing for transverse Ising quantum many-body probe** (a) Fitting coefficients a and b as a function of $\Delta\lambda_z/J$. A smooth transition from the Heisenberg limit ($b = 2$) to the standard limit ($b = 1$) is observed. Notably, for a prior distribution as wide as $0 \leq \Delta\lambda_z/J \lesssim 0.07$, the global sensor still delivers quantum-enhanced sensitivity ($b > 1$). (b) Minimizing the average uncertainty $g(B_z)$ always results in better sensitivity when compared to a probe without applying control fields. Figure taken from [51].

sensing formulation of Eq. (84), one can show that the optimal probe requires more distinct energy eigenvalues as the temperature varies over a larger interval [512]. In fact, through exploiting an evolutionary algorithm the authors of Ref. [512] find out that an effective two-level probe for local sensing turns into a three-level system with the two lowest energy eigenvalues being unique and then the rest of the spectrum gets fully degenerate as the temperature interval increases. By further enhancing the interval more and more energy levels are separated from the degenerate band. It is worth emphasizing that the bounds, given by Eq. (84) can be saturated for all these optimal thermometers.

While both the van Trees and the average uncertainty approaches focus on minimizing the variance of estimation, a new formalism for global thermometry has been developed based on minimization of the mean logarithmic error. By exploiting scale invariance and other well-behaved properties, such as symmetric invariance and monotonicity increment (decrement) from (towards) the actual hypothesis temperature value [513], the mean logarithmic error $\bar{\epsilon}_{\text{mle}}$ is defined as the global thermometry figure of merit when the temperature varies over a prior distribution

$$\bar{\epsilon}_{\text{mle}} = \int p(E, \theta) \log^2 \left[\frac{\tilde{\Theta}(E)}{\theta} \right] dE d\theta. \quad (88)$$

In the above, E is the energy, θ is the hypothesis for the true temperature T , $p(E, \theta) = p(E|\theta)p(\theta)$ their joint probability, and $\tilde{\Theta}(E)$ the optimal estimator of T given by

$$\frac{k_B \tilde{\Theta}(E)}{\epsilon_0} = \exp \left[\int p(\theta|E) \log \left(\frac{k_B \theta}{\epsilon_0} \right) d\theta \right], \quad (89)$$

with k_B the Boltzmann constant, ϵ_0 an arbitrary constant with energy units, and $p(\theta|E)$ the posterior function given by the Bayes rule $p(\theta|E) = p(E|\theta)p(\theta)/p(E)$. Notably, the mean logarithmic error $\bar{\epsilon}_{\text{mle}}$ applies to both

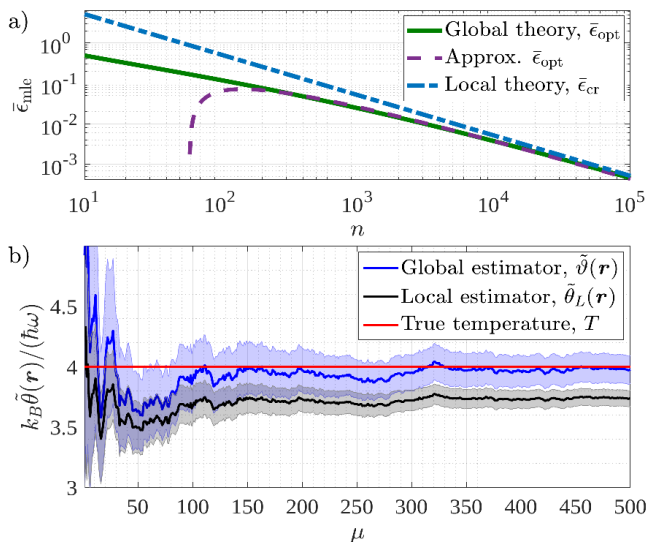


FIG. 21. **Global sensing for temperature estimation:** (a) Log-log plot of the global optimum $\bar{\epsilon}_{\text{opt}}$ and local Cramér–Rao-like bound (dot-dashed blue) for a gas of n non-interacting spin-1/2 particles in thermal equilibrium. The global optimum is lower than the local bound unless $n \rightarrow \infty$, indicating that the local bound misses information for small n . (b) Data analysis in global thermometry. The global estimate converges to the true temperature after $\mu \simeq 10^2$ shots (μ are energy measurements on the n -spin gas). In contrast, the local theory leads to a biased estimate even for $\mu \simeq 500$. Figure taken from [513].

biased and unbiased estimators. Furthermore, to observe the failure of local thermometry and the performance of the global quantum thermometer, refer to the example using the mean logarithmic error for a non-interacting gas of n spin-1/2 particles at thermal equilibrium in Ref. [513], see Fig. 21.

XV. SUMMARY AND OUTLOOK

Exploiting quantum features, such as entanglement, can enhance the precision of a sensor well-beyond the capacity of a classical sensor, the so-called quantum-enhanced sensing. Such enhanced in precision has placed quantum sensing as one of the pillars of emerging quantum technologies. In addition to such enhancement, the size versatility of quantum probes allows for achieving extremely high spatial resolution. The potential applications are immense covering from biological monitoring to mining, atomic clocks, navigation and space exploration.

Interferometric quantum sensing has been the first demonstration of entanglement as a resource for sensing purposes. These types of sensors are very susceptible to decoherence and any interaction between particles is detrimental for their precision. An alternative approach is to exploit quantum many-body systems for sensing. Unlike interferometry-based quantum sensors, in many-

body probes interaction plays a crucial role. In this review, we have explored different aspects of quantum sensing using many-body systems.

Quantum many-body sensors have been used in two scenarios, namely equilibrium and non-equilibrium. In the former, quantum criticality has been identified as a resource for achieving quantum enhanced sensitivity. There are several types of quantum criticalities, each with their own characteristics. However, in order to achieve quantum enhanced sensitivity the criticality has to be accompanied by some sort of gap closing, for instance, Hamiltonian or Liouvillian spectral gap closing. This remarkable feature can be a useful guideline for identifying potential quantum sensors in new materials, which might be even designed by artificial intelligence. Although criticality-based quantum sensors offer several advantages, they also come with some drawbacks. First, the region over which quantum enhanced precision is achievable can be very narrow, requiring probe’s fine tuning. Second, preparing the probe near its critical point can be very resource-consuming because the preparation process slows down significantly as it approaches criticality. In order to avoid these drawbacks, non-equilibrium quantum probes have also been proposed. In such systems quantum superposition and entanglement can be generated during the dynamics and thus complex initialization is not needed. Moreover, in non-equilibrium quantum probes, the evolution time acts as an additional parameter that can be used as a resource to enhance precision. In fact, the precision is often enhanced monotonically as time goes on. Nonetheless, unlike criticality-based sensors, in non-equilibrium probes the criteria for achieving quantum enhanced sensitivity with respect to resources, e.g. system size, is not well-characterized. We summarize the advantages and disadvantages of each approach in Table II.

Despite current progress on many-body quantum sensing, there are still several open problems to explore. While criticality has been identified as a resource for sensing in equilibrium scenarios, the criteria which results in quantum enhanced sensing is not specified in non-equilibrium probes. Another problem which requires further investigation is the performance of quantum sensors under imperfect situations, such as the presence of decoherence. In general terms, while quantum sensors are naturally expected to be sensitive to the desired parameters, we would like them to be robust against other system’s parameters or noisy imperfections. Despite several works on noisy quantum metrology [312, 314, 514–522], the notion of robustness has not yet been formulated quantitatively for quantum sensors. Furthermore, a general issue for quantum sensors arise in the multi-parameter Cramér-Rao inequality as the bounds are not tight and thus saturating them may not be achievable. Developing tighter bounds and strategies towards achieving them in many-body sensors require closer connections between quantum metrology and control theory. One important problem in multi-parameter sensing is the sit-

Sensing Strategy	Pros	Cons
Inteferometric Quantum Sensors		
External parameter is induced by phase shift $U(\theta) = e^{i\theta G}$	1. Heisenberg scaling possible 2. Universal optimal measurement	1. Difficult preparation 2. Sensitive to decoherence and particle loss 3. Works only for phase shift operations
Many-Body Quantum Sensors at Equilibrium		
Ground or Thermal State based for Hamiltonians of the form $H=H_0+H_1(\theta)$	1. Quantum enhanced sensitivity achievable by gap-closing phase transitions 2. Super-Heisenberg scaling possible 3. Robust against imperfections	1. Fine tuning is needed (local sensing) 2. Optimal measurement parameter-value dependent 3. Preparation might be resource consuming
Non-Equilibrium Many-Body Quantum Sensors		
Non-Equilibrium Steady State based	1. Initialization does not matter 2. Super-Heisenberg scaling possible 3. Works even with partial accessibility 4. Dissipation can also be harnessed	1. Fine tuning is needed (local sensing) 2. Optimal measurement parameter-value dependent 3. Reaching steady state is time consuming
Transient State based	1. Easy initialization 2. Super-Heisenberg scaling possible 3. Time control for better precision 4. May operate across the entire phase (no fine tuning) 5. Sequential measurements are adoptable	1. Decoherence is a limiting factor 2. Optimal measurement parameter-value dependent

TABLE II. **Quantum-enhanced sensing strategies.** A comparison between different means of quantum sensing is provided in this Table. This review is mainly focused on quantum many-body probes at equilibrium and non-equilibrium configurations.

uation where Fisher information matrix is singular and thus sensing becomes impossible. Specifying the criteria which results in singularity of the Fisher information matrix in many-body systems and recipes to fix them requires further attention. Finally, experimental realization of quantum many-body sensors is a big objective which ultimately defines the success of these probes. Many physical platforms can implement many-body sensors, including nuclear magnetic resonance systems, Rydberg atoms, optical lattices, superconducting simulators, nitrogen vacancies and levitated objects. progress on these setups as well as new physical platforms open further opportunities for developing many-body quantum sensors with wide range of applications.

ACKNOWLEDGMENTS

AB acknowledges support from the National Natural Science Foundation of China (Grants No. 12050410253, No. 92065115, and No. 12274059), and the Ministry of Science and Technology of China (Grant No. QNJ2021167001L). VM acknowledges funding by the National Natural Science Foundation of China (Grants

No. 12050410251 and No. 12374482). RY acknowledges support from the National Natural Science Foundation of China for the International Young Scientists Fund (Grant No. 12250410242).

REFERENCES

- [1] Jonathan P Dowling and Gerard J Milburn, “Quantum technology: the second quantum revolution,” *Philosophical Transactions of the Royal Society of London. Series A: Mathematical, Physical and Engineering Sciences* **361**, 1655–1674 (2003).
- [2] Seth Lloyd, “Universal quantum simulators,” *Science* **273**, 1073–1078 (1996).
- [3] Iulia M Georgescu, Sahel Ashhab, and Franco Nori, “Quantum simulation,” *Reviews of Modern Physics* **86**, 153–185 (2014).
- [4] Anton Zeilinger, “Experiment and the foundations of quantum physics,” *Reviews of Modern Physics* **71**, S288 (1999).
- [5] Nicolas Gisin and Rob Thew, “Quantum communication,” *Nature photonics* **1**, 165–171 (2007).
- [6] Christian L Degen, Friedemann Reinhard, and Paola Cappellaro, “Quantum sensing,” *Reviews of modern physics* **89**, 035002 (2017).

- [7] Scott E Crawford, Roman A Shugayev, Hari P Paudel, Ping Lu, Madhava Syamlal, Paul R Ohodnicki, Benjamin Chorpening, Randall Gentry, and Yuhua Duan, “Quantum sensing for energy applications: Review and perspective,” *Advanced Quantum Technologies* **4**, 2100049 (2021).
- [8] Marco Lanzagorta, Jeffrey Uhlmann, and Salvador E Venegas-Andraca, “Quantum sensing in the maritime environment,” in *OCEANS 2015-MTS/IEEE Washington* (IEEE, 2015) pp. 1–9.
- [9] Yuzhou Wu, Fedor Jelezko, Martin B Plenio, and Tanja Weil, “Diamond quantum devices in biology,” *Angewandte Chemie International Edition* **55**, 6586–6598 (2016).
- [10] Michael A Taylor and Warwick P Bowen, “Quantum metrology and its application in biology,” *Physics Reports* **615**, 1–59 (2016).
- [11] Nabeel Aslam, Hengyun Zhou, Elana K Urbach, Matthew J Turner, Ronald L Walsworth, Mikhail D Lukin, and Hongkun Park, “Quantum sensors for biomedical applications,” *Nature Reviews Physics* **5**, 157–169 (2023).
- [12] Rainer Kaltenbaek, Antonio Acin, Laszlo Bacsardi, Paolo Bianco, Philippe Bouyer, Eleni Diamanti, Christoph Marquardt, Yasser Omar, Valerio Pruneri, Ernst Rasel, *et al.*, “Quantum technologies in space,” *Experimental Astronomy* **51**, 1677–1694 (2021).
- [13] Lorenzo Maccone and Changliang Ren, “Quantum radar,” *Physical Review Letters* **124**, 200503 (2020).
- [14] Athena Karsa, Alasdair Fletcher, Gaetana Spedalieri, and Stefano Pirandola, “Quantum illumination and quantum radar: a brief overview,” *Reports on Progress in Physics* **87**, 094001 (2024).
- [15] Anthony J. Brady, Christina Gao, Roni Harnik, Zhen Liu, Zheshen Zhang, and Quntao Zhuang, “Entangled sensor-networks for dark-matter searches,” *PRX Quantum* **3**, 030333 (2022).
- [16] K. M. Backes, D. A. Palken, S. Al Kenany, B. M. Brubaker, S. B. Cahn, A. Droster, Gene C. Hilton, Sumita Ghosh, H. Jackson, S. K. Lamoreaux, A. F. Leder, K. W. Lehnert, S. M. Lewis, M. Malnou, R. H. Maruyama, N. M. Rapidis, M. Simanovskaia, Sukhman Singh, D. H. Speller, I. Urdinaran, Leila R. Vale, E. C. van Assendelft, K. van Bibber, and H. Wang, “A quantum enhanced search for dark matter axions,” *Nature* **590**, 238–242 (2021).
- [17] Runqi Kang, Man Jiao, Yu Tong, Yang Liu, Youpeng Zhong, Yi-Fu Cai, Jingwei Zhou, Xing Rong, and Jiangfeng Du, “Near-quantum-limited haloscope search for dark-photon dark matter enhanced by a high- q superconducting cavity,” *Phys. Rev. D* **109**, 095037 (2024).
- [18] Yuanhong Wang, Haowen Su, Min Jiang, Ying Huang, Yushu Qin, Chang Guo, Zehao Wang, Dongdong Hu, Wei Ji, Pavel Fadeev, Xinhua Peng, and Dmitry Budker, “Limits on axions and axionlike particles within the axion window using a spin-based amplifier,” *Phys. Rev. Lett.* **129**, 051801 (2022).
- [19] Min Jiang, Haowen Su, Antoine Garcon, Xinhua Peng, and Dmitry Budker, “Search for axion-like dark matter with spin-based amplifiers,” *Nature Physics* **17**, 1402–1407 (2021).
- [20] Romana Schirhagl, Kevin Chang, Michael Loretz, and Christian L. Degen, “Nitrogen-vacancy centers in diamond: Nanoscale sensors for physics and biology,” *Annual Review of Physical Chemistry* **65**, 83–105 (2014).
- [21] Tongtong Zhang, Goutam Pramanik, Kai Zhang, Michal Gulka, Lingzhi Wang, Jixiang Jing, Feng Xu, Zifu Li, Qiang Wei, Petr Cigler, and Zhiqin Chu, “Toward quantitative bio-sensing with nitrogen–vacancy center in diamond,” *ACS Sensors* **6**, 2077–2107 (2021), pMID: 34038091.
- [22] Taizhou Hong, Yuanhong Wang, Zhenhan Shao, Qing Li, Min Jiang, and Xinhua Peng, “Femtotesla atomic magnetometer for zero- and ultralow-field nuclear magnetic resonance,” (2024).
- [23] Min Jiang, Haowen Su, Antoine Garcon, Xinhua Peng, and Dmitry Budker, “Search for axion-like dark matter with spin-based amplifiers,” *Nature Physics* **17**, 1402–1407 (2021).
- [24] Vittorio Giovannetti, Seth Lloyd, and Lorenzo Maccone, “Quantum-enhanced measurements: beating the standard quantum limit,” *Science* **306**, 1330–1336 (2004).
- [25] Vittorio Giovannetti, Seth Lloyd, and Lorenzo Maccone, “Advances in quantum metrology,” *Nature Photonics* **5**, 222–229 (2011).
- [26] Vittorio Giovannetti, Seth Lloyd, and Lorenzo Maccone, “Quantum metrology,” *Physical Review Letters* **96**, 010401 (2006).
- [27] Harald Cramer, *Mathematical methods of statistics* (Princeton University Press Princeton, 1946) pp. xvi, 575 p. ;.
- [28] C. Radhakrishna Rao, “Information and the accuracy attainable in the estimation of statistical parameters,” in *Breakthroughs in Statistics: Foundations and Basic Theory*, edited by Samuel Kotz and Norman L. Johnson (Springer New York, New York, NY, 1992) pp. 235–247.
- [29] Morgan W. Mitchell, Jeff S. Lundeen, and Aephraim M. Steinberg, “Super-resolving phase measurements with a multiphoton entangled state,” *Nature* **429**, 161 (2004).
- [30] L. Pezzé, A. Smerzi, G. Khoury, J. F. Hodelin, and D. Bouwmeester, “Phase detection at the quantum limit with multiphoton mach-zehnder interferometry,” *Phys. Rev. Lett.* **99**, 223602 (2007).
- [31] Takafumi Ono, Ryo Okamoto, and Shigeki Takeuchi, “An entanglement-enhanced microscope,” *Nature communications* **4**, 2426 (2013).
- [32] Dietrich Leibfried, Murray D Barrett, T Schaez, Joseph Britton, J Chiaverini, Wayne M Itano, John D Jost, Christopher Langer, and David J Wineland, “Toward heisenberg-limited spectroscopy with multiparticle entangled states,” *Science* **304**, 1476–1478 (2004).
- [33] Weiting Wang, Yukai Wu, Yuwei Ma, Weizhou Cai, Ling Hu, Xianghao Mu, Yuan Xu, Zi-Jie Chen, Haiyan Wang, YP Song, *et al.*, “Heisenberg-limited single-mode quantum metrology in a superconducting circuit,” *Nature communications* **10**, 4382 (2019).
- [34] Cristian Bonato, Machiel S Blok, Hossein T Dinani, Dominic W Berry, Matthew L Markham, Daniel J Twitchen, and Ronald Hanson, “Optimized quantum sensing with a single electron spin using real-time adaptive measurements,” *Nature nanotechnology* **11**, 247–252 (2016).
- [35] Antonella De Pasquale, Davide Rossini, Paolo Facchi, and Vittorio Giovannetti, “Quantum parameter estimation affected by unitary disturbance,” *Phys. Rev. A* **88**, 052117 (2013).

- [36] Paolo Zanardi and Nikola Paunković, “Ground state overlap and quantum phase transitions,” *Phys. Rev. E* **74**, 031123 (2006).
- [37] Meghana Raghunandan, Jörg Wrachtrup, and Hendrik Weimer, “High-density quantum sensing with dissipative first order transitions,” *Phys. Rev. Lett.* **120**, 150501 (2018).
- [38] Toni L Heugel, Matteo Biondi, Oded Zilberberg, and Ramasubramanian Chitra, “Quantum transducer using a parametric driven-dissipative phase transition,” *Phys. Rev. Lett.* **123**, 173601 (2019).
- [39] Li-Ping Yang and Zubin Jacob, “Engineering first-order quantum phase transitions for weak signal detection,” *Journal of Applied Physics* **126**, 174502 (2019).
- [40] Paolo Zanardi, HT Quan, Xiaoguang Wang, and CP Sun, “Mixed-state fidelity and quantum criticality at finite temperature,” *Phys. Rev. A* **75**, 032109 (2007).
- [41] Shi-Jian Gu, Ho-Man Kwok, Wen-Qiang Ning, Hai-Qing Lin, *et al.*, “Fidelity susceptibility, scaling, and universality in quantum critical phenomena,” *Phys. Rev. B* **77**, 245109 (2008).
- [42] Paolo Zanardi, Matteo GA Paris, and Lorenzo Campos Venuti, “Quantum criticality as a resource for quantum estimation,” *Phys. Rev. A* **78**, 042105 (2008).
- [43] Carmen Invernizzi, Michael Korbman, Lorenzo Campos Venuti, and Matteo GA Paris, “Optimal quantum estimation in spin systems at criticality,” *Phys. Rev. A* **78**, 042106 (2008).
- [44] Shi-Jian Gu, “Fidelity approach to quantum phase transitions,” *Int. J. Mod. Phys. B* **24**, 4371–4458 (2010).
- [45] Søren Gammelmark and Klaus Mølmer, “Phase transitions and heisenberg limited metrology in an ising chain interacting with a single-mode cavity field,” *New J. Phys.* **13**, 053035 (2011).
- [46] Michael Skotiniotis, Pavel Sekatski, and Wolfgang Dür, “Quantum metrology for the ising hamiltonian with transverse magnetic field,” *New J. Phys.* **17**, 073032 (2015).
- [47] Marek M Rams, Piotr Sierant, Omyoti Dutta, Paweł Horodecki, and Jakub Zakrzewski, “At the limits of criticality-based quantum metrology: Apparent superheisenberg scaling revisited,” *Phys. Rev. X* **8**, 021022 (2018).
- [48] Bo-Bo Wei, “Fidelity susceptibility in one-dimensional disordered lattice models,” *Phys. Rev. A* **99**, 042117 (2019).
- [49] Yaoming Chu, Shaoliang Zhang, Baiyi Yu, and Jianming Cai, “Dynamic framework for criticality-enhanced quantum sensing,” *Phys. Rev. Lett.* **126**, 010502 (2021).
- [50] Ran Liu, Yu Chen, Min Jiang, Xiaodong Yang, Ze Wu, Yuchen Li, Haidong Yuan, Xinhua Peng, and Jiangfeng Du, “Experimental critical quantum metrology with the heisenberg scaling,” *npj Quantum Information* **7**, 1–7 (2021).
- [51] Victor Montenegro, Utkarsh Mishra, and Abolfazl Bayat, “Global sensing and its impact for quantum many-body probes with criticality,” *Phys. Rev. Lett.* **126**, 200501 (2021).
- [52] Safoura S Mirkhalaf, Daniel Benedicto Orenes, Morgan W Mitchell, and Emilia Witkowska, “Criticality-enhanced quantum sensing in ferromagnetic bose-einstein condensates: Role of readout measurement and detection noise,” *Phys. Rev. A* **103**, 023317 (2021).
- [53] R. Di Candia, F. Minganti, K. V. Petrovnin, G. S. Paraoanu, and S. Felicetti, “Critical parametric quantum sensing,” *npj Quantum Inf* **9**, 23 (2023).
- [54] Jan Carl Budich and Emil J Bergholtz, “Non-hermitian topological sensors,” *Phys. Rev. Lett.* **125**, 180403 (2020).
- [55] Saubhik Sarkar, Chiranjib Mukhopadhyay, Abhijeet Alase, and Abolfazl Bayat, “Free-fermionic topological quantum sensors,” *Phys. Rev. Lett.* **129**, 090503 (2022).
- [56] Florian Koch and Jan Carl Budich, “Quantum non-hermitian topological sensors,” *Phys. Rev. Res.* **4**, 013113 (2022).
- [57] Min Yu, Xiangbei Li, Yaoming Chu, Bruno Mera, F Nur Ünal, Pengcheng Yang, Yu Liu, Nathan Goldman, and Jianming Cai, “Experimental demonstration of topological bounds in quantum metrology,” *Natl. Sci. Rev.*, [nwae065](#) (2024).
- [58] S Sarkar, F Ciccarello, A Carollo, and A Bayat, “Critical non-hermitian topology induced quantum sensing,” *New J. Phys.* **26**, 073010 (2024).
- [59] Weijian Chen, Şahin Kaya Özdemir, Guangming Zhao, Jan Wiersig, and Lan Yang, “Exceptional points enhance sensing in an optical microcavity,” *Nature* **548**, 192–196 (2017).
- [60] Shang Yu, Yu Meng, Jian-Shun Tang, Xiao-Ye Xu, Yi-Tao Wang, Peng Yin, Zhi-Jin Ke, Wei Liu, Zhi-Peng Li, Yuan-Ze Yang, Geng Chen, Yong-Jian Han, Chuan-Feng Li, and Guang-Can Guo, “Experimental investigation of quantum \mathcal{PT} -enhanced sensor,” *Phys. Rev. Lett.* **125**, 240506 (2020).
- [61] Alexander McDonald and Aashish A. Clerk, “Exponentially-enhanced quantum sensing with non-hermitian lattice dynamics,” *Nature Communications* **11**, 5382 (2020).
- [62] Jan Wiersig, “Enhancing the sensitivity of frequency and energy splitting detection by using exceptional points: Application to microcavity sensors for single-particle detection,” *Phys. Rev. Lett.* **112**, 203901 (2014).
- [63] Hossein Hodaei, Absar U. Hassan, Steffen Wittek, Hipolito Garcia-Gracia, Ramy El-Ganainy, Demetrios N. Christodoulides, and Mercedes Khajavikhan, “Enhanced sensitivity at higher-order exceptional points,” *Nature* **548**, 187–191 (2017).
- [64] Zhong-Peng Liu, Jing Zhang, Şahin Kaya Özdemir, Bo Peng, Hui Jing, Xin-You Lü, Chun-Wen Li, Lan Yang, Franco Nori, and Yu-xi Liu, “Metrology with \mathcal{PT} -symmetric cavities: Enhanced sensitivity near the \mathcal{PT} -phase transition,” *Phys. Rev. Lett.* **117**, 110802 (2016).
- [65] W. Langbein, “No exceptional precision of exceptional-point sensors,” *Phys. Rev. A* **98**, 023805 (2018).
- [66] Chong Chen, Liang Jin, and Ren-Bao Liu, “Sensitivity of parameter estimation near the exceptional point of a non-hermitian system,” *New Journal of Physics* **21**, 083002 (2019).
- [67] Heming Wang, Yu-Hung Lai, Zhiquan Yuan, Myoung-Gyun Suh, and Kerry Vahala, “Petermann-factor sensitivity limit near an exceptional point in a brillouin ring laser gyroscope,” *Nature Communications* **11**, 1610 (2020).
- [68] Mengzhen Zhang, William Sweeney, Chia Wei Hsu, Lan Yang, A. D. Stone, and Liang Jiang, “Quantum noise theory of exceptional point amplifying sensors,” *Phys.*

- Rev. Lett.* **123**, 180501 (2019).
- [69] Hoi-Kwan Lau and Aashish A. Clerk, “Fundamental limits and non-reciprocal approaches in non-hermitian quantum sensing,” *Nature Communications* **9**, 4320 (2018).
- [70] Rodion Kononchuk, Jizhe Cai, Fred Ellis, Ramathanas Thevamaran, and Tsampikos Kottos, “Exceptional-point-based accelerometers with enhanced signal-to-noise ratio,” *Nature* **607**, 697–702 (2022).
- [71] Jan Wiersig, “Review of exceptional point-based sensors,” *Photon. Res.* **8**, 1457–1467 (2020).
- [72] Lei Xiao, Yaoming Chu, Quan Lin, Haiqing Lin, Wei Yi, Jianming Cai, and Peng Xue, “Non-hermitian sensing in the absence of exceptional points,” [arxiv:2403.08218](https://arxiv.org/abs/2403.08218) (2024).
- [73] Xinglei Yu, Xinzhi Zhao, Liangsheng Li, Xiao-Min Hu, Xiangmei Duan, Haidong Yuan, and Chengjie Zhang, “Toward heisenberg scaling in non-hermitian metrology at the quantum regime,” *Science Advances* **10**, eadk7616 (2024).
- [74] Xingjian He, Rozhin Yousefjani, and Abolfazl Bayat, “Stark localization as a resource for weak-field sensing with super-Heisenberg precision,” *Phys. Rev. Lett.* **131**, 010801 (2023).
- [75] Rozhin Yousefjani, Xingjian He, and Abolfazl Bayat, “Long-range interacting Stark many-body probes with super-Heisenberg precision,” *Chin. Phys. B* **32**, 100313 (2023).
- [76] Rozhin Yousefjani, Xingjian He, Angelo Carollo, and Abolfazl Bayat, “Nonlinearity-enhanced quantum sensing in stark probes,” [arXiv:2404.10382](https://arxiv.org/abs/2404.10382) (2024).
- [77] Samuel Fernández-Lorenzo and Diego Porras, “Quantum sensing close to a dissipative phase transition: Symmetry breaking and criticality as metrological resources,” *Phys. Rev. A* **96**, 013817 (2017).
- [78] Kristian Baumann, Christine Guerlin, Ferdinand Brennecke, and Tilman Esslinger, “Dicke quantum phase transition with a superfluid gas in an optical cavity,” *Nature* **464**, 1301–1306 (2010).
- [79] Markus P Baden, Kyle J Arnold, Arne L Grimsmo, Scott Parkins, and Murray D Barrett, “Realization of the Dicke model using cavity-assisted raman transitions,” *Phys. Rev. Lett.* **113**, 020408 (2014).
- [80] Jens Klinder, Hans Keßler, Matthias Wolke, Ludwig Mathey, and Andreas Hemmerich, “Dynamical phase transition in the open dicke model,” *Proc. Natl. Acad. Sci. U.S.A.* **112**, 3290–3295 (2015).
- [81] SRK Rodriguez, W Casteels, F Storme, N Carlon Zambon, I Sagnes, L Le Gratiet, E Galopin, A Lemaître, A Amo, C Ciuti, *et al.*, “Probing a dissipative phase transition via dynamical optical hysteresis,” *Phys. Rev. Lett.* **118**, 247402 (2017).
- [82] Mattias Fitzpatrick, Neereja M Sundaresan, Andy CY Li, Jens Koch, and Andrew A Houck, “Observation of a dissipative phase transition in a one-dimensional circuit QED lattice,” *Phys. Rev. X* **7**, 011016 (2017).
- [83] Johannes M Fink, Andrés Dombi, Andrés Vukics, Andreas Wallraff, and Peter Domokos, “Observation of the photon-blockade breakdown phase transition,” *Phys. Rev. X* **7**, 011012 (2017).
- [84] Theodoros Ilias, Dayou Yang, Susana F Huelga, and Martin B Plenio, “Criticality-enhanced quantum sensing via continuous measurement,” *PRX Quantum* **3**, 010354 (2022).
- [85] Theodoros Ilias, Dayou Yang, Susana F. Huelga, and Martin B. Plenio, “Criticality-enhanced electromagnetic field sensor with single trapped ions,” *npj Quantum Inf.* **10**, 36 (2024).
- [86] S. Alipour, M. Mehboudi, and A. T. Reza khani, “Quantum metrology in open systems: Dissipative cramer-rao bound,” *Phys. Rev. Lett.* **112**, 120405 (2014).
- [87] Utkarsh Mishra and Abolfazl Bayat, “Driving enhanced quantum sensing in partially accessible many-body systems,” *Phys. Rev. Lett.* **127**, 080504 (2021).
- [88] Utkarsh Mishra and Abolfazl Bayat, “Integrable quantum many-body sensors for ac field sensing,” *Sci. Rep.* **12**, 1–13 (2022).
- [89] Victor Montenegro, Marco G Genoni, Abolfazl Bayat, and Matteo GA Paris, “Quantum metrology with boundary time crystals,” *Commun. Phys.* **6**, 304 (2023).
- [90] Albert Cabot, Federico Carollo, and Igor Lesanovsky, “Continuous sensing and parameter estimation with the boundary time crystal,” *Phys. Rev. Lett.* **132**, 050801 (2024).
- [91] Changyuan Lyu, Sayan Choudhury, Chenwei Lv, Yangqian Yan, and Qi Zhou, “Eternal discrete time crystal beating the heisenberg limit,” *Phys. Rev. Res.* **2**, 033070 (2020).
- [92] Fernando Iemini, Rosario Fazio, and Anna Sanpera, “Floquet time crystals as quantum sensors of ac fields,” *Phys. Rev. A* **109**, L050203 (2024).
- [93] Rozhin Yousefjani, Krzysztof Sacha, and Abolfazl Bayat, “Discrete time crystal phase as a resource for quantum enhanced sensing,” [arXiv:2405.00328](https://arxiv.org/abs/2405.00328) (2024).
- [94] Subir Sachdev, “Quantum phase transitions,” *Physics world* **12**, 33 (1999).
- [95] Cenke Xu, “Unconventional quantum critical points,” *Int. J. Mod. Phys. B* **26**, 1230007 (2012).
- [96] Evert van Nieuwenburg, Yuval Baum, and Gil Refael, “From bloch oscillations to many-body localization in clean interacting systems,” *Proceedings of the National Academy of Sciences* **116**, 9269–9274 (2019).
- [97] Maximilian Schulz, CA Hooley, Roderich Moessner, and F Pollmann, “Stark many-body localization,” *Physical review letters* **122**, 040606 (2019).
- [98] Dong-Sheng Ding, Zong-Kai Liu, Bao-Sen Shi, Guang-Can Guo, Klaus Mølmer, and Charles S Adams, “Enhanced metrology at the critical point of a many-body rydberg atomic system,” *Nature Physics* **18**, 1447–1452 (2022).
- [99] S. Sachdev and an O’Reilly Media Company Safari, *Quantum Phase Transitions, Second Edition* (Cambridge University Press, 2011).
- [100] Matthias Vojta, “Quantum phase transitions,” *Reports on Progress in Physics* **66**, 2069 (2003).
- [101] Aditi Mitra, “Quantum quench dynamics,” *Annual Review of Condensed Matter Physics* **9**, 245–259 (2018).
- [102] Andrew J Daley, Hannes Pichler, Johannes Schachenmayer, and Peter Zoller, “Measuring entanglement growth in quench dynamics of bosons in an optical lattice,” *Physical review letters* **109**, 020505 (2012).
- [103] Pasquale Calabrese and John Cardy, “Time dependence of correlation functions following a quantum quench,” *Physical review letters* **96**, 136801 (2006).
- [104] Pasquale Calabrese, Fabian HL Essler, and Maurizio Fagotti, “Quantum quench in the transverse-field ising chain,” *Physical review letters* **106**, 227203 (2011).
- [105] Sima Pouyandeh, Farhad Shahbazi, and Abolfazl

- Bayat, “Measurement-induced dynamics for spin-chain quantum communication and its application for optical lattices,” *Phys. Rev. A* **90**, 012337 (2014).
- [106] Abolfazl Bayat, Bedoor Alkurtass, Pasquale Sodano, Henrik Johannesson, and Sougato Bose, “Measurement quench in many-body systems,” *Physical Review Letters* **121**, 030601 (2018).
- [107] Brian Skinner, Jonathan Ruhman, and Adam Nahum, “Measurement-induced phase transitions in the dynamics of entanglement,” *Physical Review X* **9**, 031009 (2019).
- [108] Yaodong Li, Xiao Chen, and Matthew PA Fisher, “Quantum zeno effect and the many-body entanglement transition,” *Physical Review B* **98**, 205136 (2018).
- [109] Shih-I Chu and Dmitry A Telnov, “Beyond the floquet theorem: generalized floquet formalisms and quasienergy methods for atomic and molecular multiphoton processes in intense laser fields,” *Physics reports* **390**, 1–131 (2004).
- [110] Vladimir Gritsev and Anatoli Polkovnikov, “Integrable floquet dynamics,” *SciPost Physics* **2**, 021 (2017).
- [111] Takashi Oka and Sota Kitamura, “Floquet engineering of quantum materials,” *Annual Review of Condensed Matter Physics* **10**, 387–408 (2019).
- [112] Hassan Manshouri, Moslem Zarei, Mehdi Abdi, Sougato Bose, and Abolfazl Bayat, “Quantum enhanced sensitivity through many-body bloch oscillations,” [arXiv:2406.13921](https://arxiv.org/abs/2406.13921) (2024).
- [113] Ayan Sahoo, Utkarsh Mishra, and Debraj Rakshit, “Localization-driven quantum sensing,” *Physical Review A* **109**, L030601 (2024).
- [114] H. Carmichael, *An Open Systems Approach to Quantum Optics* (Springer, Berlin, 1993).
- [115] Ingrid Rotter, “A non-hermitian hamilton operator and the physics of open quantum systems,” *J. Phys. A: Math. Theor.* **42**, 153001 (2009).
- [116] Heinz-Peter Breuer, Francesco Petruccione, *et al.*, *The theory of open quantum systems* (Oxford University Press on Demand, 2002).
- [117] M. B. Plenio and P. L. Knight, “The quantum-jump approach to dissipative dynamics in quantum optics,” *Rev. Mod. Phys.* **70**, 101–144 (1998).
- [118] A. J. Daley, “Quantum trajectories and open many-body quantum systems,” *Advances in Physics* **63**, 77–149 (2014).
- [119] Daniel A Lidar, Isaac L Chuang, and K Birgitta Whaley, “Decoherence-free subspaces for quantum computation,” *Physical Review Letters* **81**, 2594 (1998).
- [120] Lu-Ming Duan and Guang-Can Guo, “Preserving coherence in quantum computation by pairing quantum bits,” *Phys. Rev. Lett.* **79**, 1953–1956 (1997).
- [121] Lorenza Viola, Emanuel Knill, and Seth Lloyd, “Dynamical decoupling of open quantum systems,” *Physical Review Letters* **82**, 2417 (1999).
- [122] Kaveh Khodjasteh and Daniel A Lidar, “Fault-tolerant quantum dynamical decoupling,” *Physical review letters* **95**, 180501 (2005).
- [123] J. F. Poyatos, J. I. Cirac, and P. Zoller, “Quantum reservoir engineering with laser cooled trapped ions,” *Phys. Rev. Lett.* **77**, 4728–4731 (1996).
- [124] Christopher J Myatt, Brian E King, Quentin A Turchette, Cass A Sackett, David Kielpinski, Wayne M Itano, CWDJ Monroe, and David J Wineland, “Decoherence of quantum superpositions through coupling to engineered reservoirs,” *Nature* **403**, 269–273 (2000).
- [125] Susanne Pielawa, Giovanna Morigi, David Vitali, and Luiz Davidovich, “Generation of einstein-podolsky-rosen-entangled radiation through an atomic reservoir,” *Physical review letters* **98**, 240401 (2007).
- [126] Susanne Pielawa, Luiz Davidovich, David Vitali, and Giovanna Morigi, “Engineering atomic quantum reservoirs for photons,” *Physical Review A* **81**, 043802 (2010).
- [127] Peter Groszkowski, Martin Koppenhöfer, Hoi-Kwan Lau, and A. A. Clerk, “Reservoir-engineered spin squeezing: Macroscopic even-odd effects and hybrid-systems implementations,” *Phys. Rev. X* **12**, 011015 (2022).
- [128] BM Escher, RL de Matos Filho, and Luiz Davidovich, “General framework for estimating the ultimate precision limit in noisy quantum-enhanced metrology,” *Nature Physics* **7**, 406–411 (2011).
- [129] Fabrizio Minganti, Alberto Biella, Nicola Bartolo, and Cristiano Ciuti, “Spectral theory of liouvillians for dissipative phase transitions,” *Physical Review A* **98**, 042118 (2018).
- [130] Matteo GA Paris, “Quantum estimation for quantum technology,” *International Journal of Quantum Information* **7**, 125–137 (2009).
- [131] Johannes Jakob Meyer, “Fisher information in noisy intermediate-scale quantum applications,” *Quantum* **5**, 539 (2021).
- [132] Jing Liu, Haidong Yuan, Xiao-Ming Lu, and Xiaoguang Wang, “Quantum fisher information matrix and multiparameter estimation,” *Journal of Physics A: Mathematical and Theoretical* **53**, 023001 (2020).
- [133] Jun Ye and Peter Zoller, “Essay: Quantum sensing with atomic, molecular, and optical platforms for fundamental physics,” *Physical Review Letters* **132**, 190001 (2024).
- [134] Albert Einstein, *The Principle of Relativity* (Dover Publications, 1923).
- [135] A. Einstein, “Zur elektrodynamik bewegter körper,” *Annalen der Physik* **322**, 891–921 (1905).
- [136] A. A. Michelson and E. W. Morley, “On the relative motion of the earth and the luminiferous ether,” *American Journal of Science* **s3-34**, 333–345 (1887).
- [137] Bruno Rossi and David B. Hall, “Variation of the rate of decay of mesotrons with momentum,” *Phys. Rev.* **59**, 223–228 (1941).
- [138] J. C. Hafele and Richard E. Keating, “Around-the-world atomic clocks: Predicted relativistic time gains,” *Science* **177**, 166–168 (1972).
- [139] J. C. Hafele and Richard E. Keating, “Around-the-world atomic clocks: Observed relativistic time gains,” *Science* **177**, 168–170 (1972).
- [140] “Observation of gravitational waves from a binary black hole merger,” *Phys. Rev. Lett.* **116**, 061102 (2016).
- [141] F. Englert and R. Brout, “Broken symmetry and the mass of gauge vector mesons,” *Phys. Rev. Lett.* **13**, 321–323 (1964).
- [142] Peter W. Higgs, “Broken symmetries and the masses of gauge bosons,” *Phys. Rev. Lett.* **13**, 508–509 (1964).
- [143] G. S. Guralnik, C. R. Hagen, and T. W. B. Kibble, “Global conservation laws and massless particles,” *Phys. Rev. Lett.* **13**, 585–587 (1964).
- [144] The CMS Collaboration, “A portrait of the higgs boson by the cms experiment ten years after the discovery,”

- Nature **607**, 60–68 (2022).
- [145] Jasminder S Sidhu and Pieter Kok, “Geometric perspective on quantum parameter estimation,” *AVS Quantum Science* **2**, 014701 (2020).
- [146] G Mauro D’ariano, Matteo GA Paris, and Massimiliano F Sacchi, “Parameter estimation in quantum optics,” *Physical Review A* **62**, 023815 (2000).
- [147] Carl W Helstrom, *Quantum Detection and Estimation Theory* (Academic Press, 1976).
- [148] A.S. Holevo, *Probabilistic and Statistical Aspects of Quantum Theory* (Edizioni della Normale, Pisa, 2011).
- [149] Ingemar Bengtsson and Karol Życzkowski, *Geometry of quantum states: an introduction to quantum entanglement* (Cambridge university press, 2017).
- [150] Harry L. Van Trees, *Detection, Estimation, and Modulation Theory, Part I*, 2nd ed. (Wiley-Interscience, 2004).
- [151] Samuel L. Braunstein and Carlton M. Caves, “Statistical distance and the geometry of quantum states,” *Phys. Rev. Lett.* **72**, 3439–3443 (1994).
- [152] E. A. Morozova and N. N. Chentsov, “Markov invariant geometry on manifolds of states,” *Journal of Soviet Mathematics* **56**, 2648–2669 (1991).
- [153] C.W. Helstrom, “Minimum mean-squared error of estimates in quantum statistics,” *Physics Letters A* **25**, 101–102 (1967).
- [154] H. Yuen and M. Lax, “Multiple-parameter quantum estimation and measurement of nonselfadjoint observables,” *IEEE Transactions on Information Theory* **19**, 740–750 (1973).
- [155] C. Helstrom and R. Kennedy, “Noncommuting observables in quantum detection and estimation theory,” *IEEE Transactions on Information Theory* **20**, 16–24 (1974).
- [156] Francesco Albarelli, Marco Barbieri, Marco G Genoni, and Ilaria Gianani, “A perspective on multiparameter quantum metrology: From theoretical tools to applications in quantum imaging,” *Physics Letters A* **384**, 126311 (2020).
- [157] Jing Liu, Haidong Yuan, Xiao-Ming Lu, and Xiaoguang Wang, “Quantum fisher information matrix and multiparameter estimation,” *Journal of Physics A: Mathematical and Theoretical* **53**, 023001 (2019).
- [158] Stefano Olivares and Matteo G A Paris, “Bayesian estimation in homodyne interferometry,” *Journal of Physics B: Atomic, Molecular and Optical Physics* **42**, 055506 (2009).
- [159] Z. Hradil, R. Myška, J. Peřina, M. Zawisky, Y. Hasegawa, and H. Rauch, “Quantum phase in interferometry,” *Phys. Rev. Lett.* **76**, 4295–4298 (1996).
- [160] Lucien M. Le Cam, *Asymptotic methods in statistical decision theory*, Springer series in statistics (Springer-Verlag, New York, 1986).
- [161] Jesús Rubio and Jacob Dunningham, “Quantum metrology in the presence of limited data,” *New Journal of Physics* **21**, 043037 (2019).
- [162] Jesús Rubio and Jacob Dunningham, “Bayesian multiparameter quantum metrology with limited data,” *Physical Review A* **101**, 032114 (2020).
- [163] Jing Liu, Xiao-Xing Jing, and Xiaoguang Wang, “Quantum metrology with unitary parametrization processes,” *Scientific reports* **5**, 8565 (2015).
- [164] Wei Zhong, Zhe Sun, Jian Ma, Xiaoguang Wang, and Franco Nori, “Fisher information under decoherence in Bloch representation,” *Physical Review A* **87**, 022337 (2013).
- [165] François Chapeau-Blondeau, “Optimized probing states for qubit phase estimation with general quantum noise,” *Physical Review A* **91**, 052310 (2015).
- [166] B Maroufi, R Laghmach, H El Hadfi, and M Daoud, “On the analytical derivation of quantum Fisher information and skew information for two qubit x states,” *International Journal of Theoretical Physics* **60**, 3103–3114 (2021).
- [167] O. Pinel, P. Jian, N. Treps, C. Fabre, and D. Braun, “Quantum parameter estimation using general single-mode gaussian states,” *Phys. Rev. A* **88**, 040102 (2013).
- [168] Alex Monras, “Phase space formalism for quantum estimation of gaussian states,” [arXiv:1303.3682](https://arxiv.org/abs/1303.3682) (2013).
- [169] Zhang Jiang, “Quantum fisher information for states in exponential form,” *Phys. Rev. A* **89**, 032128 (2014).
- [170] Carlo Sparaciari, Stefano Olivares, and Matteo GA Paris, “Bounds to precision for quantum interferometry with gaussian states and operations,” *JOSA B* **32**, 1354–1359 (2015).
- [171] Paulina Marian and Tudor A. Marian, “Quantum fisher information on two manifolds of two-mode gaussian states,” *Phys. Rev. A* **93**, 052330 (2016).
- [172] Carlo Sparaciari, Stefano Olivares, and Matteo GA Paris, “Gaussian-state interferometry with passive and active elements,” *Physical Review A* **93**, 023810 (2016).
- [173] Lahcen Bakmou, Mohammed Daoud, *et al.*, “Multiparameter quantum estimation theory in quantum gaussian states,” *Journal of Physics A: Mathematical and Theoretical* **53**, 385301 (2020).
- [174] Alexander S Holevo, *Probabilistic and Statistical Aspects of Quantum Theory; 2nd ed.*, Publications of the Scuola Normale Superiore. Monographs (Springer, Dordrecht, 2011).
- [175] Alexander S. Holevo, “Commutation superoperator of a state and its applications to the noncommutative statistics,” *Reports on Mathematical Physics* **12**, 251–271 (1977).
- [176] Sammy Ragy, Marcin Jarzyna, and Rafał Demkowicz-Dobrzański, “Compatibility in multiparameter quantum metrology,” *Physical Review A* **94**, 052108 (2016).
- [177] Angelo Carollo, Bernardo Spagnolo, Alexander A Dubkov, and Davide Valenti, “On quantumness in multi-parameter quantum estimation,” *Journal of Statistical Mechanics: Theory and Experiment* **2019**, 094010 (2019).
- [178] Federico Belliardo and Vittorio Giovannetti, “Incompatibility in quantum parameter estimation,” *New Journal of Physics* **23**, 063055 (2021).
- [179] Hongzhen Chen, Yu Chen, and Haidong Yuan, “Incompatibility measures in multiparameter quantum estimation under hierarchical quantum measurements,” *Phys. Rev. A* **105**, 062442 (2022).
- [180] Dominik Šafránek, “Simple expression for the quantum fisher information matrix,” *Physical Review A* **97**, 042322 (2018).
- [181] Alan J Laub, *Matrix analysis for scientists and engineers*, Vol. 91 (Siam, 2005).
- [182] Valeria Simoncini, “Computational methods for linear matrix equations,” *siam REVIEW* **58**, 377–441 (2016).
- [183] Lukas J Fiderer, Tommaso Tufarelli, Samanta Piano, and Gerardo Adesso, “General expressions for the quantum fisher information matrix with applications to dis-

- crete quantum imaging,” *PRX Quantum* **2**, 020308 (2021).
- [184] W. K. Wootters, “Statistical distance and hilbert space,” *Phys. Rev. D* **23**, 357–362 (1981).
- [185] E. H. Lehmann and G. Casella, *Theory of Point Estimation*, Springer Texts in Statistics (Springer New York, NY, 1998).
- [186] Pieter Kok and Brendon W Lovett, *Introduction to optical quantum information processing* (Cambridge university press, 2010).
- [187] Jan Hilgevoord and Jos Uffink, “Uncertainty in prediction and in inference,” *Foundations of Physics* **21**, 323–341 (1991).
- [188] Paolo Facchi, M. S. Kim, Saverio Pascazio, Francesco V. Pepe, Domenico Pomarico, and Tommaso Tufarelli, “Bound states and entanglement generation in waveguide quantum electrodynamics,” *Phys. Rev. A* **94**, 043839 (2016).
- [189] A. Uhlmann, “The “transition probability” in the state space of a $*$ -algebra,” *Reports on Mathematical Physics* **9**, 273–279 (1976).
- [190] Harry L Van Trees and Kristine L Bell, “Bayesian bounds for parameter estimation and nonlinear filtering/tracking,” *AMC* **10**, 10–1109 (2007).
- [191] Jacob Ziv and Moshe Zakai, “Some lower bounds on signal parameter estimation,” *IEEE transactions on Information Theory* **15**, 386–391 (1969).
- [192] Mankei Tsang, “Ziv-zakai error bounds for quantum parameter estimation,” *Physical review letters* **108**, 230401 (2012).
- [193] Shoukang Chang, Wei Ye, Xuan Rao, Huan Zhang, Liqing Huang, Mengmeng Luo, Yuetao Chen, Shaoyan Gao, and Liyun Hu, “Evaluating the quantum ziv–zakai bound for phase estimation in noisy environments,” *Optics Express* **30**, 24207–24221 (2022).
- [194] Dominic W Berry, Mankei Tsang, Michael JW Hall, and Howard M Wiseman, “Quantum bell-ziv-zakai bounds and heisenberg limits for waveform estimation,” *Physical Review X* **5**, 031018 (2015).
- [195] Shoukang Chang, Wei Ye, Xuan Rao, Huan Zhang, Liqing Huang, Mengmeng Luo, Yuetao Chen, Shaoyan Gao, and Liyun Hu, “Evaluating the quantum ziv–zakai bound for phase estimation in noisy environments,” *Opt. Express* **30**, 24207–24221 (2022).
- [196] Xiao-Ming Lu and Mankei Tsang, “Quantum weissweinstein bounds for quantum metrology,” *Quantum Science and Technology* **1**, 015002 (2016).
- [197] Jing Liu and Haidong Yuan, “Valid lower bound for all estimators in quantum parameter estimation,” *New Journal of Physics* **18**, 093009 (2016).
- [198] Marco Gabbriellini, Augusto Smerzi, and Luca Pezzè, “Multipartite entanglement at finite temperature,” *Scientific reports* **8**, 1–18 (2018).
- [199] Luca Lepori, Andrea Trombettoni, Domenico Giuliano, Johannes Kombe, Jorge Yago Malo, Andrew J Daley, Augusto Smerzi, and Maria Luisa Chiofalo, “Can multipartite entanglement be characterized by two-point connected correlation functions?” *J. Phys. A: Math. Theor.* **56**, 305302 (2023).
- [200] Sergio Boixo, Steven T Flammia, Carlton M Caves, and John M Geremia, “Generalized limits for single-parameter quantum estimation,” *Physical review letters* **98**, 090401 (2007).
- [201] Nicolò Spagnolo, Chiara Vitelli, Vito Giovanni Lucivero, Vittorio Giovannetti, Lorenzo Maccone, and Fabio Sciarrino, “Phase estimation via quantum interferometry for noisy detectors,” *Physical Review Letters* **108**, 233602 (2012).
- [202] Ryo Okamoto, Minako Iefuji, Satoshi Oyama, Koichi Yamagata, Hiroshi Imai, Akio Fujiwara, and Shigeki Takeuchi, “Experimental demonstration of adaptive quantum state estimation,” *Phys. Rev. Lett.* **109**, 130404 (2012).
- [203] Ryo Okamoto, Satoshi Oyama, Koichi Yamagata, Akio Fujiwara, and Shigeki Takeuchi, “Experimental demonstration of adaptive quantum state estimation for single photonic qubits,” *Phys. Rev. A* **96**, 022124 (2017).
- [204] Shengshi Pang and Todd A Brun, “Quantum metrology for a general hamiltonian parameter,” *Physical Review A* **90**, 022117 (2014).
- [205] Jian Ma, Xiaoguang Wang, Chang-Pu Sun, and Franco Nori, “Quantum spin squeezing,” *Physics Reports* **509**, 89–165 (2011).
- [206] Luca Pezze, Augusto Smerzi, Markus K Oberthaler, Roman Schmied, and Philipp Treutlein, “Quantum metrology with nonclassical states of atomic ensembles,” *Reviews of Modern Physics* **90**, 035005 (2018).
- [207] Irénée Frérot and Tommaso Roscilde, “Quantum critical metrology,” *Physical review letters* **121**, 020402 (2018).
- [208] Lorenzo Campos Venuti and Paolo Zanardi, “Quantum critical scaling of the geometric tensors,” *Physical review letters* **99**, 095701 (2007).
- [209] David Schwandt, Fabien Alet, and Sylvain Capponi, “Quantum monte carlo simulations of fidelity at magnetic quantum phase transitions,” *Physical review letters* **103**, 170501 (2009).
- [210] A Fabricio Albuquerque, Fabien Alet, Clément Sire, and Sylvain Capponi, “Quantum critical scaling of fidelity susceptibility,” *Physical Review B* **81**, 064418 (2010).
- [211] Vladimir Gritsev and Anatoli Polkovnikov, “Universal dynamics near quantum critical points,” *arXiv:0910.3692* (2009).
- [212] Sebastian Greschner, AK Kolezhuk, and T Vekua, “Fidelity susceptibility and conductivity of the current in one-dimensional lattice models with open or periodic boundary conditions,” *Physical Review B* **88**, 195101 (2013).
- [213] Raj Kumar Pathria, *Statistical mechanics* (Elsevier, 2016).
- [214] Glen Bigan Mbeng, Angelo Russomanno, and Giuseppe E Santoro, “The quantum ising chain for beginners,” *arXiv:2009.09208* (2020).
- [215] Chiranjib Mukhopadhyay and Abolfazl Bayat, “Modular many-body quantum sensors,” *arXiv:2311.18319* (2023).
- [216] Angelo Carollo, Bernardo Spagnolo, and Davide Valenti, “Symmetric logarithmic derivative of fermionic gaussian states,” *Entropy* **20**, 485 (2018).
- [217] Alessio Serafini, *Quantum continuous variables: a primer of theoretical methods* (CRC press, 2017).
- [218] Dieter Jaksch, Christoph Bruder, Juan Ignacio Cirac, Crispin W Gardiner, and Peter Zoller, “Cold bosonic atoms in optical lattices,” *Physical Review Letters* **81**, 3108 (1998).
- [219] Dieter Jaksch and Peter Zoller, “The cold atom hubbard toolbox,” *Annals of physics* **315**, 52–79 (2005).
- [220] Maciej Lewenstein, Anna Sanpera, Veronica Ahufinger,

- Bogdan Damski, Aditi Sen, and Ujjwal Sen, “Ultracold atomic gases in optical lattices: mimicking condensed matter physics and beyond,” *Advances in Physics* **56**, 243–379 (2007).
- [221] JA Dunningham, K Burnett, and Stephen M Barnett, “Interferometry below the standard quantum limit with bose-einstein condensates,” *Physical review letters* **89**, 150401 (2002).
- [222] JA Dunningham and K Burnett, “Sub-shot-noise-limited measurements with bose-einstein condensates,” *Physical Review A* **70**, 033601 (2004).
- [223] Jessica J Cooper, David W Hallwood, and Jacob A Dunningham, “Scheme for implementing atomic multiport devices,” *Journal of Physics B: Atomic, Molecular and Optical Physics* **42**, 105301 (2009).
- [224] JJ Cooper, DW Hallwood, and JA Dunningham, “Entanglement-enhanced atomic gyroscope,” *Physical Review A* **81**, 043624 (2010).
- [225] Louis Garbe, Matteo Bina, Arne Keller, Matteo GA Paris, and Simone Felicetti, “Critical quantum metrology with a finite-component quantum phase transition,” *Physical review letters* **124**, 120504 (2020).
- [226] Z. H. Wang, Q. Zheng, Xiaoguang Wang, and Yong Li, “The energy-level crossing behavior and quantum fisher information in a quantum well with spin-orbit coupling,” *Scientific Reports* **6** (2016), 10.1038/srep22347.
- [227] Xin Zhu, Jia-Hao Lü, Wen Ning, Fan Wu, Li-Tuo Shen, Zhen-Biao Yang, and Shi-Biao Zheng, “Criticality-enhanced quantum sensing in the anisotropic quantum rabi model,” *Sci. China Phys. Mech. Astron.* **66** (2023), 10.1007/s11433-022-2073-9.
- [228] Pierre Pfeuty, “The one-dimensional ising model with a transverse field,” *ANNALS OF PHYSICS* **57**, 79–90 (1970).
- [229] Raffaele Salvia, Mohammad Mehboudi, and Martí Perarnau-Llobet, “Critical quantum metrology assisted by real-time feedback control,” *Phys. Rev. Lett.* **130**, 240803 (2023).
- [230] Wan-Fang Liu, Jian Ma, and Xiaoguang Wang, “Quantum fisher information and spin squeezing in the ground state of the xy model,” *Journal of Physics A: Mathematical and Theoretical* **46**, 045302 (2013).
- [231] En-Jia Ye, Zheng-Da Hu, and Wei Wu, “Scaling of quantum fisher information close to the quantum phase transition in the xy spin chain,” *Physica B: Condensed Matter* **502**, 151–154 (2016).
- [232] Fatih Ozaydin and Azmi Ali Altintas, “Quantum metrology: Surpassing the shot-noise limit with dzyaloshinskii-moriya interaction,” *Scientific Reports* **5**, 1–6 (2015).
- [233] Biao-Liang Ye, Bo Li, Zhi-Xi Wang, Xianqing Li-Jost, and Shao-Ming Fei, “Quantum fisher information and coherence in one-dimensional xy spin models with dzyaloshinsky-moriya interactions,” *SCIENCE CHINA Physics, Mechanics & Astronomy* **61**, 1–7 (2018).
- [234] Fatih Ozaydin and Azmi Ali Altintas, “Parameter estimation with dzyaloshinskii-moriya interaction under external magnetic fields,” *Optical and Quantum Electronics* **52**, 1–10 (2020).
- [235] Qiang Zheng, Yao Yao, and Xun-Wei Xu, “Probing berezinskii-kosterlitz-thouless phase transition of spin-half xxz chain by quantum fisher information,” *Communications in Theoretical Physics* **63**, 279 (2015).
- [236] Biao-Liang Ye, Li-Yuan Xue, Yu-Liang Fang, Sheng Liu, Qi-Cheng Wu, Yan-Hui Zhou, and Chui-Ping Yang, “Quantum coherence and quantum fisher information in the xxz system,” *Physica E: Low-dimensional Systems and Nanostructures* **115**, 113690 (2020).
- [237] James Lambert and ES Sørensen, “Estimates of the quantum fisher information in the $s=1$ antiferromagnetic heisenberg spin chain with uniaxial anisotropy,” *Physical Review B* **99**, 045117 (2019).
- [238] Leonardo Lucchesi and Maria Luisa Chiofalo, “Many-body entanglement in short-range interacting fermi gases for metrology,” *Physical Review Letters* **123**, 060406 (2019).
- [239] P. W. Anderson, “Absence of diffusion in certain random lattices,” *Phys. Rev.* **109**, 1492–1505 (1958).
- [240] Serge Aubry and Gilles André, “Analyticity breaking and anderson localization in incommensurate lattices,” *Proceedings, VIII International Colloquium on Group-Theoretical Methods in Physics* **3** (1980).
- [241] L Bakmou, Abdallah Slaoui, Mohammed Daoud, and R Ahl Laamara, “Quantum fisher information matrix in heisenberg xy model,” *Quantum Information Processing* **18**, 1–20 (2019).
- [242] Giovanni Di Francesco, Bernardo Spagnolo, Davide Valenti, and Angelo Carollo, “Multiparameter quantum critical metrology,” *arXiv:2203.12676* (2022).
- [243] Min Jiang, Yunlan Ji, Qing Li, Ran Liu, Dieter Suter, and Xinhua Peng, “Multiparameter quantum metrology using strongly interacting spin systems,” *arXiv:2104.00211* (2021).
- [244] Feng Pan and JP Draayer, “Analytical solutions for the lmg model,” *Physics Letters B* **451**, 1–10 (1999).
- [245] Hiroyuki Morita, Hiromasa Ohnishi, João da Providência, and Seiya Nishiyama, “Exact solutions for the lmg model hamiltonian based on the bethe ansatz,” *Nuclear Physics B* **737**, 337–350 (2006).
- [246] Sébastien Dusuel and Julien Vidal, “Finite-size scaling exponents of the lipkin-meshkov-glick model,” *Phys. Rev. Lett.* **93**, 237204 (2004).
- [247] Sébastien Dusuel and Julien Vidal, “Continuous unitary transformations and finite-size scaling exponents in the lipkin-meshkov-glick model,” *Phys. Rev. B* **71**, 224420 (2005).
- [248] Ho-Man Kwok, Wen-Qiang Ning, Shi-Jian Gu, Hai-Qing Lin, *et al.*, “Quantum criticality of the lipkin-meshkov-glick model in terms of fidelity susceptibility,” *Physical Review E* **78**, 032103 (2008).
- [249] Jian Ma, Lei Xu, Heng-Na Xiong, and Xiaoguang Wang, “Reduced fidelity susceptibility and its finite-size scaling behaviors in the lipkin-meshkov-glick model,” *Phys. Rev. E* **78**, 051126 (2008).
- [250] Giulio Salvatori, Antonio Mandarino, and Matteo GA Paris, “Quantum metrology in lipkin-meshkov-glick critical systems,” *Physical Review A* **90**, 022111 (2014).
- [251] Louis Garbe, Obinna Abah, Simone Felicetti, and Ricardo Puebla, “Critical quantum metrology with fully-connected models: from heisenberg to kibble-zurek scaling,” *Quantum Science and Technology* **7**, 035010 (2022).
- [252] Samuel Fernández-Lorenzo, Jacob A Dunningham, and Diego Porras, “Heisenberg scaling with classical long-range correlations,” *Physical Review A* **97**, 023843 (2018).
- [253] C. Monroe, W. C. Campbell, L.-M. Duan, Z.-X. Gong, A. V. Gorshkov, P. W. Hess, R. Islam, K. Kim, N. M. Linke, G. Pagano, P. Richerme, C. Senko, and N. Y.

- Yao, “Programmable quantum simulations of spin systems with trapped ions,” *Rev. Mod. Phys.* **93**, 025001 (2021).
- [254] Jing Yang, Shengshi Pang, Adolfo del Campo, and Andrew N Jordan, “Super-heisenberg scaling in hamiltonian parameter estimation in the long-range kitaev chain,” *Physical Review Research* **4**, 013133 (2022).
- [255] David J Luitz, Nicolas Laflorencie, and Fabien Alet, “Many-body localization edge in the random-field heisenberg chain,” *Physical Review B* **91**, 081103 (2015).
- [256] Qiujiang Guo, Chen Cheng, Zheng-Hang Sun, Zixuan Song, Hekang Li, Zhen Wang, Wenhui Ren, Hang Dong, Dongning Zheng, Yu-Ran Zhang, *et al.*, “Observation of energy-resolved many-body localization,” *Nature Physics* **17**, 234–239 (2021).
- [257] Rozhin Yousefjani and Abolfazl Bayat, “Mobility edge in long-range interacting many-body localized systems,” *Physical Review B* **107**, 045108 (2023).
- [258] Rozhin Yousefjani, Sougato Bose, and Abolfazl Bayat, “Floquet-induced localization in long-range many-body systems,” *Physical Review Research* **5**, 013094 (2023).
- [259] Shi-Xin Zhang and Hong Yao, “Universal properties of many-body localization transitions in quasiperiodic systems,” *Physical review letters* **121**, 206601 (2018).
- [260] Marko Žnidarič and Marko Ljubotina, “Interaction instability of localization in quasiperiodic systems,” *Proceedings of the National Academy of Sciences* **115**, 4595–4600 (2018).
- [261] William Morong, Fangli Liu, Patrick Becker, KS Collins, Lei Feng, Antonis Kyprianidis, Guido Pagano, Tianyu You, AV Gorshkov, and Christopher Monroe, “Observation of stark many-body localization without disorder,” *Nature* **599**, 393–398 (2021).
- [262] Robert Hofstadter and John A. McIntyre, “Experimental study of the compton effect at 1.2 mev,” *Phys. Rev.* **76**, 1269–1270 (1949).
- [263] Douglas R. Hofstadter, “Energy levels and wave functions of bloch electrons in rational and irrational magnetic fields,” *Phys. Rev. B* **14**, 2239–2249 (1976).
- [264] Vieri Mastropietro, “Localization of interacting fermions in the aubry-andré model,” *Phys. Rev. Lett.* **115**, 180401 (2015).
- [265] Vieri Mastropietro, “Localization in interacting fermionic chains with quasi-random disorder,” *Communications in Mathematical Physics* **351**, 283–309 (2017).
- [266] Vedika Khemani, D. N. Sheng, and David A. Huse, “Two universality classes for the many-body localization transition,” *Phys. Rev. Lett.* **119**, 075702 (2017).
- [267] Piero Naldesi, Elisa Ercolessi, and Tommaso Roscilde, “Detecting a many-body mobility edge with quantum quenches,” *SciPost Phys.* **1**, 010 (2016).
- [268] F. Setiawan, Dong-Ling Deng, and J. H. Pixley, “Transport properties across the many-body localization transition in quasiperiodic and random systems,” *Phys. Rev. B* **96**, 104205 (2017).
- [269] Ayan Sahoo and Debraj Rakshit, “Enhanced sensing of stark weak field under the influence of aubry-andré harper criticality,” *arXiv:2408.03232* (2024).
- [270] Andrey R Kolovsky, “Interplay between anderson and stark localization in 2d lattices,” *Physical review letters* **101**, 190602 (2008).
- [271] Titas Chanda, Ruixiao Yao, and Jakub Zakrzewski, “Coexistence of localized and extended phases: Many-body localization in a harmonic trap,” *Physical Review Research* **2**, 032039 (2020).
- [272] Ruixiao Yao and Jakub Zakrzewski, “Many-body localization of bosons in an optical lattice: Dynamics in disorder-free potentials,” *Physical Review B* **102**, 104203 (2020).
- [273] Chong Chen, Ping Wang, and Ren-Bao Liu, “Effects of local decoherence on quantum critical metrology,” *Physical Review A* **104**, L020601 (2021).
- [274] Shou-cheng Zhang, “Topological states of quantum matter,” *Physics* **1**, 6 (2008).
- [275] Tudor D Stanescu, *Introduction to topological quantum matter & quantum computation* (CRC Press, 2016).
- [276] Nathan Goldman, Jan Carl Budich, and Peter Zoller, “Topological quantum matter with ultracold gases in optical lattices,” *Nature Physics* **12**, 639–645 (2016).
- [277] Alexander Alldridge, Christopher Max, and Martin R Zirnbauer, “Bulk-boundary correspondence for disordered free-fermion topological phases,” *Communications in Mathematical Physics* **377**, 1761–1821 (2020).
- [278] Abhijeet Alase, *Boundary physics and bulk-boundary correspondence in topological phases of matter* (Dartmouth College, 2019).
- [279] B Andrei Bernevig, “Topological insulators and topological superconductors,” in *Topological Insulators and Topological Superconductors* (Princeton university press, 2013).
- [280] Xie Chen, Zheng-Cheng Gu, Zheng-Xin Liu, and Xiaogang Wen, “Symmetry protected topological orders and the group cohomology of their symmetry group,” *Phys. Rev. B* **87**, 155114 (2013).
- [281] WP Su, JR Schrieffer, and Ao J Heeger, “Solitons in polyacetylene,” *Physical review letters* **42**, 1698 (1979).
- [282] Xiao-Liang Qi and Shou-Cheng Zhang, “Topological insulators and superconductors,” *Reviews of Modern Physics* **83**, 1057 (2011).
- [283] Zhan Wu, Long Zhang, Wei Sun, Xiao-Tian Xu, Bao-Zong Wang, Si-Cong Ji, Youjin Deng, Shuai Chen, Xiong-Jun Liu, and Jian-Wei Pan, “Realization of two-dimensional spin-orbit coupling for bose-einstein condensates,” *Science* **354**, 83–88 (2016).
- [284] Sayan Mondal, Ayan Sahoo, Ujjwal Sen, and Debraj Rakshit, “Multicritical quantum sensors driven by symmetry-breaking,” *arXiv:2407.14428* (2024).
- [285] Damian F Abasto, Alioscia Hama, and Paolo Zanardi, “Fidelity analysis of topological quantum phase transitions,” *Physical Review A* **78**, 010301 (2008).
- [286] Shuo Yang, Shi-Jian Gu, Chang-Pu Sun, and Hai-Qing Lin, “Fidelity susceptibility and long-range correlation in the kitaev honeycomb model,” *Physical Review A* **78**, 012304 (2008).
- [287] Jian-Hui Zhao and Huan-Qiang Zhou, “Singularities in ground-state fidelity and quantum phase transitions for the kitaev model,” *Physical Review B* **80**, 014403 (2009).
- [288] Shi-Jian Gu and Hai-Qing Lin, “Scaling dimension of fidelity susceptibility in quantum phase transitions,” *EPL (Europhysics Letters)* **87**, 10003 (2009).
- [289] Bruno Mera, Anwei Zhang, and Nathan Goldman, “Relating the topology of dirac hamiltonians to quantum geometry: When the quantum metric dictates chern numbers and winding numbers,” *SciPost Physics* **12**, 018 (2022).

- [290] Yuto Ashida, Zongping Gong, and Masahito Ueda, “Non-hermitian physics,” *Advances in Physics* **69**, 249–435 (2020).
- [291] Emil J. Bergholtz, Jan Carl Budich, and Flore K. Kunst, “Exceptional topology of non-hermitian systems,” *Rev. Mod. Phys.* **93**, 015005 (2021).
- [292] Dorje C Brody, “Biorthogonal quantum mechanics,” *Journal of Physics A: Mathematical and Theoretical* **47**, 035305 (2013).
- [293] Daniel Leykam, Konstantin Y. Bliokh, Chunli Huang, Y. D. Chong, and Franco Nori, “Edge modes, degeneracies, and topological numbers in non-hermitian systems,” *Phys. Rev. Lett.* **118**, 040401 (2017).
- [294] Naomichi Hatano and David R Nelson, “Localization transitions in non-hermitian quantum mechanics,” *Physical review letters* **77**, 570 (1996).
- [295] Leonardo Banchi, Samuel L. Braunstein, and Stefano Pirandola, “Quantum fidelity for arbitrary gaussian states,” *Phys. Rev. Lett.* **115**, 260501 (2015).
- [296] Rebekka Koch and Jan Carl Budich, “Bulk-boundary correspondence in non-hermitian systems: stability analysis for generalized boundary conditions,” *The European Physical Journal D* **74**, 70 (2020).
- [297] Flore K. Kunst, Elisabet Edvardsson, Jan Carl Budich, and Emil J. Bergholtz, “Biorthogonal bulk-boundary correspondence in non-hermitian systems,” *Phys. Rev. Lett.* **121**, 026808 (2018).
- [298] Elisabet Edvardsson and Eddy Ardonne, “Sensitivity of non-hermitian systems,” *Phys. Rev. B* **106**, 115107 (2022).
- [299] Zhiwei Guo, Tengzhou Zhang, Juan Song, Haitao Jiang, and Hong Chen, “Sensitivity of topological edge states in a non-hermitian dimer chain,” *Photonics Research* **9**, 574–582 (2021).
- [300] Wenkui Ding, Xiaoguang Wang, and Shu Chen, “Fundamental sensitivity limits for non-hermitian quantum sensors,” *Phys. Rev. Lett.* **131**, 160801 (2023).
- [301] Kohei Kawabata, Ken Shiozaki, Masahito Ueda, and Masatoshi Sato, “Symmetry and topology in non-hermitian physics,” *Phys. Rev. X* **9**, 041015 (2019).
- [302] Nobuyuki Okuma, Kohei Kawabata, Ken Shiozaki, and Masatoshi Sato, “Topological origin of non-hermitian skin effects,” *Phys. Rev. Lett.* **124**, 086801 (2020).
- [303] Kai Zhang, Zhesen Yang, and Chen Fang, “Correspondence between winding numbers and skin modes in non-hermitian systems,” *Phys. Rev. Lett.* **125**, 126402 (2020).
- [304] Kai Zhang, Zhesen Yang, and Chen Fang, “Universal non-hermitian skin effect in two and higher dimensions,” *Nature Communications* **13**, 2496 (2022).
- [305] Linhu Li, Ching Hua Lee, Sen Mu, and Jiangbin Gong, “Critical non-hermitian skin effect,” *Nature Communications* **11**, 5491 (2020).
- [306] S. Longhi, “Topological phase transition in non-hermitian quasicrystals,” *Phys. Rev. Lett.* **122**, 237601 (2019).
- [307] Shunyu Yao and Zhong Wang, “Edge states and topological invariants of non-hermitian systems,” *Phys. Rev. Lett.* **121**, 086803 (2018).
- [308] Shunyu Yao, Fei Song, and Zhong Wang, “Non-hermitian chern bands,” *Phys. Rev. Lett.* **121**, 136802 (2018).
- [309] Lei Xiao, Tianshu Deng, Kunkun Wang, Gaoyan Zhu, Zhong Wang, Wei Yi, and Peng Xue, “Non-hermitian bulk-boundary correspondence in quantum dynamics,” *Nature Physics* **16**, 761–766 (2020).
- [310] Lei Xiao, Tianshu Deng, Kunkun Wang, Zhong Wang, Wei Yi, and Peng Xue, “Observation of non-bloch parity-time symmetry and exceptional points,” *Phys. Rev. Lett.* **126**, 230402 (2021).
- [311] Francesco Albarelli, Matteo AC Rossi, Dario Tamascelli, and Marco G Genoni, “Restoring heisenberg scaling in noisy quantum metrology by monitoring the environment,” *Quantum* **2**, 110 (2018).
- [312] Matteo AC Rossi, Francesco Albarelli, Dario Tamascelli, and Marco G Genoni, “Noisy quantum metrology enhanced by continuous nondemolition measurement,” *Phys. Rev. Lett.* **125**, 200505 (2020).
- [313] Alex W Chin, Susana F Huelga, and Martin B Plenio, “Quantum metrology in non-markovian environments,” *Phys. Rev. Lett.* **109**, 233601 (2012).
- [314] R Chaves, JB Brask, Marcin Markiewicz, J Kolodyński, and A Acín, “Noisy metrology beyond the standard quantum limit,” *Physical review letters* **111**, 120401 (2013).
- [315] Jonatan Bohr Brask, Rafael Chaves, and Jan Kolodyński, “Improved quantum magnetometry beyond the standard quantum limit,” *Phys. Rev. X* **5**, 031010 (2015).
- [316] Andrea Smirne, Jan Kolodyński, Susana F Huelga, and Rafał Demkowicz-Dobrzański, “Ultimate precision limits for noisy frequency estimation,” *Physical review letters* **116**, 120801 (2016).
- [317] Markus Heyl, “Dynamical quantum phase transitions: a review,” *Reports on Progress in Physics* **81**, 054001 (2018).
- [318] R Jafari and Henrik Johannesson, “Loschmidt echo revivals: Critical and noncritical,” *Physical review letters* **118**, 015701 (2017).
- [319] Longwen Zhou, Qing-hai Wang, Hailong Wang, and Jiangbin Gong, “Dynamical quantum phase transitions in non-hermitian lattices,” *Phys. Rev. A* **98**, 022129 (2018).
- [320] Yecheng Jing, Jian-Jun Dong, Yu-Yu Zhang, and Zi-Xiang Hu, “Biorthogonal dynamical quantum phase transitions in non-hermitian systems,” *Phys. Rev. Lett.* **132**, 220402 (2024).
- [321] Francisco J González, Ariel Norambuena, and Raúl Coto, “Dynamical quantum phase transition in diamond: Applications in quantum metrology,” *Physical Review B* **106**, 014313 (2022).
- [322] Qingze Guan and Robert J Lewis-Swan, “Identifying and harnessing dynamical phase transitions for quantum-enhanced sensing,” *Physical Review Research* **3**, 033199 (2021).
- [323] Krzysztof Sacha, “Modeling spontaneous breaking of time-translation symmetry,” *Physical Review A* **91**, 033617 (2015).
- [324] Vedika Khemani, Achilleas Lazarides, Roderich Moessner, and Shivaji L Sondhi, “Phase structure of driven quantum systems,” *Physical review letters* **116**, 250401 (2016).
- [325] Dominic V Else, Bela Bauer, and Chetan Nayak, “Floquet time crystals,” *Physical review letters* **117**, 090402 (2016).
- [326] Fernando Iemini, Rosario Fazio, and Anna Sanpera, “Floquet time crystals as quantum sensors of ac fields,” *Physical Review A* **109**, L050203 (2024).

- [327] Dominic Gribben, Anna Sanpera, Rosario Fazio, Jamir Marino, and Fernando Iemini, “Quantum enhancements and entropic constraints to boundary time crystals as sensors of ac fields,” [arXiv:2406.06273](#) (2024).
- [328] JE Lang, Ren-Bao Liu, and TS Monteiro, “Dynamical-decoupling-based quantum sensing: Floquet spectroscopy,” *Physical Review X* **5**, 041016 (2015).
- [329] Guoqing Wang, Yi-Xiang Liu, Jennifer M Schloss, Scott T Alsid, Danielle A Braje, Paola Cappellaro, *et al.*, “Sensing of arbitrary-frequency fields using a quantum mixer,” *Physical Review X* **12**, 021061 (2022).
- [330] Min Jiang, Yushu Qin, Xin Wang, Yuanhong Wang, Haowen Su, Xinhua Peng, and Dmitry Budker, “Floquet spin amplification,” *Physical Review Letters* **128**, 233201 (2022).
- [331] Shengshi Pang and Andrew N Jordan, “Optimal adaptive control for quantum metrology with time-dependent hamiltonians,” *Nature communications* **8**, 1–9 (2017).
- [332] Hengyun Zhou, Joonhee Choi, Soonwon Choi, Renate Landig, Alexander M. Douglas, Junichi Isoya, Fedor Jelezko, Shinobu Onoda, Hitoshi Sumiya, Paola Cappellaro, Helena S. Knowles, Hongkun Park, and Mikhail D. Lukin, “Quantum metrology with strongly interacting spin systems,” *Phys. Rev. X* **10**, 031003 (2020).
- [333] Min Yu, Yu Liu, Pengcheng Yang, Musang Gong, Qingyun Cao, Shaoliang Zhang, Haibin Liu, Markus Heyl, Tomoki Ozawa, Nathan Goldman, *et al.*, “Quantum fisher information measurement and verification of the quantum cramer-rao bound in a solid-state qubit,” *npj Quantum Information* **8**, 1–8 (2022).
- [334] Peter A Ivanov, “Enhanced parameter estimation with periodically driven quantum probe,” *Entropy* **23**, 1333 (2021).
- [335] Angelo Russomanno, Giuseppe E Santoro, and Rosario Fazio, “Entanglement entropy in a periodically driven ising chain,” *Journal of Statistical Mechanics: Theory and Experiment* **2016**, 073101 (2016).
- [336] Takashi Ishii, Tomotaka Kuwahara, Takashi Mori, and Naomichi Hatano, “Heating in integrable time-periodic systems,” *Phys. Rev. Lett.* **120**, 220602 (2018).
- [337] Garry Goldstein, Paola Cappellaro, Jero R Maze, JS Hodges, L Jiang, Anders Søndberg Sørensen, and MD Lukin, “Environment-assisted precision measurement,” *Physical review letters* **106**, 140502 (2011).
- [338] Martin B Plenio, Vlatko Vedral, and Peter L Knight, “Quantum error correction in the presence of spontaneous emission,” *Physical Review A* **55**, 67 (1997).
- [339] Morten Kjaergaard, Mollie E Schwartz, Jochen Braumüller, Philip Krantz, Joel I-J Wang, Simon Gustavsson, and William D Oliver, “Superconducting qubits: Current state of play,” *Annual Review of Condensed Matter Physics* **11**, 369–395 (2020).
- [340] Kastler, Alfred, “Quelques suggestions concernant la production optique et la détection optique d’une inégalité de population des niveaux de quantification spatiale des atomes. application à l’expérience de stern et gerlach et à la résonance magnétique,” *J. Phys. Radium* **11**, 255–265 (1950).
- [341] GAML Alzetta, A Gozzini, L Moi, and G Orriols, “An experimental method for the observation of rf transitions and laser beat resonances in oriented na vapour,” *Il Nuovo Cimento B (1971-1996)* **36**, 5–20 (1976).
- [342] EetGORRIOLS Arimondo and G Orriols, “Nonabsorbing atomic coherences by coherent two-photon transitions in a three-level optical pumping,” *Nuovo Cimento Lettere* **17**, 333–338 (1976).
- [343] A. Aspect, E. Arimondo, R. Kaiser, N. Vansteenkiste, and C. Cohen-Tannoudji, “Laser cooling below the one-photon recoil energy by velocity-selective coherent population trapping,” *Phys. Rev. Lett.* **61**, 826–829 (1988).
- [344] ARR Carvalho, P Milman, RL de Matos Filho, and L Davidovich, “Decoherence, pointer engineering and quantum state protection,” in *Modern Challenges in Quantum Optics* (Springer, 2001) pp. 65–79.
- [345] Frank Verstraete, Michael M. Wolf, and J. Ignacio Cirac, “Quantum computation and quantum-state engineering driven by dissipation,” *Nature Physics* **5**, 633–636 (2009).
- [346] Sebastian Diehl, A Micheli, Adrian Kantian, B Kraus, HP Büchler, and Peter Zoller, “Quantum states and phases in driven open quantum systems with cold atoms,” *Nature Physics* **4**, 878–883 (2008).
- [347] Fernando Pastawski, Lucas Clemente, and Juan Ignacio Cirac, “Quantum memories based on engineered dissipation,” *Physical Review A* **83**, 012304 (2011).
- [348] Julio T Barreiro, Markus Müller, Philipp Schindler, Daniel Nigg, Thomas Monz, Michael Chwalla, Markus Hennrich, Christian F Roos, Peter Zoller, and Rainer Blatt, “An open-system quantum simulator with trapped ions,” *Nature* **470**, 486–491 (2011).
- [349] Daniel A Lidar, “Review of decoherence-free subspaces, noiseless subsystems, and dynamical decoupling,” *Quantum information and computation for chemistry*, 295–354 (2014).
- [350] G Massimo Palma, Kalle-Antti Suominen, and Artur Ekert, “Quantum computers and dissipation,” *Proceedings of the Royal Society of London. Series A: Mathematical, Physical and Engineering Sciences* **452**, 567–584 (1996).
- [351] Paolo Zanardi, “Dissipative dynamics in a quantum register,” *Physical Review A* **56**, 4445 (1997).
- [352] Lorenza Viola and Emanuel Knill, “Robust dynamical decoupling of quantum systems with bounded controls,” *Physical Review Letters* **90**, 037901 (2003).
- [353] M. J. Kastoryano, F. Reiter, and A. S. Sørensen, “Dissipative preparation of entanglement in optical cavities,” *Phys. Rev. Lett.* **106**, 090502 (2011).
- [354] A. F. Alharbi and Z. Ficek, “Deterministic creation of stationary entangled states by dissipation,” *Phys. Rev. A* **82**, 054103 (2010).
- [355] Ryan Sweke, Ilya Sinayskiy, and Francesco Petruccione, “Dissipative preparation of large w states in optical cavities,” *Phys. Rev. A* **87**, 042323 (2013).
- [356] Dong-Xiao Li, Xiao-Qiang Shao, Jin-Hui Wu, and XX Yi, “Dissipation-induced w state in a rydberg-atom-cavity system,” *Optics Letters* **43**, 1639–1642 (2018).
- [357] Jaeyoon Cho, Sougato Bose, and M. S. Kim, “Optical pumping into many-body entanglement,” *Phys. Rev. Lett.* **106**, 020504 (2011).
- [358] Kai Stannigel, Peter Rabl, and Peter Zoller, “Driven-dissipative preparation of entangled states in cascaded quantum-optical networks,” *New Journal of Physics* **14**, 063014 (2012).
- [359] Kuan-Liang Liu and Hsi-Sheng Goan, “Non-markovian entanglement dynamics of quantum continuous variable systems in thermal environments,” *Phys. Rev. A* **76**, 022312 (2007).

- [360] Gao-xiang Li, Li-hui Sun, and Zbigniew Ficek, “Multi-mode entanglement of n harmonic oscillators coupled to a non-markovian reservoir,” *Journal of Physics B: Atomic, Molecular and Optical Physics* **43**, 135501 (2010).
- [361] G. D. de Moraes Neto, W. Rosado, F. O. Prado, and M. H. Y. Moussa, “Steady entanglement in bosonic dissipative networks,” *Phys. Rev. A* **90**, 062322 (2014).
- [362] GD de Moraes Neto, VF Teizen, V Montenegro, and E Vernek, “Steady many-body entanglements in dissipative systems,” *Physical Review A* **96**, 062313 (2017).
- [363] Jan Kołodzyński and Rafał Demkowicz-Dobrzański, “Phase estimation without a priori phase knowledge in the presence of loss,” *Phys. Rev. A* **82**, 053804 (2010).
- [364] Rafał Demkowicz-Dobrzański, Jan Kołodzyński, and Mădălin Guță, “The elusive heisenberg limit in quantum-enhanced metrology,” *Nature communications* **3**, 1–8 (2012).
- [365] Sergey Knysh, Vadim N Smelyanskiy, and Gabriel A Durkin, “Scaling laws for precision in quantum interferometry and the bifurcation landscape of the optimal state,” *Physical Review A* **83**, 021804 (2011).
- [366] M Kacprowicz, R Demkowicz-Dobrzański, W Wasilewski, K Banaszek, and IA Walmsley, “Experimental quantum-enhanced estimation of a lossy phase shift,” *Nature Photonics* **4**, 357–360 (2010).
- [367] C. L. Latune, B. M. Escher, R. L. de Matos Filho, and L. Davidovich, “Quantum limit for the measurement of a classical force coupled to a noisy quantum-mechanical oscillator,” *Phys. Rev. A* **88**, 042112 (2013).
- [368] BM Escher, L Davidovich, N Zagury, and RL de Matos Filho, “Quantum metrological limits via a variational approach,” *Physical review letters* **109**, 190404 (2012).
- [369] Tony E. Lee, Sarang Gopalakrishnan, and Mikhail D. Lukin, “Unconventional magnetism via optical pumping of interacting spin systems,” *Phys. Rev. Lett.* **110**, 257204 (2013).
- [370] Eric M Kessler, Geza Giedke, Atac Imamoglu, Susanne F Yelin, Mikhail D Lukin, and J Ignacio Cirac, “Dissipative phase transition in a central spin system,” *Physical Review A* **86**, 012116 (2012).
- [371] Emanuele G. Dalla Torre, Eugene Demler, Thierry Giamarchi, and Ehud Altman, “Dynamics and universality in noise-driven dissipative systems,” *Phys. Rev. B* **85**, 184302 (2012).
- [372] Jamir Marino and Sebastian Diehl, “Driven markovian quantum criticality,” *Physical review letters* **116**, 070407 (2016).
- [373] Filippo Vicentini, Fabrizio Minganti, Riccardo Rota, Giuliano Orso, and Cristiano Ciuti, “Critical slowing down in driven-dissipative bose-hubbard lattices,” *Physical Review A* **97**, 013853 (2018).
- [374] R Rota, F Minganti, A Biella, and C Ciuti, “Dynamical properties of dissipative xyz heisenberg lattices,” *New Journal of Physics* **20**, 045003 (2018).
- [375] R. Rota, F. Storme, N. Bartolo, R. Fazio, and C. Ciuti, “Critical behavior of dissipative two-dimensional spin lattices,” *Phys. Rev. B* **95**, 134431 (2017).
- [376] F. Letscher, O. Thomas, T. Niederprüm, M. Fleischauer, and H. Ott, “Bistability versus metastability in driven dissipative rydberg gases,” *Phys. Rev. X* **7**, 021020 (2017).
- [377] Vincent R. Overbeck, Mohammad F. Maghrebi, Alexey V. Gorshkov, and Hendrik Weimer, “Multicritical behavior in dissipative ising models,” *Phys. Rev. A* **95**, 042133 (2017).
- [378] Luca Capriotti, Alessandro Cuccoli, Andrea Fubini, Valerio Tognetti, and Ruggero Vaia, “Dissipation-driven phase transition in two-dimensional josephson arrays,” *Phys. Rev. Lett.* **94**, 157001 (2005).
- [379] J. Eisert and T. Prosen, “Noise-driven quantum criticality,” [arXiv:1012.5013](https://arxiv.org/abs/1012.5013) (2010).
- [380] L. M. Sieberer, S. D. Huber, E. Altman, and S. Diehl, “Nonequilibrium functional renormalization for driven-dissipative bose-einstein condensation,” *Phys. Rev. B* **89**, 134310 (2014).
- [381] Peter A Ivanov, “Enhanced two-parameter phase-space-displacement estimation close to a dissipative phase transition,” *Physical Review A* **102**, 052611 (2020).
- [382] H. J. Carmichael, “Breakdown of photon blockade: A dissipative quantum phase transition in zero dimensions,” *Phys. Rev. X* **5**, 031028 (2015).
- [383] Mónica Benito, Carlos Sánchez Muñoz, and Carlos Navarrete-Benlloch, “Degenerate parametric oscillation in quantum membrane optomechanics,” *Phys. Rev. A* **93**, 023846 (2016).
- [384] J. J. Mendoza-Arenas, S. R. Clark, S. Felicetti, G. Romero, E. Solano, D. G. Angelakis, and D. Jaksch, “Beyond mean-field bistability in driven-dissipative lattices: Bunching-antibunching transition and quantum simulation,” *Phys. Rev. A* **93**, 023821 (2016).
- [385] W. Casteels, F. Storme, A. Le Boité, and C. Ciuti, “Power laws in the dynamic hysteresis of quantum nonlinear photonic resonators,” *Phys. Rev. A* **93**, 033824 (2016).
- [386] Nicola Bartolo, Fabrizio Minganti, Wim Casteels, and Cristiano Ciuti, “Exact steady state of a kerr resonator with one- and two-photon driving and dissipation: Controllable wigner-function multimodality and dissipative phase transitions,” *Phys. Rev. A* **94**, 033841 (2016).
- [387] Wim Casteels, Rosario Fazio, and Christiano Ciuti, “Critical dynamical properties of a first-order dissipative phase transition,” *Physical Review A* **95**, 012128 (2017).
- [388] Wim Casteels and Cristiano Ciuti, “Quantum entanglement in the spatial-symmetry-breaking phase transition of a driven-dissipative bose-hubbard dimer,” *Phys. Rev. A* **95**, 013812 (2017).
- [389] M. Foss-Feig, P. Niroula, J. T. Young, M. Hafezi, A. V. Gorshkov, R. M. Wilson, and M. F. Maghrebi, “Emergent equilibrium in many-body optical bistability,” *Phys. Rev. A* **95**, 043826 (2017).
- [390] Matteo Biondi, Gianni Blatter, Hakan E. Türeci, and Sebastian Schmidt, “Nonequilibrium gas-liquid transition in the driven-dissipative photonic lattice,” *Phys. Rev. A* **96**, 043809 (2017).
- [391] Alberto Biella, Florent Storme, José Lebreuilly, Davide Rossini, Rosario Fazio, Iacopo Carusotto, and Cristiano Ciuti, “Phase diagram of incoherently driven strongly correlated photonic lattices,” *Phys. Rev. A* **96**, 023839 (2017).
- [392] Vincenzo Savona, “Spontaneous symmetry breaking in a quadratically driven nonlinear photonic lattice,” *Phys. Rev. A* **96**, 033826 (2017).
- [393] Carlos Sánchez Muñoz, Antonio Lara, Jorge Puebla, and Franco Nori, “Hybrid systems for the generation of nonclassical mechanical states via quadratic interac-

- tions,” *Phys. Rev. Lett.* **121**, 123604 (2018).
- [394] LM Sieberer, Sebastian D Huber, Ehud Altman, and S Diehl, “Dynamical critical phenomena in driven-dissipative systems,” *Physical review letters* **110**, 195301 (2013).
- [395] Jiasen Jin, Alberto Biella, Oscar Viyuela, Leonardo Mazza, Jonathan Keeling, Rosario Fazio, and Davide Rossini, “Cluster mean-field approach to the steady-state phase diagram of dissipative spin systems,” *Phys. Rev. X* **6**, 031011 (2016).
- [396] Tony E. Lee, H. Häffner, and M. C. Cross, “Antiferromagnetic phase transition in a nonequilibrium lattice of rydberg atoms,” *Phys. Rev. A* **84**, 031402 (2011).
- [397] Ching-Kit Chan, Tony E. Lee, and Sarang Gopalakrishnan, “Limit-cycle phase in driven-dissipative spin systems,” *Phys. Rev. A* **91**, 051601 (2015).
- [398] Mohammad F. Maghrebi and Alexey V. Gorshkov, “Nonequilibrium many-body steady states via keldysh formalism,” *Phys. Rev. B* **93**, 014307 (2016).
- [399] S V Lawande, R R Puri, and S S Hassan, “Non-resonant effects in the fluorescent dicke model. i. exact steady state analysis,” *Journal of Physics B: Atomic and Molecular Physics* **14**, 4171 (1981).
- [400] R.R. Puri, S.V. Lawande, and S.S. Hassan, “Dispersion in the driven dicke model,” *Optics Communications* **35**, 179–184 (1980).
- [401] Hendrik Weimer, “Variational principle for steady states of dissipative quantum many-body systems,” *Phys. Rev. Lett.* **114**, 040402 (2015).
- [402] Matteo Marcuzzi, Emanuele Levi, Sebastian Diehl, Juan P Garrahan, and Igor Lesanovsky, “Universal nonequilibrium properties of dissipative rydberg gases,” *Physical review letters* **113**, 210401 (2014).
- [403] Federico Carollo, Edward Gillman, Hendrik Weimer, and Igor Lesanovsky, “Critical behavior of the quantum contact process in one dimension,” *Physical Review Letters* **123**, 100604 (2019).
- [404] Philipp Werner, Klaus Völker, Matthias Troyer, and Sudip Chakravarty, “Phase diagram and critical exponents of a dissipative ising spin chain in a transverse magnetic field,” *Phys. Rev. Lett.* **94**, 047201 (2005).
- [405] Angelo Carollo, Bernardo Spagnolo, and Davide Valenti, “Uhlmann curvature in dissipative phase transitions,” *Scientific reports* **8**, 1–16 (2018).
- [406] Jiasen Jin, Wen-Bin He, Fernando Iemini, Diego Ferreira, Ying-Dan Wang, Stefano Chesi, and Rosario Fazio, “Determination of the critical exponents in dissipative phase transitions: Coherent anomaly approach,” *Physical Review B* **104**, 214301 (2021).
- [407] M-L Cai, Z-D Liu, Y Jiang, Y-K Wu, Q-X Mei, W-D Zhao, L He, X Zhang, Z-C Zhou, and L-M Duan, “Probing a dissipative phase transition with a trapped ion through reservoir engineering,” *Chinese Physics Letters* **39**, 020502 (2022).
- [408] Giovanni Ferioli, Antoine Glicenstein, Igor Ferrier-Barbut, and Antoine Browaeys, “A non-equilibrium superradiant phase transition in free space,” *Nature Physics* **19**, 1345–1349 (2023).
- [409] J Benary, C Baals, E Bernhart, J Jiang, M Röhrle, and H Ott, “Experimental observation of a dissipative phase transition in a multi-mode many-body quantum system,” *New Journal of Physics* **24**, 103034 (2022).
- [410] Ferdinand Brennecke, Rafael Mottl, Kristian Baumann, Renate Landig, Tobias Donner, and Tilman Esslinger, “Real-time observation of fluctuations at the driven-dissipative dicke phase transition,” *Proceedings of the National Academy of Sciences* **110**, 11763–11767 (2013).
- [411] Francesco Ferri, Rodrigo Rosa-Medina, Fabian Finger, Nishant Dogra, Matteo Soriente, Oded Zilberberg, Tobias Donner, and Tilman Esslinger, “Emerging dissipative phases in a superradiant quantum gas with tunable decay,” *Physical Review X* **11**, 041046 (2021).
- [412] Thomas Fink, Anne Schade, Sven Höfling, Christian Schneider, and Ataç Imamoglu, “Signatures of a dissipative phase transition in photon correlation measurements,” *Nature Physics* **14**, 365–369 (2018).
- [413] Hamid Ohadi, A Dreismann, YG Rubo, F Pinsker, Y del Valle-Inclan Redondo, SI Tsintzos, Z Hatzopoulos, PG Savvidis, and JJ Baumberg, “Spontaneous spin bifurcations and ferromagnetic phase transitions in a spinor exciton-polariton condensate,” *Physical Review X* **5**, 031002 (2015).
- [414] Michele C Collodo, Anton Potočnik, Simone Gasparinetti, Jean-Claude Besse, Marek Pechal, Mahdi Sameti, Michael J Hartmann, Andreas Wallraff, and Christopher Eichler, “Observation of the crossover from photon ordering to delocalization in tunably coupled resonators,” *Physical Review Letters* **122**, 183601 (2019).
- [415] Dong-Sheng Ding, Hannes Busche, Bao-Sen Shi, Guang-Can Guo, and Charles S. Adams, “Phase diagram and self-organizing dynamics in a thermal ensemble of strongly interacting rydberg atoms,” *Phys. Rev. X* **10**, 021023 (2020).
- [416] G. S. Agarwal, A. C. Brown, L. M. Narducci, and G. Vetri, “Collective atomic effects in resonance fluorescence,” *Phys. Rev. A* **15**, 1613–1624 (1977).
- [417] H J Carmichael and D F Walls, “Hysteresis in the spectrum for cooperative resonance fluorescence,” *Journal of Physics B: Atomic and Molecular Physics* **10**, L685 (1977).
- [418] D. F. Walls, P. D. Drummond, S. S. Hassan, and H. J. Carmichael, “Non-Equilibrium Phase Transitions in Cooperative Atomic Systems,” *Progress of Theoretical Physics Supplement* **64**, 307–320 (1978).
- [419] D F Walls, “Cooperative fluorescence from n coherently driven two-level atoms,” *Journal of Physics B: Atomic and Molecular Physics* **13**, 2001 (1980).
- [420] H J Carmichael, “Analytical and numerical results for the steady state in cooperative resonance fluorescence,” *Journal of Physics B: Atomic and Molecular Physics* **13**, 3551 (1980).
- [421] S Morrison and AS Parkins, “Dissipation-driven quantum phase transitions in collective spin systems,” *Journal of Physics B: Atomic, Molecular and Optical Physics* **41**, 195502 (2008).
- [422] F Iemini, A Russomanno, J Keeling, M Schirò, M Dalmonte, and R Fazio, “Boundary time crystals,” *Physical review letters* **121**, 035301 (2018).
- [423] Federico Carollo and Igor Lesanovsky, “Exact solution of a boundary time-crystal phase transition: time-translation symmetry breaking and non-markovian dynamics of correlations,” *Physical Review A* **105**, L040202 (2022).
- [424] Cristóbal Lledó and Marzena H Szymańska, “A dissipative time crystal with or without z2 symmetry breaking,” *New Journal of Physics* **22**, 075002 (2020).
- [425] Frank Wilczek, “Quantum time crystals,” *Physical re-*

- view letters **109**, 160401 (2012).
- [426] Alfred Shapere and Frank Wilczek, “Classical time crystals,” *Physical review letters* **109**, 160402 (2012).
- [427] Tongcang Li, Zhe-Xuan Gong, Zhang-Qi Yin, HT Quan, Xiaobo Yin, Peng Zhang, L-M Duan, and Xiang Zhang, “Space-time crystals of trapped ions,” *Physical review letters* **109**, 163001 (2012).
- [428] Fabrizio Minganti, Ievgen I Arkhipov, Adam Miranowicz, and Franco Nori, “Correspondence between dissipative phase transitions of light and time crystals,” [arXiv:2008.08075](https://arxiv.org/abs/2008.08075) (2020).
- [429] Krzysztof Sacha and Jakub Zakrzewski, “Time crystals: a review,” *Reports on Progress in Physics* **81**, 016401 (2017).
- [430] Albert Cabot, Leah Sophie Muhle, Federico Carollo, and Igor Lesanovsky, “Quantum trajectories of dissipative time crystals,” *Phys. Rev. A* **108**, L041303 (2023).
- [431] Antônio C Lourenço, Luis Fernando dos Prazeres, Thiago O Maciel, Fernando Iemini, and Eduardo I Duzzioni, “Genuine multipartite correlations in a boundary time crystal,” *Physical Review B* **105**, 134422 (2022).
- [432] K Tucker, B Zhu, R J Lewis-Swan, J Marino, F Jimenez, J G Restrepo, and A M Rey, “Shattered time: can a dissipative time crystal survive many-body correlations?” *New Journal of Physics* **20**, 123003 (2018).
- [433] Matthew A. Norcia, Robert J. Lewis-Swan, Julia R. K. Cline, Bihui Zhu, Ana M. Rey, and James K. Thompson, “Cavity-mediated collective spin-exchange interactions in a strontium superradiant laser,” *Science* **361**, 259–262 (2018).
- [434] Athreya Shankar, John Cooper, Justin G. Bohnet, John J. Bollinger, and Murray Holland, “Steady-state spin synchronization through the collective motion of trapped ions,” *Physical Review A* **95** (2017), [10.1103/physreva.95.033423](https://doi.org/10.1103/physreva.95.033423).
- [435] Naoto Shiraishi and Takashi Mori, “Systematic construction of counterexamples to the eigenstate thermalization hypothesis,” *Physical review letters* **119**, 030601 (2017).
- [436] Christopher J Turner, Alexios A Michailidis, Dmitry A Abanin, Maksym Serbyn, and Zlatko Papić, “Weak ergodicity breaking from quantum many-body scars,” *Nature Physics* **14**, 745–749 (2018).
- [437] Maksym Serbyn, Dmitry A Abanin, and Zlatko Papić, “Quantum many-body scars and weak breaking of ergodicity,” *Nature Physics* **17**, 675–685 (2021).
- [438] Josh M Deutsch, “Quantum statistical mechanics in a closed system,” *Physical review A* **43**, 2046 (1991).
- [439] Mark Srednicki, “Chaos and quantum thermalization,” *Physical Review E* **50**, 888 (1994).
- [440] Marcos Rigol, Vanja Dunjko, and Maxim Olshanii, “Thermalization and its mechanism for generic isolated quantum systems,” *Nature* **452**, 854–858 (2008).
- [441] Shane Dooley, “Robust quantum sensing in strongly interacting systems with many-body scars,” *PRX Quantum* **2**, 020330 (2021).
- [442] Shane Dooley, Silvia Pappalardi, and John Goold, “Entanglement enhanced metrology with quantum many-body scars,” *Physical Review B* **107**, 035123 (2023).
- [443] Jean-Yves Desaulès, Francesca Pietracaprina, Zlatko Papić, John Goold, and Silvia Pappalardi, “Extensive multipartite entanglement from su(2) quantum many-body scars,” *Physical Review Letters* **129**, 020601 (2022).
- [444] Daniel K Mark and Olexei I Motrunich, “ η -pairing states as true scars in an extended hubbard model,” *Physical Review B* **102**, 075132 (2020).
- [445] Shigeru Machida and Mikio Namiki, “Theory of Measurement of Quantum Mechanics: Mechanism of Reduction of Wave Packet. I,” *Progress of Theoretical Physics* **63**, 1457–1473 (1980).
- [446] Shigeru Machida and Mikio Namiki, “Theory of Measurement in Quantum Mechanics: Mechanism of Reduction of Wave Packet. II,” *Progress of Theoretical Physics* **63**, 1833–1847 (1980).
- [447] W. H. Furry, “Note on the quantum-mechanical theory of measurement,” *Phys. Rev.* **49**, 393–399 (1936).
- [448] H. D. Zeh, “On the interpretation of measurement in quantum theory,” *Foundations of Physics* **1**, 69–76 (1970).
- [449] Paul Busch, Gianni Cassinelli, and Pekka J. Lahti, “On the quantum theory of sequential measurements,” *Foundations of Physics* **20**, 757–775 (1990).
- [450] Heinz-Jürgen Schmidt and Jochen Gemmer, “Sequential measurements and entropy,” *Journal of Physics: Conference Series* **1638**, 012007 (2020).
- [451] Masashi Ban, “On sequential measurements with indefinite causal order,” *Physics Letters A* **403**, 127383 (2021).
- [452] Brian Skinner, Jonathan Ruhman, and Adam Nahum, “Measurement-induced phase transitions in the dynamics of entanglement,” *Phys. Rev. X* **9**, 031009 (2019).
- [453] Maxwell Block, Yimu Bao, Soonwon Choi, Ehud Altman, and Norman Y. Yao, “Measurement-induced transition in long-range interacting quantum circuits,” *Phys. Rev. Lett.* **128**, 010604 (2022).
- [454] Tristan Benoist, Jan-Luka Fatras, and Clément Pellegrini, “Limit theorems for quantum trajectories,” [arXiv:2302.06191](https://arxiv.org/abs/2302.06191) (2023).
- [455] Erkkka Haapasalo, Teiko Heinosaari, and Yui Kuramochi, “Saturation of repeated quantum measurements,” *Journal of Physics A: Mathematical and Theoretical* **49**, 33LT01 (2016).
- [456] Tristan Benoist, Martin Fraas, Yan Pautrat, and Clément Pellegrini, “Invariant measure for quantum trajectories,” *Probability Theory and Related Fields* **174**, 307–334 (2019).
- [457] Daniel Klaus Burgarth, Paolo Facchi, Vittorio Giovannetti, Hiromichi Nakazato, Saverio Pascazio, and Kazuya Yuasa, “Exponential rise of dynamical complexity in quantum computing through projections,” *Nat. Commun.* **5**, 1–6 (2014).
- [458] Tomás Rybár and Mário Ziman, “Process estimation in the presence of time-invariant memory effects,” *Phys. Rev. A* **92**, 042315 (2015).
- [459] Abolfazl Bayat, “Scaling of tripartite entanglement at impurity quantum phase transitions,” *Phys. Rev. Lett.* **118**, 036102 (2017).
- [460] Wen-Long Ma, Ping Wang, Weng-Hang Leong, and Ren-Bao Liu, “Phase transitions in sequential weak measurements,” *Physical Review A* **98**, 012117 (2018).
- [461] Soonwon Choi, Yimu Bao, Xiao-Liang Qi, and Ehud Altman, “Quantum error correction in scrambling dynamics and measurement-induced phase transition,” *Physical Review Letters* **125**, 030505 (2020).
- [462] Xiaozhou Feng, Brian Skinner, and Adam Nahum, “Measurement-induced phase transitions on dynamical

- quantum trees,” *PRX Quantum* **4**, 030333 (2023).
- [463] Takaaki Minato, Koudai Sugimoto, Tomotaka Kuwahara, and Keiji Saito, “Fate of measurement-induced phase transition in long-range interactions,” *Physical review letters* **128**, 010603 (2022).
- [464] Michael J Gullans and David A Huse, “Dynamical purification phase transition induced by quantum measurements,” *Physical Review X* **10**, 041020 (2020).
- [465] Maxwell Block, Yimu Bao, Soonwon Choi, Ehud Altman, and Norman Y Yao, “Measurement-induced transition in long-range interacting quantum circuits,” *Physical Review Letters* **128**, 010604 (2022).
- [466] Daniel Burgarth, Vittorio Giovannetti, Airi N Kato, and Kazuya Yuasa, “Quantum estimation via sequential measurements,” *New Journal of Physics* **17**, 113055 (2015).
- [467] Madalin Guta and Jukka Kiukas, “Information geometry and local asymptotic normality for multi-parameter estimation of quantum markov dynamics,” *Journal of Mathematical Physics* **58**, 052201 (2017).
- [468] Catalin Catana, Luc Bouten, and Mădălin Guță, “Fisher informations and local asymptotic normality for continuous-time quantum markov processes,” *Journal of Physics A: Mathematical and Theoretical* **48**, 365301 (2015).
- [469] Victor Montenegro, Gareth Siôn Jones, Sougato Bose, and Abolfazl Bayat, “Sequential measurements for quantum-enhanced magnetometry in spin chain probes,” *Phys. Rev. Lett.* **129**, 120503 (2022).
- [470] Hideo Mabuchi, “Dynamical identification of open quantum systems,” *Quantum and Semiclassical Optics: Journal of the European Optical Society Part B* **8**, 1103 (1996).
- [471] Merlijn van Horssen and Mădălin Guță, “Sanov and central limit theorems for output statistics of quantum markov chains,” *Journal of Mathematical Physics* **56**, 022109 (2015).
- [472] H Mabuchi, “Dynamical identification of open quantum systems,” *Quantum and Semiclassical Optics: Journal of the European Optical Society Part B* **8**, 1103 (1996).
- [473] Jianning Li and Dianzhen Cui, “Fisher information of sequential measurements and the optimization in composite systems,” *Phys. Rev. A* **108**, 012419 (2023).
- [474] Eoin O’Connor, Steve Campbell, and Gabriel T Landi, “Fisher information rates in sequentially measured quantum systems,” *New J. Phys.* **26**, 033048 (2024).
- [475] Lewis A. Clark, Adam Stokes, and Almut Beige, “Quantum jump metrology,” *Phys. Rev. A* **99**, 022102 (2019).
- [476] Antonella De Pasquale, Kazuya Yuasa, and Vittorio Giovannetti, “Estimating temperature via sequential measurements,” *Physical Review A* **96**, 012316 (2017).
- [477] Lewis A Clark, Adam Stokes, and Almut Beige, “Quantum jump metrology,” *Physical Review A* **99**, 022102 (2019).
- [478] Kawthar Al Rasbi, Almut Beige, and Lewis A. Clark, “Quantum jump metrology in a two-cavity network,” *Phys. Rev. A* **106**, 062619 (2022).
- [479] Mădălin Guță, “Fisher information and asymptotic normality in system identification for quantum markov chains,” *Physical Review A* **83**, 062324 (2011).
- [480] Antonella De Pasquale, Kazuya Yuasa, and Vittorio Giovannetti, “Estimating temperature via sequential measurements,” *Phys. Rev. A* **96**, 012316 (2017).
- [481] Atirach Ritboon, Lukáš Slodička, and Radim Filip, “Sequential phonon measurements of atomic motion,” *Quantum Science and Technology* **7**, 015023 (2022).
- [482] Maël Bompais and Nina H. Amini, “On asymptotic stability of non-demolition quantum trajectories with measurement imperfections,” *arXiv:2304.02462* (2023).
- [483] Maël Bompais, Nina H. Amini, and Clément Pellegrini, “Parameter estimation for quantum trajectories: Convergence result,” in *2022 IEEE 61st Conference on Decision and Control (CDC)* (2022) pp. 5161–5166.
- [484] Stefano Gherardini, Andrea Smirne, Matthias M. Müller, and Filippo Caruso, “Advances in sequential measurement and control of open quantum systems,” *Proceedings* **12** (2019), 10.3390/proceedings2019012011.
- [485] Jay Gambetta and H. M. Wiseman, “State and dynamical parameter estimation for open quantum systems,” *Phys. Rev. A* **64**, 042105 (2001).
- [486] Matthias M. Müller, Stefano Gherardini, Augusto Smerzi, and Filippo Caruso, “Fisher information from stochastic quantum measurements,” *Phys. Rev. A* **94**, 042322 (2016).
- [487] Eleonora Nagali, Simone Felicetti, Pierre-Louis de Assis, Vincenzo D’Ambrosio, Radim Filip, and Fabio Sciarino, “Testing sequential quantum measurements: how can maximal knowledge be extracted?” *Scientific Reports* **2** (2012), 10.1038/srep00443.
- [488] Alexander Holm Küllerich and Klaus Mølmer, “Quantum zeno effect in parameter estimation,” *Phys. Rev. A* **92**, 032124 (2015).
- [489] Marco Radaelli, Gabriel T Landi, Kavan Modi, and Felix C Binder, “Fisher information of correlated stochastic processes,” *New Journal of Physics* **25**, 053037 (2023).
- [490] Jay Gambetta and Howard Mark Wiseman, “State and dynamical parameter estimation for open quantum systems,” *Physical Review A* **64**, 042105 (2001).
- [491] P. Six, Ph. Campagne-Ibarcq, L. Bretheau, B. Huard, and P. Rouchon, “Parameter estimation from measurements along quantum trajectories,” in *2015 54th IEEE Conference on Decision and Control (CDC)* (2015) pp. 7742–7748.
- [492] Maël Bompais, Nina H. Amini, and Clément Pellegrini, “Parameter estimation for quantum trajectories: Convergence result,” *arxiv:2204.00343* .
- [493] Yaoling Yang, Victor Montenegro, and Abolfazl Bayat, “Extractable information capacity in sequential measurements metrology,” *Phys. Rev. Res.* **5**, 043273 (2023).
- [494] Jaroslav Hájek, “A characterization of limiting distributions of regular estimates,” *Zeitschrift für Wahrscheinlichkeitstheorie und Verwandte Gebiete* **14**, 323–330 (1970).
- [495] Arnold Janssen and Vladimir Ostrovski, “The convolution theorem of hájek and le cam-revisited,” *arXiv:1309.4984* (2013).
- [496] Nobuo Inagaki, “On the limiting distribution of a sequence of estimators with uniformity property,” *Annals of the Institute of Statistical Mathematics* **22**, 1–13 (1970).
- [497] J. Dauwels, “Computing bayesian cramer-rao bounds,” in *Proceedings. International Symposium on Information Theory, 2005. ISIT 2005.* (2005) pp. 425–429.
- [498] Richard D. Gill and Boris Y. Levit, “Applications of the

- van Trees inequality: a Bayesian Cramér-Rao bound,” *Bernoulli* **1**, 59 – 79 (1995).
- [499] A. A. Borovkov, *Mathematical Statistics. Parameter Estimation* (Moscow: Nauka, 1984).
- [500] H. L. van Trees, *Detection, Estimation and Modulation Theory, Part 1* (Wiley & Sons, 1968).
- [501] Chris A.J. Klaassen, “The asymptotic spread of estimators,” *Journal of Statistical Planning and Inference* **23**, 267–285 (1989).
- [502] Gabriel O. Alves and Gabriel T. Landi, “Bayesian estimation for collisional thermometry,” *Phys. Rev. A* **105**, 012212 (2022).
- [503] Mathias R. Jørgensen, Jan Kołodyński, Mohammad Mehboudi, Martí Perarnau-Llobet, and Jonatan B. Brask, “Bayesian quantum thermometry based on thermodynamic length,” *Phys. Rev. A* **105**, 042601 (2022).
- [504] Mohammad Mehboudi, Mathias R. Jørgensen, Stella Seah, Jonatan B. Brask, Jan Kołodyński, and Martí Perarnau-Llobet, “Fundamental limits in bayesian thermometry and attainability via adaptive strategies,” *Phys. Rev. Lett.* **128**, 130502 (2022).
- [505] E. Weinstein and A.J. Weiss, “A general class of lower bounds in parameter estimation,” *IEEE Transactions on Information Theory* **34**, 338–342 (1988).
- [506] Steve Campbell, Mohammad Mehboudi, Gabriele De Chiara, and Mauro Paternostro, “Global and local thermometry schemes in coupled quantum systems,” *New Journal of Physics* **19**, 103003 (2017).
- [507] Antonella De Pasquale and Thomas M Stace, “Quantum thermometry,” in *Thermodynamics in the quantum regime* (Springer, 2018) pp. 503–527.
- [508] Jasper Chan, TP Alegre, Amir H Safavi-Naeini, Jeff T Hill, Alex Krause, Simon Gröblacher, Markus Aspelmeyer, and Oskar Painter, “Laser cooling of a nanomechanical oscillator into its quantum ground state,” *Nature* **478**, 89–92 (2011).
- [509] V. Montenegro, M. G. Genoni, A. Bayat, and M. G. A. Paris, “Mechanical oscillator thermometry in the nonlinear optomechanical regime,” *Phys. Rev. Res.* **2**, 043338 (2020).
- [510] Luis A Correa, Mohammad Mehboudi, Gerardo Adesso, and Anna Sanpera, “Individual quantum probes for optimal thermometry,” *Phys. Rev. Lett.* **114**, 220405 (2015).
- [511] Matteo G A Paris, “Achieving the landau bound to precision of quantum thermometry in systems with vanishing gap,” *Journal of Physics A: Mathematical and Theoretical* **49**, 03LT02 (2015).
- [512] Wai-Keong Mok, Kishor Bharti, Leong-Chuan Kwek, and Abolfazl Bayat, “Optimal probes for global quantum thermometry,” *Communications physics* **4**, 62 (2021).
- [513] Jesús Rubio, Janet Anders, and Luis A Correa, “Global quantum thermometry,” *Physical Review Letters* **127**, 190402 (2021).
- [514] BM Escher, RL de Matos Filho, and L Davidovich, “Quantum metrology for noisy systems,” *Brazilian Journal of Physics* **41**, 229–247 (2011).
- [515] Jan Kołodyński and Rafał Demkowicz-Dobrzański, “Efficient tools for quantum metrology with uncorrelated noise,” *New Journal of Physics* **15**, 073043 (2013).
- [516] Rafał Demkowicz-Dobrzański and Lorenzo Maccone, “Using entanglement against noise in quantum metrology,” *Physical review letters* **113**, 250801 (2014).
- [517] Rafał Demkowicz-Dobrzański, Jan Czajkowski, and Pavel Sekatski, “Adaptive quantum metrology under general markovian noise,” *Physical Review X* **7**, 041009 (2017).
- [518] Wolfgang Dür, Michalis Skotiniotis, Florian Froewis, and Barbara Kraus, “Improved quantum metrology using quantum error correction,” *Physical Review Letters* **112**, 080801 (2014).
- [519] Rosanna Nichols, Thomas R Bromley, Luis A Correa, and Gerardo Adesso, “Practical quantum metrology in noisy environments,” *Physical Review A* **94**, 042101 (2016).
- [520] Uesli Alushi, Wojciech Górecki, Simone Felicetti, and Roberto Di Candia, “Optimality and noise resilience of critical quantum sensing,” *Physical Review Letters* **133**, 040801 (2024).
- [521] Philippe Faist, Mischa P Woods, Victor V Albert, Joseph M Renes, Jens Eisert, and John Preskill, “Time-energy uncertainty relation for noisy quantum metrology,” *PRX Quantum* **4**, 040336 (2023).
- [522] Florentin Reiter, Anders Søndberg Sørensen, Peter Zoller, and CA Muschik, “Dissipative quantum error correction and application to quantum sensing with trapped ions,” *Nature communications* **8**, 1822 (2017).